A STUDY OF SOME INTEGRAL EQUATIONS AND APPLICATIONS TO WATER WAVE PROPAGATION PROBLEMS

Thesis
Submitted for the Degree of
Doctor of Philosophy
in Science

By

Anushree Samanta

Department of Mathematics
Jadavpur University
Kolkata - 700032

November 2022

যাদবপুর বিশ্ববিদ্যালয়

FACULTY OF SCIENCE
DEPARTMENT OF MATHEMATICS

JADAVPUR UNIVERSITY
Kolkata-700 032, India
Telephone : 91 (33) 2414 6717

CERTIFICATE FROM THE SUPERVISOR

This is to certify that the thesis entitled " A STUDY OF SOME INTEGRAL EQUATIONS AND APPLICATIONS TO WATER WAVE PROPAGATION PROBLEMS " submitted by ANUSHREE SAMANTA, who got her name registered on 07.02.2018 for the award of Ph.D. (Science) degree of Jadavpur University, is absolutely based upon her own work under the supervision of Prof. Sudeshna Banerjea, Department of Mathematics, Jadavpur University and Dr Rumpa Chakraborty, Department of Mathematics, Diamond Harbour Women's University, West Bengal and that neither this thesis nor any part of it has been submitted for any degree/diploma or any other academic award anywhere before.

Sudeshna Banerjea.

(Sudeshna Banerjea)
Department of Mathematics
Jadavpur University
Kolkata-700032
India.

Professor
DEPARTMENT OF MATHEMATICS
Jadavpur University
Kolkata – 700 032, West Bengal

Rumpa Chakraborty

(Rumpa Chakraborty)
Department of Mathematics
Diamond Harbour Women's University
Diamond Harbour, Sarisha, South 24 Pargana
Pin 743368, West Bengal, India.

Dr. RUMPA CHAKRABORTY
Assistant Professor
Department of Mathematics
Diamond Harbour Women's University
South 24 Parganas, West Bengal-743368

Dedicated to

My beloved parents and younger sister

Ajit Kumar Samanta

Kalpana Samanta

Anwesha Samanta

Acknowledgement

I would like to express my sincere gratitude to my Ph.D supervisor Prof. Sudeshna Banerjea, Department of Mathematics, Jadavpur University, for the continuous support of my Ph.D study and research, for her patience, motivation and enthusiasm. Her guidance helped me in research and writing this thesis.

I would also like to express my gratitude to my co-supervisor Dr. Rumpa Chakraborty, Diamond Harbour Womens University, for her guidance, encouragement and co-operation throughout my research tenure. I convey my gratitude to Prof. B. N. Mandal, Retired professor, Physics and Applied Mathematics Unit, Indian Statistical Institute, Kolkata, for his encouragement and insightful comments. I would like to thank my Research Advisory Committee (RAC) members, Prof. Subenoy Chakraborty and Prof. Subhas Chanda Mandal, Jadavpur University, for their guidance, support, valuable comments on my research topics. I sincerely thank the present and former Heads of the department of Mathematic, Jadavpur University, for providing me all the necessary infrastructural facilities. My sincere thank to all the office staffs of the department for their help and cooperation.

I take this opportunity to thank the Department of Science and Technology (DST), Government of India, for awarding me the INSPIRE Fellowship (No.- IF170841), providing me with the financial means to complete this research endeavour.

My sincere thanks and gratefulness to all the research scholars of the Department of Mathematics of Jadavpur University, specially Piyali Kundu, Gour Das, Pallab Dey, Sreeparna Majee, Monalisa Masanta and my senior Dibakar Mondal for their help and support throughout my research tenure.

Last but not the least, my deepest gratitude goes to my parents and my younger sister who endured this long process with me, always offering support and love.

November, 2022 Anushree Samanta

Contents

Abstract

The thesis is concerned with a study of numerical solution of integral equations with regular and singular kernel by boundary element method and their applications to water wave scattering problems by thin curved barrier and rectangular thick barrier present in water region. The work in the present thesis is based on following problems.

[1] Boundary element approach of solving Fredholm and Volterra integral equations.

[2] Line element method of solving singular integral equations.

[3] Hypersingular integral equation formulation of the problem of water wave scattering by a circular arc shaped impermeable barrier submerged in a water of finite depth.

[4] Water wave interaction with a circular arc shaped porous barrier submerged in a water of finite depth.

[5] Scattering of water waves by thick rectangular barrier in presence of ice cover.

[6] Numerical approach to the problem of oblique wave scattering by a wide rectangular impediment with a vent placed under a finite depth water body with ice covered surface.

The problems in [1] and [2] illustrate the application of boundary element method (BEM) to solve Fredholm and Volterra integral equations of second kind and also singular integral equations of first kind with weakly singular kernel and hypersingular equations of first and second kind. In this approach, the the range of integration is divided into finite number of line elements. Next, discretizing the interval of definition of the integral equation into same number of line elements and assuming that the unknown function satisfying the integral equation is constant in each small line element, it is then converted into a system of linear algebraic equations. The unknown function is then evaluated on each line element by solving the system of linear algebraic equations.

The error analysis of this method is also discussed here. Some examples are considered here for illustrating the method.

Under the assumption of linearised theory of water waves, the problem of scattering of water waves by a thin circular arc shaped barrier, rigid and porous, submerged in ocean of finite depth, are studied in problems [3] and [4] respectively. By judicious application of Green's integral theorem, the corresponding boundary value problem is reduced to a hypersingular integral equation of first kind for the rigid barrier and of second kind for the porous barrier. This hypersingular integral equation in each problem is solved by using two methods. The first method is based on the Boundary Element Method (BEM) as described in problems [1] and [2]. The second method is a collocation method where the unknown function satisfying the integral equation is approximated by an infinite series involving Chebyshev polynomials. Choosing the collocation points suitably the integral equation is reduced to a system of linear equations. Using the solution of the integral equation, the quantities of physical interest, i.e, reflection and transmission coefficients are obtained and studied graphically in each problem in [3] and [4].

In problem [5], the problem of water wave scattering of a normally incident wave train by a thick rectangular barriers present in water with ice cover is studied. The four basic configurations of thick rectangular barrier viz, partially immersed, bottom standing, submerged to a finite depth and wall with a gap extending full depth of water region are considered. The problem [6] is concerned with the study of the problem of scattering of an obliquely incident wave by a thick rectangular wall with a gap totally submerged in water of finite depth with ice cover. Multi term Galerkin approximations involving ultraspherical Gegenbauer polynomials is used for solving the integral equations arising in the mathematical analysis for the problems in [5] and [6]. In problem [6], the corresponding integral equation is also solved by using boundary element method. Numerical estimates for the reflection and transmission coefficients are obtained for various values of different parameters and are studied graphically.

PART I

General Introduction

Chapter 1

Introduction

1 Preamble

The theory of integral equations constitute an important topic in Mathematics as this is one of the most useful mathematical tools in both pure and applied mathematics. Integral equations arise in a natural way in course of solving the initial and boundary value problems associated with mathematical modelling of physical phenomena. The solutions of integral equations play an important role to understand the qualitative features of the physical phenomena in the natural sciences.

Development of the theory of integral equation is closely associated with the history of mathematics, specifically applied mathematics. The origin of integral equation may be attributed to N.H.Abel who in 1826 first reduced the problem of finding the path of descent of a particle along a smooth vertical curve under the action of gravity in an interval of time, to an integral equation. Later in 1896, V. Volterra developed the general theory of solution of a class of linear integral equation where the upper limit of integral is variable. Such type of integral equations are known after him. I. Fredholm in 1900 developed the theory of integral equation in which the limits of integral are constants and these integral equations are known as Fredholm integral equations.

It may be noted that an extensive literature exists for the theory of second kind integral equations of Fredholm or Volterra type but the literature concerning first kind integral

equation is rather limited. In some cases the first kind integral equations with special forms of kernels possess exact solutions. These are mostly singular integral equations in which the kernels have singularities of different forms.
Study of singular integral equations is significant due to their occurrence and application in various physical problems in mathematical physics as has been demonstrated in Abel integral equation. The kernel of Abel integral equation is a weakly singular kernel as it has square root singularity. A weakly singular integral can be defined in Riemann sense and so it is amenable to numerical methods. However a strongly singular integral needs to be defined in special way. The kernel of Cauchy type singular integral equation involves strong singularity and the corresponding integral is defined in the sense of Cauchy principal value. Similarly the kernel of hypersingular integral equation involves hypersingular integral which is defined as Hadamard finite part integral.
The literature on singular integral equations with Cauchy kernel was enriched around the middle of twentieth century by contribution of Russian mathematicians like N. I. Muskhelishvili, S. G. Mikhlin, F. D. Gakhov, I. I. Piralov and others. They carried out a lot of work on Cauchy type singular integral equations by using the complex variable theory exploiting the concept of analytic functions and Riemann Hilbert boundary value problem. Extensive references of the works by these mathematicians can be found in the treatise of Muskhelishvili (1953), Mikhlin (1957), Gakhov (1966).

A major part of the development of singular integral equations involve devising methods by which these can be investigated for obtaining their solutions successfully. It may be noted that the methods of complex variable theory leading to the solution of Riemann Hilbert problems for solving singular integral equations are cumbersome. Certain elementary and straightforward methods also produce the solutions relatively. Notable works by Peters (1963), Case (1966), Estrada and Kanwal (1989,2000), Chakrabarti (1980,1981,1984,1986,1989.2006,2007), Chakrabarti and Chakrabarti (1977), Chakrabarti and George (1994), Chakrabarti and Manam (2003), Chakrabarti and Williams (1980), Mandal and Goswami (1983), Mandal (1986), MacCammy (1965,1985), Banerjea and Mandal (1993,1995), Williams (1978) may be mentioned in this connection. This has resulted in the creation of somewhat new interest in

the investigation of singular integral equations by simple and straightforward methods to obtain their solutions.

Hypersingular integral equations of first kind also arise in various physical problems of continuum mechanics. Examples range from potential flow past a rigid thin plate, acoustic scattering by hard plate, water wave interaction with thin impermeable barriers in the linearized theory of water waves (Martin et. al. (1997)), to crack problems in two dimensional elasticity (Ioakimidis (1982)) and stress field around cracks in fracture mechanics (Chan et. al. (2003)). The problem of two dimensional flow past a flat rigid plate in an infinite fluid can be reduced to finding the solution of a simple hypersingular integral equation with the condition that the unknown function vanishes at the end points of the range of integration. The solution of the hypersingular integral equation of first kind was obtained by Parsons and Martin (1992,1994) by using a collocation method based on approximating the unknown function by Chebychev's polynomial. A number of water wave scattering problems involving thin straight or curved plates have been investigated by formulating them in terms of hypersingular integral equations (cf. Parsons and Martin (1992,1994), Mandal et. al. (1995), Banerjea et. al. (1996), Mandal and Gayen (2002), Kanoria and Mandal (2002), Dutta and Banerjea (2009), Mondal and Banerjea (2016)). Recently boundary element method has been applied to solve numerically the integral equation with regular, weakly singular and hypersingular integral equations (cf. Banerjea et. al. (2019), Samanta et. al. (2022)). Hypersingular integral equations of second kind have been investigated in the literature rarely. Occurrence of hypersingular integral equations of second kind can be traced to Prandtl's (1918) singular integro-differential equation (cf. Dragos (1983)) arising in connection with the theory of lifting in aerodynamics. A Gauss type quadrature formula was given by Dragos (1994) for its numerical solution. Chakrabarti et. al. (1997), used a straight forward analysis involving complex function-theoretic method to determine the exact solution of special type of hypersingular integral equation of second kind. Later Gayen et. al. (2014), Mondal and Banerjea (2016), Mondal et. al. (2021) used collocation method used by Parsons and Martin (1992) to solve hypersingular integral equations of second kind. Recently boundary element method has been applied to solve hypersingular integral equation of second kind numerically and this solution

is used to solve some water wave problems (cf. Mondal et. al. (2021).

The subject of surface gravity waves is varied and fascinating from the point of view of types of physical problems which occur as well as mathematical ideas needed to tackle them. The theory of water waves deals with the study of some general aspect of wave motion or study of behaviour of waves in presence of some configurations of interest to the ship designers and oceanographers. Unfortunately even the simplest problem appears to be difficult to tackle mathematically unless some assumptions are made about the medium as well as the wave motion. Consequently water is assumed to be incompressible, inviscid and homogeneous fluid. Thus if one assumes that the motion in water to be irrotational, then the problems concerning propagation of water waves reduce to a boundary value problem consisting of Laplace equation together with appropriate boundary conditions. Again the boundary conditions including the free surface condition are nonlinear in nature. Thus further assumptions are required regarding the wave motion to simplify the boundary conditions so as to handle the boundary value problem mathematically. The nature of assumptions provides a natural way to classify the theory of water waves. Consequently two approximate theories, *viz*, the linearised theory and the shallow water theory are developed from the basic hydrodynamic theory.

The linearised theory is based on the assumption that the amplitude of wave motion is small compared to the wavelength(cf. Stoker (1957)). Consequently the motion is assumed to be small so that the velocity components and the free surface elevation /depression and their partial derivatives are small so that their products and powers can be neglected. Thus if the motion is assumed to be irrotational then within the framework of linearised theory the concerned boundary value problem consists in solving Laplace's equation together with linearised free surface condition and bottom condition. There are varied classes of problems in the literature which are studied mathematically within the framework of linearised theory. The present thesis is concerned with the study of wave motion under the assumption of linearised theory.

Shallow water theory is developed from the basic hydrodynamic theory on the assumption that the depth of water is small compared to the wavelength. This theory

gives a set of nonlinear equations even for first order approximation. The first order approximation leads to the theory of long waves. The higher order approximation gives solution corresponding to continuous permanent wave profiles of finite amplitude that can propagate without change of form or shape if viscosity is neglected (cf. Stoker (1957)).

From mathematical point of view the theory of water waves has been a source of intriguing and often difficult mathematical problem. Virtually every classical mathematical technique appears somewhere within its confine. The founding fathers of this subject are Euler, Lagrange, Cauchy, Poisson. Further contributions in the theory of water waves have been made by Stokes, Lord Kelvin, Kirchhoff and Lamb who constructed a number of explicit solutions. In the twentieth century Havelock, Kochin, Sretensky, Stoker, John and others applied Fredholm theory of boundary integral equations to the field of water waves. A general exposition of the classical theory is given in the books of Lamb (1932), Stoker (1957), Wehausen and Laitone (1960), Sretensky (1977), Lighthill (1978), Whitham (1979), Crapper (1984), Mandal and Chakrabarti (2000) & Kuznetsov et. al. (2001). Various aspects of linear theory of water waves have been discussed in the works of Havelock (1929) and Ursell (1947). Applications and mathematical methods associated with the theory of water waves have been discussed in Wehausen (1971), Newman (1977), Mei (1983), Linton and Melver (2001).

The present thesis is concerned with the study of some integral equations and its application to some problems on interaction of water waves with marine structures, under the assumption of linearised theory. The validity of using the linearized theory in water wave problems has been verified a number of times experimentally. Ursell, Dean and Yu(1959) experimented on the height of water waves generated by a flat vertical piston wave-maker and obtained results which are in very good agreement with theoretical results obtained under the assumption of linearized theory for small amplitude gravity waves. Dean and Ursell(1959), Yu and Ursell(1961) also experimented with a circular cylinder in deep water as well as in finite depth water. In both the experiments the experimental result of wave amplitude almost coincides with the theoretical results.

Other experiments were performed from time to time. These experimental evidences confirm and establish the validity of the linearized theory of water waves.

With this preamble we now describe the problems in the thesis.

2 A brief description of the problems in the thesis

The work in the thesis is concerned with a study of integral equations and its applications to water wave scattering problems by thin curved barrier and rectangular thick barrier present in water region. The thesis is divided into four parts. The Part I of the thesis is an introductory part which comprises of two chapters. Apart from a general introduction in chapter one, some mathematical preliminaries are discussed in chapter two.

In Part II of the thesis, there are two chapters viz, Chapter 3 and 4. In this part, the boundary element method of solution of integral equation with regular and singular kernel are discussed in chapters 3 and 4 respectively.

The boundary element method (BEM) is a powerful computational technique, providing numerical solutions to a range of scientific and engineering problems. The method is easier to apply than the more traditional finite element method. Acoustics, compressible fluid flow problems [cf. Luminita (2007)] are tackled by this numerical technique. Boundary integral equations are classical tool for the analysis of boundary value problems consisting of partial differential equation and boundary conditions. The term boundary element method (BEM) denotes a method for the approximate numerical solution of these boundary integral equations. The approximate solution of the boundary value problem obtained by BEM has the distinguishing feature that it is an exact solution of the differential equation in its domain and is parametrized by a finite set of parameters on the boundary [cf. Beer et. al. (2008), Kirkup (2007), Brebbia and Dominguez (1994)].

The advantage of BEM over other numerical methods is that only the boundary of the domain needs to be discretized. Especially in two dimensions where the boundary is just a curve, this allows very simple data input and storage methods. The boundary element method is especially advantageous in the case of problems with infinite

or semi-infinite domains, although only the finite surface of the infinite domain has to be discretized. Thus the solution at any arbitrary point of the domain can be found after determining the unknown boundary data. For the same level of accuracy, the boundary element method uses a lesser number of nodes and elements as compared to the other numerical methods like, finite element method. A detail explanation is given by Pozrikidis (2002), Becker (1992), Beer and Watson (1992).

As mentioned apriori, the theory of Integral Equations constitute an important topic in Mathematics. Modeling of physical phenomena in the language of mathematics gives rise to boundary value problems with a governing differential equation and associated boundary conditions. Using suitable procedure, the boundary value problem can be reduced to an integral equation of first or second kind. It is already mentioned that the literature on second kind integral equation is very rich whereas the literature on first kind integral equations is very limited. Moreover, if the kernel of the integral equation is complicated then the analytical methods for solving the integral equation may not be available. In this situation numerical methods are adopted. A number of numerical methods are available in the literature viz, Galerkin method, collocation method where the unknown function satisfying the integral equation is approximated by a polynomial. An approximate solution of integral equation using various numerical method has been studied by a number of researchers. Mandal and Bhattacharyya (2007,2008) obtained approximate numerical solutions of some classes of integral equations and singular integro-differential equation by using Bernstein polynomials as basis. Mandal and Bhattacharyya (2007) considered Fredholm integral equations of second kind and hypersingular integral equations of first and second kind. They explained the method with illustrative examples and compared the approximate solutions with exact solutions numerically by evaluating the absolute error associated with the approximate solutions. An excellent agreement between the exact and approximate solutions was observed. Also Mandal and Bhattacharyya (2008) used a method based on polynomial approximation using Bernstein polynomial basis to obtain approximate numerical solution of a singular integro-differential equation with Cauchy kernel. The numerical results obtained by them agreed favorably with those obtained by various Galerkin methods earlier in the literature.

In Chapter 3, we applied boundary element method (BEM) to solve Fredholm and Volterra integral equations of second kind. In this approach, the the range of integration is divided into finite number of line elements. Next, discretizing the interval of definition of the integral equation into same number of line elements and assuming that the unknown function satisfying the integral equation is constant in each line element, it is then converted into a system of linear algebraic equations over the line elements. It may be noted that for Volterra integral equation, a lower triangular matrix associated with the system of linear algebraic equations is obtained. The unknown function is then evaluated on each line element by solving the system of linear algebraic equations. The convergence of the method is studied by increasing the number of line elements. Some numerical examples of both Fredholm and Volterra integral equations are considered which are solved by using BEM. From the numerical data, it is observed that quite accurate results are obtained for both types of integral equations.
In Chapter 4, we have applied boundary element method to solve integral equations i) of first kind with weakly singular kernel, viz, Abel integral equation and integral equation with log kernel, ii) of first and second kind with hypersingular kernel.
These integral equations occur while solving the boundary value problems arising in Mathematical physics, particularly in solid mechanics and theory of water waves.

The analytical solutions of Abel integral equation, integral equation with log kernel and hypersingular integral equation are well known (cf. Mandal and Chakrabarti (2011)). However if the kernel of the integral equation involves singularity with complicated form, the exact solution may not be easy to obtain in which case numerical methods are helpful. Moreover, the integral equations with log kernel and Abel integral equations involve weakly singular kernel while the kernel of the hypersingular integral equation involves strong singularity. It is important to note here that the integrals with weak singularity are amenable to the numerical techniques as the integrals can be defined in ordinary Riemann sense. However the integrals with strong singularity has to be defined in a special manner and for that reason the numerical evaluation of integrals with strong singularity needs special attention. The exact solution of hypersingular integral equation is available in the literature (cf. Mandal and Chakrabarti (2011), Dutta and Banerjea (2009)) by function theoretic method or method based on

utilizing the known solution of Cauchy type singular integral equation of first kind. However, for solving hypersingular integral equation with complicated kernel, Parsons and Martin (1992) suggested an elegant numerical method based on approximating the unknown function satisfying the integral equation by Chebychev's polynomial.
Following the method used in Chapter 3, (cf. Banerjea et. al. (2019)), the range of integration of the given integral equations in Chapter 4, is divided into finite number of line elements. Next, discretizing the interval of definition into same number of line elements, the given integral equation is reduced to a system of algebraic equations over the line elements. It may be mentioned that the coefficient matrix of the system of linear equations associated with the Abel integral equation is a lower triangular matrix. Solving the system of linear algebraic equations, the unknown function is evaluated on each line element. Some examples are considered here for illustrating the method. It is observed that use of this method produces very accurate results. The error analysis of the method is discussed here.
Usually boundary element method is used to solve boundary value problems involving partial differential equation in a domain in higher dimension. In Chapters 3 and 4 we have used this method to solve integral equations in one dimension. To the best of our knowledge, this method has not been used in the literature to solve integral equation although Gray in 1991, Guiggiani in 1992 developed an algorithm to study hypersingular boundary integral equation and evaluation of hypersingular integrals by the boundary element method in three-dimensional crack problems.

In Part III of the thesis,the problem of water wave propagation in presence of thin curved barrier is studied. There two chapters in this part viz, Chapters 5 and 6. In Chapters 5 and 6, under the assumption of linearised theory of water waves, the problem of scattering of water waves by a thin circular arc shaped barrier, rigid and porous respectively, submerged in ocean of finite depth, are studied. The phenomena of water wave propagation in presence of obstacles of different shapes termed as breakwaters has been a subject of considerable interest among the researchers since early twentieth century because of numerous practical applications. A breakwater is a coastal structure that breaks waves and reduces the wave energy reaching the beach so that a harbour or

an anchorage is protected from the effect of water waves and also the beach erosion is prevented. Breakwaters are usually rigid structures which extend up to the full depth of ocean. However, these fixed structures are expensive as large quantity of construction material is required and also difficult to construct, particularly when the ocean is very deep. An useful alternative is to construct floating breakwaters. The phenomena of water wave propagation in presence of a floating breakwater has been a subject of interest as the floating breakwaters are relatively easier to construct and are cost effective rather than the fixed structures (cf. Sobhani et. al (1988)). Breakwaters in the shape of a circular arc submerged in water was studied by many researchers because it is known that the increase in arc length of a circular arc-shaped rigid breakwater reduces the reflection (cf Parsons and Martin (1994)). Parsons and Martin (1994) considered the scattering problem where the circular arc shaped barrier was submerged in water of infinite depth. He pioneered in solving the corresponding boundary value problem by first kind hypersingular integral equation formulation where he used collocation method based on approximating the unknown function satisfying hypersingular integral equation by Chebyshev's polynomial. The collocation method used in Parsons and Martin (1994) is an efficient method of solving hypersingular integral equation. McIver and Urka (1995) studied the problem using matched series expansion and also Schwinger variational principal method to obtain numerical results for the reflection coefficient for a symmetric circular-arc-shaped plate submerged in deep water. Later Kanoria and Mandal (2002) and Mondal et. al. (2017) adopted hypersingular integral equation formulation used in Parsons and Martin (1994) to study the wave propagation problem involving circular arc shaped barrier not symmetric about the vertical axis, present in deep water and in water of finite depth covered by ice respectively.

In Chapter 5, we have considered the problem of scattering of water waves by a thin rigid curved barrier in the form of an arc of a circle submerged in ocean of finite depth. We applied Green's Integral theorem to reduce the corresponding boundary value problem to first kind hypersingular integral equation. This hypersingular integral equation is solved by using two methods.

The first method is based on the Boundary Element Method (BEM) which is described in Chapters 3 and 4 (cf. Banerjea et. al.(2019), Samanta et. al. (2022)).

The second method is based on the work of Parson and Martin (1994), which is a collocation method where the unknown function satisfying the integral equation is approximated by an infinite series involving Chebyshev polynomials. Choosing the collocation points suitably the integral equation is reduced to a system of linear equations. This system of linear equations is solved numerically to obtain the solution the the integral equation.

It was observed that the solution of the integral equation by the two methods agree with each other. The second method is a well known standard and widely used method in comparison with the other method. However, the first method illustrates an application of BEM in solving integral equations numerically which is not very common and in some sense new numerical technique in solving integral equations. Using the solution of the integral equation, the reflection and transmission coefficients are evaluated and depicted graphically. From the graphical results, it was observed that the size and the position of the barrier have some impact on the reflection and transmission coefficients.

In Chapter 6, we used a second kind hypersingular integral equation formulation to study the problem of water wave scattering by a circular arc shaped porous barrier submerged in water of finite depth.

The problem of scattering of water waves by porous coastal structures like rubble mound breakwaters are important in coastal engineering as the pores in the barrier attenuates wave action by dissipating the wave energy and thereby protects the shore line or harbour. Many researchers used sophisticated mathematical techniques to study scattering problems involving porous barrier mainly in any form of straight orientation. Among them the works of Yu (1995), Mclver (1999), Evans and Porter (2011), Tsai and Young (2011), Gayen and Mandal (2014) may be mentioned.

The problem of wave interaction with perforated semicircular bottom standing barrier was considered by Liu and Li (2012, 2013) who used multipole expansion method to study the problem. Later Mondal and Banerjea in (2016) used the second kind hypersingular integral equation formulation to study the problem of scattering of water waves by a circular arc shaped porous barrier submerged in deep ocean. They used the collocation method as in Parson and Martin (1994) to solve the hypersingular integral equation and thereby obtained the reflection, transmision and the energy dissipation

coefficients.

In Chapter 6, the corresponding boundary value problem was reduced to a second kind hypersingular integral equation by a judicious application of Green's integral theorem. Following Mondal et. al. (2021), the second kind hypersingular integral equation was solved by using BEM as well as the collocation method. We may mention here that the in the present problem the hypersingular integral equation is of second kind whereas in Mondal et. al. (2021) the hypersingular integral equation was of first kind. The quantities of interest ie, reflection, transmission and energy dissipation coefficients were evaluated by using the solution of the second kind hypersingular integral equation obtained by both the methods. The reflection coefficient obtained thus by both the methods are presented in tabular form and it was found that the results matched upto five places of decimal. Also it is observed that the reflection coefficients obtained by the present methods are in good agreement with the results obtained by Liu and Li (2012).

Part IV of the thesis consists of two chapters 7 and 8. In Chapter 7, the problem of water wave propagation in presence of a thick rectangular barrier present in water with ice cover is studied. The four basic configurations of thick rectangular barrier viz, partially immersed, bottom standing, submerged to a finite depth and barrier with a gap extending full depth of water region are considered. Chapter 8 is concerned with the study of the problem of scattering of an obliquely incident wave by a thick rectangular wall with a gap totally submerged in water of finite depth with ice cover.

Ice is one of the most common material on earth, yet it is very different from all other known materials. Depending on its morphology and micro-structure, it may behave as an elastic plate or as a brittle structure or as an viscoelastic material or even as a quasi-liquid material. A mathematical model for treating the ice sheet as floating thin elastic plate is well known and a significant research has been carried out using this model to study the problems related to ocean wave interaction with sea ice (cf. Fox and Squire (1994); Squire (2007); Chung and Fox (2002); Linton and Chung (2003); Chakrabarti (2000); Gayen et al.(2005)).

The study of ocean wave interactions with a very large thin, floating elastic plate has gained immense importance since last decade as it can be used to model a wide range of

physical systems. One of its important applications consists in modelling a very large floating structure (VLFS) that is used in ocean space utilization for the construction of megafloats such as floating airports, offshore runways, floating restaurant etc. It is a technology that allows these megafloats, which are considered to be artificial lands to float on rising sea level and has a minimal effect on marine habitat, natural and tidal current flow (cf. Wang et. al. (2010), Wadhams (1978)). Owing to the large surface area and relatively small depth, VLFS behaves elastically under wave action (cf. Wang et. al. (2010)). In the polar region, surface gravity waves propagate from the open ocean into ice-covered seas. Understanding the modus operandi of formation of sea ice and its distribution, it is imperative to explain the geophysical phenomena occurring in the polar regions and in the marginal ice zone. A precinct between ocean and atmosphere, the sea ice arrests the escape of heat from the ocean to the air above. Consequently it plays a crucial role in conservation of marine life. An uninterrupted expanse of unbroken ice over a vast stretch in the polar region often encounters waves propagating at free surface. It is well known that waves may weaken and rupture the continuous sea ice causing fissures which may lead to melting of sea ice. This phenomena is an indicator of global climatic change. The amplitude of the waves travelling beneath the ice needs to be studied as it causes the ice-cover to bend. The bending of ice-cover is attributed to its elastic property. In order to minimize the impact of wave action on a VLFS or ice sheet, various anti motion structures and devices such as breakwaters, submerged plates, oscillating water column breakwater, air cushion, curtain pile breakwater are designed (cf. Wang (2010); Tari and Ohkubo (2000)). Also, a number of experiments measuring wave propagation through marginal ice zone have been reported of which first measurement was carried out by a ship borne wave recorder (cf Kohout and Meylan (2008)). Later, measurements were carried out by a echo sounder from a submerged hovering submarine, acoustic Doppler Current Profiler mounted on an autonomous under water vehicle (cf Kohout and Meylan (2008), Wadhams (1978)). Thus the study of the waves in presence of thin or thick plate under ice cover or VLFS is important. Mathematically, the boundary value problem (BVP) related to study of water waves in ocean with ice-cover is interesting as it involves fifth order derivative of the potential function in the boundary condition on ice cover

whereas the governing partial differential equation is of second order.

The problems of water wave scattering by breakwaters modelled as thin vertical barriers of various configurations have been studied extensively in the literature under the assumption of linear theory during the last fifty years. However, the rigid breakwaters in form of thin plates are vulnerable to huge wave load. In this situation an alternative is to construct breakwater in form of thick rectangular barrier. When the breakwaters are modelled as thick vertical barriers with rectangular cross sections in water of uniform finite depth, the corresponding water-wave scattering problems for normal incidence of a surface wave train were investigated by Mei and Black (1969) for surface piercing and bottom-standing barriers. They used a variational formulation to obtain numerical estimates for the reflection coefficient and presented graphically the numerical results. Later Mandal and Kanoria (2000), Kanoria et al. (1999) and Kanoria (1999) considered the problems of oblique and normal wave scattering by thick barriers respectively, wherein the barriers have four types of configurations such as surface-piercing or bottom standing or a submerged block, or a thick wall with a gap. They used multi-term Galerkin approximation method involving ultraspherical Gegenbauer polynomials for solving first kind integral equations arising in the mathematical analysis to obtain very accurate numerical estimates for the reflection coefficient.
There are some notable work of water wave scattering by rectangular trench (cf. Kirby and Dalrymple (1983), Lee and Ayer (1981), Miles (1982)). Recently Sasmal et al. (2019) solved the problem of wave scattering over rectangular trench in presence of ice cover. They considered the multi-term Galerkin approximation techniques. The problems of scattering of normally incident wave train by a thick barrier for its four basic configurations and scattering of oblique incident wave train by a totally submerged wall with a gap present in water with ice cover are studied in Chapter 7 and 8 respectively by using multi term Galerkin approximations involving ultraspherical Gegenbauer polynomials for solving the integral equations arising in the mathematical analysis (cf Mandal and Kanoria (2000)). In Chapter 8 the corresponding integral equation is also solved by using boundary element method and the result is in good agreement with the result obtained by Galerkin approximation. Numerical estimates

for the reflection and transmission coefficients obtained for various values of different parameters are depicted graphically. It is also found that the width of the barriers affects the reflection and transmission coefficients significantly, and there exists an infinite number of discrete wave frequencies at which waves are completely transmitted, as was also observed by Kanorai et al. (1999). From the numerical study, it is clearly understood that presence of ice cover significantly affects the nature of reflection and transmission coefficients.

This completes the description of the contents of the present thesis.

The work reported in the present thesis is mainly based on the following papers:

1. Sudeshna Banerjea, Rumpa Chakraborty and Anushree Samanta. Boundary element approach of solving fredholm and volterra integral equations, *Int. J. Mathematical Modelling and Numerical Optimisation.* 9(1), (2019), pp. 1-11.

2. Anushree Samanta, Rumpa Chakraborty and Sudeshna Banerjea . Line element method of solving singular integral equations, *Indian Journal of Pure and Applied Mathematics.* 53(2), (2022), pp. 528-541.

3. Dibakar Mondal, Anushree Samanta and Sudeshna Banerjea. Hypersingular integral equation formulation of the problem of water wave scattering by a circular arc shaped impermeable barrier submerged in a water of finite depth. *Quarterly Journal of Mechanics and Applied Mathematics*, 74(4), (2021), pp. 491-505.

4. Anushree Samanta, Dibakar Mondal and Sudeshna Banerjea. Water wave interaction with a circular arc shaped porous barrier submerged in a water of finite depth, *Journal of Engineering Mathematics.* 138(1), (2023), 4.

5. Anushree Samanta, Rumpa Chakraborty . Scattering of water waves by thick rectangular barriers in presence of ice cover, *Journal of Ocean Engineering and Science.* 5(3), (2020), pp. 279-293.

6. Anushree Samanta, Rumpa Chakraborty. Numerical approach on oblique wave scattering by a wide rectangular impediment with a vent placed under a finite depth water body with ice covered surface, *J. Offshore Mech. Arct. Eng.*. 145(1), (2023), pp. 010903.

Chapter 2

Mathematical preliminaries

Some mathematical preliminaries used in the problems of the present thesis are briefly studied in the chapter.

1 Basic Equations of the Theory of Water Waves and Havelock's Expansion of Water Wave Potential

(A) Water With A Free Surface

We consider the motion in a homogeneous, incompressible fluid (water) of density ρ under the action of gravity and bounded above by a free surface. A rectangular cartesian co-ordinate system is chosen in which the y-axis is taken vertically downwards and the plane y=0 is the position of the undisturbed free surface. The fluid occupies the half space $y \geq 0$ if it is infinitely deep or the region $0 \leq y \leq h$ if it is of uniform finite depth h. The basic equations are derived from the equation of continuity (equation of conservation of mass) and Euler's equation of motion (equation of conservation of momentum). These are respectively given by

$$\nabla.\mathbf{q} = 0 \tag{2.1.1}$$

and

$$\frac{\partial \mathbf{q}}{\partial t} + (\mathbf{q}.\nabla)\mathbf{q} = \nabla(-\frac{p}{\rho} + gy) \tag{2.1.2}$$

where $\mathbf{q} = (u, v, w)$ is the fluid velocity, p is the pressure, g is the acceleration due to gravity and ∇ is the gradient operator. We assume that the motion in the fluid starts from rest so that it is irrotational and can be described by a velocity potential function $\Phi(x, y, z, t)$. Hence,

$$\mathbf{q} = \nabla\Phi \tag{2.1.3}$$

so that the equation of continuity becomes

$$\nabla^2\Phi = 0, \quad \text{in the fluid region} \tag{2.1.4}$$

where $\nabla^2 \equiv (\frac{\partial^2}{\partial x^2} + \frac{\partial^2}{\partial y^2} + \frac{\partial^2}{\partial z^2})$ is the Laplace operator. Using the relation (2.1.3), the equation of motion (2.1.2) can be integrated to give Bernoulli equation

$$\frac{\partial \Phi}{\partial t} + \frac{1}{2}|\mathbf{q}|^2 + \frac{p}{\rho} - gy = C(t)$$

where $C(t)$ is a constant depending upon time t only and can be absorbed in Φ by redefining Φ so that the linearized form of the Bernoulli equation is

$$\frac{\partial \Phi}{\partial t} = gy - \frac{p}{\rho}. \tag{2.1.5}$$

Let $y = \eta(x, z, t)$ denote the free surface depression. The pressure at the free surface is equal to the atmospheric pressure which is a constant and may be taken to be equal to zero (by a suitable choice of scale), so that equation (2.1.5) gives rise to

$$\frac{\partial}{\partial t}\Phi(x, y, z, t) = g\eta(x, z, t) \quad \text{on} \quad y = \eta(x, z, t).$$

Expanding $\frac{\partial \Phi}{\partial t}(x, y, z, t)$ by Taylor's series about $y = 0$ and neglecting the terms of sec-

ond and higher orders of smallness, this reduces to the linearized dynamical boundary condition at the free surface as given by

$$\frac{\partial \Phi}{\partial t} = g\eta \quad \text{on} \quad y = 0. \tag{2.1.6}$$

We write the equation of the free surface as

$$F(x, y, z, t) \equiv y - \eta(x, z, t) = 0. \tag{2.1.7}$$

Sine $F = 0$ is a boundary of the fluid, we must have

$$\frac{\partial F}{\partial t} + u\frac{\partial F}{\partial x} + v\frac{\partial F}{\partial y} + w\frac{\partial F}{\partial z} = 0 \quad \text{on} \quad y = \eta,$$

which by using the relation (2.1.7) produces

$$\frac{\partial \eta}{\partial t} + u\frac{\partial \eta}{\partial x} - v + w\frac{\partial \eta}{\partial z} = 0 \quad \text{on} \quad y = \eta.$$

Since the velocity components and the free surface depression together with their partial derivatives are small quantities, their squares, higher powers and products can be neglected so that this equation becomes

$$\frac{\partial \eta}{\partial t} = \frac{\partial \Phi}{\partial y}(x, y, z, t) \quad \text{on} \quad y = \eta(x, z, t).$$

Again, expanding $\frac{\partial \Phi}{\partial y}(x, y, z, t)$ about $y = 0$ and neglecting terms of second and higher orders of smallness, the linearized kinematical boundary condition at the free surface is obtained as

$$\frac{\partial \Phi}{\partial y} = \frac{\partial \eta}{\partial t} \quad \text{on} \quad y = 0. \tag{2.1.8}$$

This condition implies that the velocity of fluid particles on the free surface normal to it is the same as the velocity of the free surface.

Elimination of η between the equations (2.1.6) and (2.1.8) produces the linearized free

surface condition as given by

$$\frac{\partial^2\Phi}{\partial t^2} = g\frac{\partial\Phi}{\partial y} \quad \text{on} \quad y = 0. \tag{2.1.9}$$

The condition of no motion at the bottom gives

$$\nabla\Phi \to 0 \quad \text{as} \quad y \to \infty \tag{2.1.10a}$$

if the fluid extends infinitely downwards. However, if the fluid is of uniform finite depth h below the mean free surface, then

$$\frac{\partial\Phi}{\partial y} = 0 \quad \text{on} \quad y = h. \tag{2.1.10b}$$

The free surface depression $\eta(x, z, t)$ is obtained from equation (2.1.6) in terms of the velocity potential Φ as

$$\eta(x, z, t) = \frac{1}{g}\frac{\partial\Phi}{\partial t}(x, 0, z, t). \tag{2.1.11}$$

The basic equations of the linearized theory of water waves are given by the equations (2.1.4), (2.1.9) and (2.1.10a) or (2.1.10b).
If we assume the motion to be simple harmonic in time with angular frequency σ, then the velocity potential Φ can be expressed as

$$\Phi(x, y, z, t) = Re(\phi(x, y, z)e^{-i\sigma t}) \tag{2.1.12}$$

so that from equations (2.1.4), (2.1.9) and (2.1.10a,b) we find the potential function ϕ satisfies

$$\nabla^2\phi = 0 \quad \text{in the fluid region,} \tag{2.1.13}$$

$$K\phi + \phi_y = 0 \quad \text{on} \quad y = 0 \tag{2.1.14}$$

where $K = \frac{\sigma^2}{g}$,

$$\nabla\phi \to 0 \quad \text{as} \quad y \to \infty \tag{2.1.15a}$$

for infinitely deep fluid, or

$$\frac{\partial\phi}{\partial y} = 0 \quad \text{on} \quad y = h \tag{2.1.15b}$$

for fluid of uniform finite depth.
The equations (2.1.13) to (2.1.15a) or (2.1.15b) are also regarded as basic equations of the linearized theory of water waves for time harmonic irrotational motion in the fluid. A detailed discussion can be found in Mandal and Chakrabarti (2000).

For the two-dimensional motion, a representation for the water wave potential ϕ can be obtained by employing the method of separation of variables for solving the two-dimensional Laplace equation

$$\nabla^2\phi = 0 \quad \text{in the fluid region} \tag{2.1.16}$$

where $\nabla^2 \equiv \frac{\partial^2}{\partial x^2} + \frac{\partial^2}{\partial y^2}$, along with the free surface and bottom conditions. In this case, the solution for the potential function $\phi(x, y)$ representing progressive waves is given by

$$\phi(x,y) = \begin{cases} \exp(-Ky \pm iKx) & \text{for deep water,} \\ \frac{\cosh k_0(h-y)}{\cosh k_0 h}\exp(\pm ik_0 x) & \text{for water of finite depth h ,} \end{cases} \tag{2.1.17}$$

where k_0 is the unique real positive root of the transcendental equation

$$k\tanh kh = K. \tag{2.1.18}$$

The local solutions are given by

$$\phi = \begin{cases} (k\cos ky - K\sin ky)e^{-k|x|}(k > 0) & \text{for deep water,} \\ \frac{\cos k_n(h-y)}{\cos k_n h}\ \exp(-k_n|x|) & \text{for water of finite depth h} \end{cases} \tag{2.1.19}$$

where $\pm ik_n$'s ($n = 1, 2, 3, ...$) are the purely imaginary roots of the transcendental equation (2.1.18). It can be shown that the equation (2.1.18) has only two real roots $\pm k_0$ and countably infinite number of purely imaginary roots $\pm ik_n (n = 1, 2, 3, ...)$ [cf. Mandal and Chakrabarti (2000)].

Thus, the progressive wave solution given by equations (2.1.17) and local solutions (2.1.19) forms the basis functions for the expansion of the function $\phi(x, y)$ satisfying Laplace's equation, free surface condition and bottom condition. Thus, in the case of fluid of infinite depth, a representation of $\phi(x, y)$ is given by

$$\begin{aligned}\phi(x,y) &= Ae^{-Ky+iKx} + Be^{-Ky-iKx} \\ &+ \begin{cases} \int_0^\infty C(k)(k\cos ky - K\sin ky)e^{-kx}dk & x > 0, \\ \int_0^\infty D(k)(k\cos ky - K\sin ky)e^{kx}dk & x < 0, \end{cases}\end{aligned} \tag{2.1.20}$$

where A, B are unknown constants and $C(k)$ and $D(k)$ are unknown functions of k. This is known as Havelock's expansion of water wave potential $\phi(x, y)$ for deep water. Similarly, in the case of fluid of finite depth 'h', Havelock's expansion of $\phi(x, y)$ is given by

$$\begin{aligned}\phi(x,y) &= A_0\frac{\cosh k_0(h-y)}{\cosh k_0 h}e^{ik_0x} + B_0\frac{\cosh k_0(h-y)}{\cosh k_0 h}e^{-ik_0x} \\ &+ \begin{cases} \sum_{n=1}^\infty C_n e^{-k_n x}\frac{\cos k_n(h-y)}{\cos k_n h} & x > 0, \\ \sum_{n=1}^\infty D_n e^{k_n x}\frac{\cos k_n(h-y)}{\cos k_n h} & x < 0, \end{cases}\end{aligned} \tag{2.1.21}$$

where A_0, B_0, C_n and D_n are unknowns.

(B) Water With An Ice-Cover

Here we derive the basic equations in the theory of water waves when the water surface is covered by a thin sheet of ice of thickness h_i and density ρ_i. The ice sheet can be modelled as a thin elastic plate with Young's modulus E and Poisson ratio ν.

We choose a rectangular cartesian coordinate system when y axis is directed vertically downwards into the water region so that water occupies the region $y \geq 0$. The x axis is along the thin ice cover at rest.

We assume the motion to start from rest so that it is irrotational and can be described by a velocity potential $\Phi(x, y, z, t)$.

The equation of continuity gives

$$\nabla^2 \Phi = 0 \tag{2.1.22}$$

in the fluid region.
The linearised Bernoulli's equation gives

$$\frac{\partial \phi}{\partial t} = gy - \frac{p}{\rho}, \tag{2.1.23}$$

where p, ρ are the pressure and density of water and g is the acceleration due to gravity. Let us consider the depression of the ice covered surface below the horizontal level as $y = \zeta(x, z, t)$.
Then Newton's equation of motion gives (cf. Fox and Squire (1994))

$$m\frac{\partial^2 \zeta}{\partial t^2} = mg + \Pi - p - L\nabla^4_{x,z}\zeta \qquad \text{on } y = \zeta. \tag{2.1.24}$$

Here $m = \rho\delta = h_i\rho_i$, Π is the atmospheric pressure, $L = \frac{Eh_i^3}{12(1-\nu^2)}$ and δ is a constant having dimension of length.
Using (2.1.23) in (2.1.24) we get after simplification

$$m\frac{\partial^2 \zeta}{\partial t^2} = mg + \Pi - \rho(g\zeta - \frac{\partial \Phi}{\partial t}) - L\nabla^4_{x,z}\zeta \qquad \text{on } y = 0. \tag{2.1.25}$$

Also the kinematic condition gives

$$\frac{\partial \zeta}{\partial t} = \frac{\partial \Phi}{\partial y} \qquad \text{on } \; y = 0. \tag{2.1.26}$$

Eliminating ζ between (2.1.25) and (2.1.26), we obtain

$$\frac{\partial^2}{\partial t^2}[\Phi - \delta\Phi_y] = g[1 + D\nabla^4_{x,z}]\Phi_y \quad \text{on } y = 0, \tag{2.1.27}$$

where $D = \frac{L}{\rho g}$.
The bottom condition for Φ is

$$\nabla\Phi \to 0 \quad \text{as } y \to \infty, \tag{2.1.28}$$

for deep water and

$$\frac{\partial\Phi}{\partial y} = 0 \quad \text{on } \ y = h, \tag{2.1.29}$$

where the water region is of uniform finite depth h.
Now let us consider two dimensional time harmonic motion with angular frequency σ so that $\Phi = Re\{\phi(x,y)e^{-i\sigma t}\}$.
Then ϕ satisfies

$$\nabla^2\phi = 0 \quad \text{in } \ y > 0. \tag{2.1.30}$$

The ice cover condition (2.1.27) becomes

$$K\phi + (1 - \delta K + D\partial^4_{xxxx})\phi_y = 0 \quad \text{on } y = 0. \tag{2.1.31}$$

The bottom condition becomes

$$\nabla\phi \to 0 \quad \text{as } \ y \to \infty, \ \text{ for deep water} \tag{2.1.32}$$

and

$$\frac{\partial\phi}{\partial y} = 0 \quad \text{on } \ y = h, \ \text{ for the water with uniform finite depth } \ h. \tag{2.1.33}$$

Thus equations(2.1.30)-(2.1.33) give the basic equations when the water surface is covered with ice.

The method of separation of variables, the progressive wave solutions and the local solutions of Laplace's equation with the ice cover condition for two dimensional harmonic motion in deep water are $e^{-\lambda_0 y \pm i\lambda_0 x}$, $e^{-\lambda_1 y \pm i\lambda_1 x}$, $e^{-\bar{\lambda}_1 y \pm i\bar{\lambda}_1 x}$ and $\{(Dk^4 + 1 - \delta k)k\cos ky - K\sin ky\}\, e^{-k|x|}$, where λ_0 is the unique real positive root of the equation

$$Dk^4 + (1 - \delta K)k - K = 0. \tag{2.1.34}$$

The other two pairs of complex conjugate zeros of (2.1.34) are $(\lambda_1, \bar{\lambda}_1)$ and $(\lambda_2, \bar{\lambda}_2)$ with Re $\lambda_1 > 0$, Im $\lambda_1 > 0$, Re $\lambda_2 < 0$ and Im $\lambda_2 > 0$ (cf. Chakrabarti et. al. (2003)). Hence for the irrotational motion in water with ice cover, Havelock's expansion for wave potential $\phi(x, y)$ is given as

$$\begin{aligned}\phi(x,y) &= P_1 e^{-\lambda_0 y + i\lambda_0 x} + P_2 e^{-\lambda_0 y - i\lambda_0 x} \\ &+ \begin{cases} P_3 e^{-\lambda_1 y + i\lambda_1 x} + P_4 e^{-\bar{\lambda}_1 y - i\bar{\lambda}_1 x} & \\ + \int_0^\infty Q(\xi)\,\{\xi(D\xi^4 + 1 - \delta K)\cos\xi y - K\sin\xi y\}\, e^{-\xi x} d\xi & x > 0, \\ P_5 e^{-\lambda_1 y - i\lambda_1 x} + P_6 e^{-\bar{\lambda}_1 y + i\bar{\lambda}_1 x} & \\ \int_0^\infty R(\xi)\{\xi(D\xi^4 + 1 - \delta K)\cos\xi y - K\sin\xi y\} e^{\xi x} d\xi & x < 0. \end{cases}\end{aligned} \tag{2.1.35}$$

Here $P_1, P_2, ..., P_6$ are the unknown constants and $Q(\xi), R(\xi)$ are functions of ξ. Again for water of uniform finite depth h, the method of separation of variables of Laplace's equation for two dimensional motion produces the progressive and local solutions, satisfying the ice cover condition and bottom condition given by (2.1.31) and (2.1.33) respectively as $\frac{\cosh\mu_0(h-y)}{\cosh\mu_0 h} e^{\pm i\mu_0 x}$, $\frac{\cosh\mu_1(h-y)}{\cosh\mu_1 h} e^{\pm i\mu_1 x}$, $\frac{\cosh\bar{\mu}_1(h-y)}{\cosh\bar{\mu}_1 h} e^{\pm i\bar{\mu}_1 x}$ and $\frac{\cos\mu_n(h-y)}{\cos\mu_n h} e^{\pm\mu_n x}$, where μ_0 is the unique positive real root of the equation

$$k(Dk^4 + 1 - \delta K)\sinh kh - K\cosh kh = 0, \tag{2.1.36}$$

and $\pm\mu_1$ and $\pm\bar{\mu}_1$ with Reμ_1 <Imμ_1, Re$\mu_1 > 0$ and Im$\mu_1 > 0$ are its four complex conjugate roots and $\pm i\mu_n$ are infinite number of purely imaginary zeros ($\mu_n > 0$ and real, n=1,2,....) of (2.1.36) with $h\mu_n \to n\pi$ as $n \to \infty$ (Chung and Fox (2002)).

Hence the Havelock's expansion of $\phi(x,y)$ for finite depth h of water is given by

$$\phi(x,y) = G_1 \frac{\cosh\mu_0(h-y)}{\cosh\mu_0 h} e^{i\mu_0 x} + G_2 \frac{\cosh\mu_0(h-y)}{\cosh\mu_0 h} e^{-i\mu_0 x}$$

$$+ \begin{cases} G_3 \frac{\cosh\mu_1(h-y)}{\cosh\mu_1 h} e^{i\mu_1 x} + G_4 \frac{\cosh\bar{\mu}_1(h-y)}{\cosh\bar{\mu}_1 h} e^{-i\bar{\mu}_1 x} + \sum_{n=1}^{\infty} S_n \frac{\cos\mu_n(h-y)}{\cos\mu_n h} e^{-\mu_n x} \\ \qquad\qquad\qquad\qquad\qquad\qquad\qquad\qquad x > 0, \\ G_5 \frac{\cosh\mu_1(h-y)}{\cosh\mu_1 h} e^{-i\mu_1 x} + G_6 \frac{\cosh\bar{\mu}_1(h-y)}{\cosh\bar{\mu}_1 h} e^{i\bar{\mu}_1 x} + \sum_{n=1}^{\infty} T_n \frac{\cos\mu_n(h-y)}{\cos\mu_n h} e^{\mu_n x} \\ \qquad\qquad\qquad\qquad\qquad\qquad\qquad\qquad x < 0, \end{cases} \tag{2.1.37}$$

where $G_1, G_2, ..., G_6, S_n$ and T_n are constants.

Havelock's expansion theorem

Let $f(x)$ be a function defined in $(0,\infty)$ which satisfies Dirichlet's conditions. Then Havelock's expansion for $f(x)$ in $(0,\infty)$ is given by

$$f(x) = Ae^{-Kx} + \int_0^{\infty} g(y)\,(y\cos xy - K\sin xy)\,dy, \tag{2.1.38}$$

where K is a non negative parameter,

$$A = 2K \int_0^{\infty} f(x)e^{-Kx}dx, \tag{2.1.39}$$

and

$$g(y) = \frac{2}{\pi}\frac{1}{y^2+K^2} \int_0^{\infty} f(x)(y\cos xy - K\sin xy)dx. \tag{2.1.40}$$

The expansion (2.1.38) combined with the relations (2.1.39) and (2.1.40) is known as Havelock's expansion theorem in the water wave theorem which is often regarded as a hybrid integral transform. This is in fact a generalisation of Fourier cosine transform. This is clear if we put K=0 in these relations.

If a function is defined in a finite interval $(0, h)$ and satisfies Dirichlet's conditions then Havelock's expansion for $f(x)$ in $(0, h)$ is given by

$$f(y) = A_0 \cosh k_0(h-y) + \sum_{n=1}^{\infty} A_n \cos k_n(h-y) \tag{2.1.41}$$

where $\pm k_0, \ \pm ik_n$ are roots of the equation (2.1.18) and

$$A_0 = \frac{4ik_0}{2k_0h + \sinh 2k_0h} \int_0^h f(t) \cosh k_0(h-t), \tag{2.1.42}$$

$$A_n = \frac{4k_n}{2k_0h + \sin 2k_nh} \int_0^h f(t) \cos k_n(h-t). \tag{2.1.43}$$

This hybrid transform was first used by Havelock in 1929 in connection with a plane vertical wave maker problem. There is a detail description of this Havelock expansion theorem in Mandal and Chakrabarti (2000).

2 Two Dimensional Source Potential

Velocity potentials due to the presence of different types of singularities in an incompressible inviscid fluid, assuming irrotational motion of small amplitude play a significant role in the study of the problem of scattering or radiation of waves due to the presence of obstacles in fluid medium. When a body or a number of bodies present in fluid undergoes some oscillations, the resulting motion in fluid can be described by a series of singularities placed on the bodies. These singularities are characterised by their giving rise to velocity potentials which are typical singular solutions of Laplace's equation in the neighbourhood of singularities.

For two dimensional problems these singularities are logarithmic type or multipole type and for three dimensional problems these are point source or point multipoles.

In the present section we shall consider only the logarithmic singularity.

(A) Line Source Submerged In Ocean With A Free Surface

We consider two dimensional time harmonic irrotational motion in an incompressible , inviscid fluid due to presence of a line source at (ξ, η). If $Re\{G(x, y; \xi, \eta)\ e^{-i\sigma t}\}$ is the velocity potential then G satisfies

$$\nabla^2 G = 0 \qquad \text{except at } (\xi, \eta), \tag{2.2.1}$$

$$KG + G_y = 0 \qquad \text{on} \quad y = 0, \tag{2.2.2}$$

$$G \sim \ln \rho \qquad \text{as} \quad \rho \to 0, \tag{2.2.3}$$

$$\rho = \{(x-\xi)^2 + (y-\eta)^2\}^{\frac{1}{2}}, \tag{2.2.4}$$

$$\nabla G \to 0 \quad \text{as } y \to \infty \text{ for deep water}, \tag{2.2.5}$$

$$G_y = 0 \quad \text{on } y = h \quad \text{for finite depth } h, \tag{2.2.6}$$

G behaves as outgoing waves as $|x - \xi| \to \infty$.
The expression for $G(x, y; \xi, \eta)$ for deep water and for water region of finite depth are given below.

(a) Deep Water

$$G(x, y; \xi, \eta) = -2\pi i e^{-K(y+\eta)+iK|x-\xi|} - 2\int_0^\infty \frac{e^{-k|x-\xi|}}{k(k^2+K^2)} L(k, y) L(k, \eta) dk, \tag{2.2.7}$$

where

$$L(k, t) = k \cos kt - K \sin kt \quad \text{for deep water.} \tag{2.2.8}$$

(b) Water region of finite depth

The solution for G satisfying conditions (2.2.1) to 2.2.4) and (2.2.6) is given by

$$G(x,y;\xi,\eta) = -4\pi i\frac{\cosh k_0(h-\eta)\cosh k_0(h-y)}{2k_0h+\sinh 2k_0h}e^{ik_0|x-\xi|}$$
$$-4\pi\sum_{n=1}^{\infty}\frac{\cos k_n(h-\eta)\cos k_n(h-y)}{2k_nh+\sin 2k_nh}e^{-k_n|x-\xi|}, \qquad (2.2.9)$$

where $\pm k_0$ and $\pm ik_n$ $(n$=1,2,....) are the roots of

$$k\tanh kh = K.$$

The detailed derivation of (2.2.7) and (2.2.9) can be found in Thorne (1953), Mandal (1987) and Mandal and Chakrabarti (2000).

(B) Line Source Submerged In Ocean With Ice Cover

Assuming linear theory and irrotational motion, let $Re\{\phi(x,y)\ e^{-i\sigma t}\}$ denotes velocity potential describing two dimensional irrotational motion due to presence of a line source at (ξ,η) in ocean with ice cover. Here $\phi(x,y)$ satisfies

$$\nabla^2\phi = 0 \qquad \text{except at } (\xi,\eta),$$

the linearised ice cover condition

$$K\phi + (D\partial^4_{xxxx} - \delta K + 1)\phi_y = 0 \quad \text{on } y = 0. \qquad (2.2.10)$$

Here $D = \frac{Eh_0^3}{12(1-\nu^2)\rho g}$, $K = \frac{\sigma^2}{g}$, g being the gravity, $\delta = \frac{\rho_i}{\rho}h_i$, E being the Young's modulus, ν being Poisson ratio of the material of ice cover, ρ being the density of water, ρ_i is the density of ice and h_i is the thickness of ice cover.

$$\phi \sim \ln\rho \qquad \text{as} \quad \rho \to 0, \qquad (2.2.11)$$

$$\rho = \{(x-\xi)^2 + (y-\eta)^2\}^{\frac{1}{2}}, \qquad (2.2.12)$$

$$\nabla\phi \to 0 \quad \text{as} \quad y \to \infty \quad \text{for deep water,} \tag{2.2.13}$$

$$\phi_y = 0 \quad \text{on } y = h \quad \text{for finite depth } h. \tag{2.2.14}$$

Here ϕ behaves as outgoing waves as $|x-\xi| \to \infty$.

Source potential due to a logarithmic singularity in water with ice cover surface for deep water is given as

$$\phi(x,y) = -2\int_0^\infty \frac{\{k(1-\delta K+Dk^4)\cosh ky_< - K\sinh ky_<\}}{k\{k(1-\delta K+Dk^4)-K\}} e^{-ky_>}\cos k(x-\xi)dk, \tag{2.2.15}$$

where $y_<$ and $y_>$ respectively denote the lesser and greater of y and η.
Alternately

$$\begin{aligned}\phi(x,y) = -2\int_0^\infty \frac{L(k,y)L(k,\eta)}{k\{k^2(1-\delta K+Dk^4)+K^2\}} e^{-k|x-\xi|}dk \\ -2\pi i \frac{1}{\lambda(1-\delta K+5DK^4\lambda^4)} e^{-K\lambda(y+\eta)+iK\lambda|x-\xi|} \\ -2\pi i\Big[\frac{1}{\lambda_1(1-\delta K+5DK^4\lambda_1^4)} e^{-K\lambda_1(y+\eta)+iK\lambda_1|x-\xi|} \\ -\frac{1}{\bar\lambda_1(1-\delta K+5DK^4\bar\lambda_1^4)} e^{-K\bar\lambda_1(y+\eta)-iK\bar\lambda_1|x-\xi|}\Big],\end{aligned} \tag{2.2.16}$$

where $L(k,y) = k(1-\delta K+Dk^4)\cos ky - K\sin ky$, real positive root $K\lambda$ and two pairs of complex conjugate zeros $K\lambda_1$, $K\bar\lambda_1$ and $K\lambda_2$, $K\bar\lambda_2$ with $\mathrm{Re}\lambda_1 > 0$, $\mathrm{Re}\lambda_2 < 0$, $\mathrm{Im}(\lambda_1,\lambda_2) > 0$ are the roots of the equation

$$\Delta(k) = (1-\delta K+Dk^4)k - K = 0. \tag{2.2.17}$$

Source potential for finite depth water with ice cover surface is given as

$$\phi(x,y) = -2\int_0^\infty \frac{\{k(1-\delta K+Dk^4)\cosh ky_< - K\sinh ky_<\}}{k\Delta_0(k)} \cosh k(h-y_>)\cos k(x-\xi)dk, \tag{2.2.18}$$

alternately

$$\phi(x,y) = -4\pi \sum_{n=1}^{\infty} f(\alpha_n;y,\eta)e^{-K\alpha_n|x-\xi|} - 4\pi i g(\mu;y,\eta)e^{iK\mu|x-\xi|}$$
$$-4\pi i g(\mu_1;y,\eta)e^{iK\mu_1|x-\xi|} + 4\pi i g(\bar{\mu}_1;y,\eta)e^{-iK\bar{\mu}_1|x-\xi|}, \tag{2.2.19}$$

where

$$f(\alpha;y,\eta) = \frac{(1-\delta K+DK^4\alpha^4)\cos K\alpha(h-\eta)\cos K\alpha(h-y)}{2K\alpha h(1-\delta K+DK^4\alpha^4)+(1-\delta K+5DK^4\alpha^4)\sin 2K\alpha h}, \tag{2.2.20}$$

$$g(\alpha;y,\eta) = if(i\alpha;y,\eta), \tag{2.2.21}$$

two real roots $\pm K\mu(\mu > 0)$, two pairs of complex conjugate zeros $K\mu_1$, $K\bar{\mu}_1$ and $-K\mu_1$, $-K\bar{\mu}_1$ with $\mathrm{Re}\mu_1 < \mathrm{Im}\mu_1$, and an infinite number of purely imaginary zeros $\pm iK\alpha_n$ ($\alpha_n > 0$ and real, n=1,2,...) are the roots of the transcendental equation

$$\Delta_0(k) = k(1-\delta K+Dk^4)\sinh kh - K\cosh kh = 0. \tag{2.2.22}$$

A detailed discussion can be found in the thesis of Rupanwita Chowdhury (Gayen) (2004).

3 Integral Equations

Integral equations arise in a natural way in course of solving varieties of initial and boundary value problems involving both linear ordinary as well as linear partial differential equations. As a result many initial and boundary value problems of mathematical physics can be solved by reducing them into appropriate integral equations.

An equation for the unknown function $\phi(x)$ of a single real variable x, $a \le x \le b$ is said to be an integral equation if $\phi(x)$ appears under the sign of integration and the integral exists in some sense.

The integral equation in which the unknown function appears linearly is called a lin-

ear integral equation, otherwise it is a nonlinear integral equation. The general one dimensional linear integral equation for an unknown function $\varphi(x)$ is of the form

$$c\varphi(x) + \lambda \int_a^b K(x,t)\varphi(t)dt = f(x), \quad a \le x \le b. \tag{2.3.1}$$

Here c is either 0 or 1 and $K(x,t)$ is a known function which is known as the kernel of the integral equation. The other known function $f(x)$ is called the forcing term. The known constant λ is the parameter of the integral equation.

The integral equation, in which the forcing term $f(x)$ is equal to zero, is called homogeneous integral equation, where as for nonhomogeneous integral equation $f(x) \neq 0$.

The integral equation (2.3.1) in which $c = 0$ is called integral equation of first kind, i.e.

$$\int_a^b K(x,t)\varphi(t)dt = f(x), \quad a \le x \le b. \tag{2.3.2}$$

The integral equation (2.3.1) in which $c = 1$ is called integral equation of second kind.

If the limits of integration appearing in the integral equation (2.3.1) are constants, then the integral equation is known as Fredholm integral equation. If any one limit of integration is known function of x, the corresponding integral equation (2.3.1) is called Volterra integral equation.

If the kernel $K(x,t)$ of integral equation (2.3.1) is square integrable, then the kernel is known as regular kernel and the corresponding integral equation is known as regular integral equation. Otherwise it is a singular integral equation (cf. Estrada and Kanwal (2000), Mandal and Chakrabarty (2011)).

If the kernel $K(x,t)$ of integral equation (2.3.1) is of the form

$$K(x,t) = \frac{f(x,t)}{(x-t)^\alpha} \tag{2.3.3}$$

where $f(x,t)$ is bounded in $[a,b] \times [a,b]$ with $f(x,x) \neq 0$ and $0 < \alpha < 1$, then the integral equation (2.3.1) is known as weakly singular integral equation.

If in the integral equation (2.3.1),

$$K(x,t) = \frac{f(x,t)}{x-t}, \tag{2.3.4}$$

where $f(x,t)$ is a differentiable function of x and t with $f(x,x) \neq 0$, then the integral equation (2.3.1) is known as singular integral equation, where the integral is to be understood in the sense of Cauchy principal value as given by

$$\int_a^b K(x,t)\varphi(t)dt = \lim_{\epsilon\to 0+}\left[\int_a^{x-\epsilon} K(x,t)\varphi(t)dt + \int_{x+\epsilon}^b K(x,t)\varphi(t)dt\right]. \tag{2.3.5}$$

If the kernel $K(x,t)$ in the integral equation (2.3.1) is of the form

$$K(x,t) = \frac{f(x,t)}{(x-t)^2} \tag{2.3.6}$$

where $f(x,t)$ is a differentiable function with $f(x,x) \neq 0$, then the integral equation (2.3.1) is known as hypersingular integral equation. A hypersingular integral $\int_a^b \frac{\psi(t)}{(x-t)^2}dt, \quad a \leq x \leq b$ is understood in the sense of two sided HADAMARD FINITE PART integral of order 2 defined by

$$\int_a^b \frac{\psi(t)}{(x-t)^2}dt = \lim_{\epsilon\to 0+}\left[\int_a^{x-\epsilon} \frac{\psi(t)}{(x-t)^2}dt + \int_{x+\epsilon}^b \frac{\psi(t)}{(x-t)^2}dt - \frac{\psi(x+\epsilon)+\psi(x-\epsilon)}{\epsilon}\right]. \tag{2.3.7}$$

4 Galerkin Method

One of the most important weighted residual method is Galerkin approximation method. To describe the method, we need some idea regarding the inner product.

Definition : In a vector space V of real valued functions whose domain is an closed interval $A = [a,b]$, an inner product of two real functions $f(x)$ and $g(x)$ is defied as

$$\big\langle f(x), g(x)\big\rangle = \int_a^b f(x)g(x)dx. \tag{2.4.1}$$

Galerkin approximation : Let us consider an operator equation as

$$(Ly)(x) = f(x), \quad x \in A \tag{2.4.2}$$

where L is a linear operator in a certain inner product space S to itself, A is a domain in S and $f(x) \in S$ represents the forcing function.
In some problems of physical interest, it is desired to evaluate an inner product $\langle y, f \rangle$, where

$$\langle y, f \rangle = \int_{x \in A} y(x) f(x) dx. \tag{2.4.3}$$

A real valued function $y(x)$ is said to solve the operator equation (2.4.2) if and only if

$$\langle Ly, \lambda \rangle = \langle \lambda, Ly \rangle = \langle \lambda, f \rangle \quad \text{for all } \lambda \in S. \tag{2.4.4}$$

Now using (2.4.1) and (2.4.4) the function $y(x)$ can be evaluated at least approximately. Here we replace $y(x)$ by $F(x)$, where F is the approximate solution of equation (2.4.2), so that

$$\langle \lambda, LF \rangle = \langle \lambda, f \rangle \quad \text{for all } \lambda \in S \tag{2.4.5}$$

whenever the approximation relation as in equation (2.4.5) holds good, then we can consider F as the approximate solution of the operator equation (2.4.2). The determination of such approximate solutions of the equation (2.4.2) involving the function F in the form of a truncated series as given by

$$F(x) = \sum_{j=1}^{n} a_j \phi_j(x) \tag{2.4.6}$$

is known as Galerkin approximation method, $\{\phi_j\}_{j=1}^{n}$ (n is finite) being the set of basic functions.
Applying the linear operator L on both side of the equation (2.4.6) and taking inner product with $\lambda \in S$ on both sides and then using the approximate identity equation

(2.4.5) , we get

$$\sum_{j=1}^{n} a_j \big\langle L\phi_j(x), \lambda(x) \big\rangle \approx \big\langle f(x), \lambda(x) \big\rangle \quad \text{for } \lambda \in S. \tag{2.4.7}$$

Single-term Galerkin approximation :

If we take $n = 1$ in equation (2.4.7), and choose $\lambda(x) = \phi_1(x)$, then we get $a_1 = \frac{\langle f, \phi_1 \rangle}{\langle L\phi_1, \phi_1 \rangle}$ producing the approximate solution for $y(x)$ as

$$F(x) = a_1 \phi_1(x). \tag{2.4.8}$$

The approximate evaluation of the quantity $\langle y, f \rangle$ in (2.4.3), can be completed by using the approximate relation $\langle y, f \rangle \approx \langle F, f \rangle$, which takes up the value $a_1 \langle \phi_1, f \rangle$, if only the single-term Galerkin approximation is used.

Multi-term Galerkin approximation :

Let us choose $\lambda(x) = \phi_k(x)$ for some fixed positive integer k, such that $1 \leq k \leq n$, then we obtain from (2.4.7), that

$$\sum_{j=1}^{n} a_j \big\langle L\phi_j(x), \phi_k(x) \big\rangle = \big\langle f(x), \phi_k(x) \big\rangle, \quad k = 1, 2, ..., n. \tag{2.4.9}$$

Thus here we obtain exactly n linear equations for the determination of the n unknown constants and these constants can be easily determined by appropriate choice of the set of functions $\{\phi_j(x)\}_{j=1}^{n}$. The approximation of y by F, where F is given by the n-term truncated series (given in (2.4.6)), is termed as multi-term Galerkin approximations. Once the n constants $a_1, a_2, ..., a_n$ are determined by solving the linear system (2.4.7), $\langle y, f \rangle$, the quantity of our physical interest, is approximately evaluated as

$$\langle y, f \rangle \approx \sum_{j=1}^{n} a_j \langle \phi_j, f \rangle. \tag{2.4.10}$$

The inner product $\langle \phi_j, f \rangle$ is defined by an integral defined as in equation (2.4.3),and is evaluated by using appropriate numerical quadrature formula.

The choice of the basis functions $\{\phi_j\}_{j=1}^{n}$ are chosen suitably by keeping in mind the regarding boundary conditions of the physical problems.

A detailed dicussion is given by Mandal and Chakrabarty (2000). Also this method is employed by various researchers in the theory of water waves. Notable among them are Evans and Morris(1972 a, b), Porter and Evans (1995).

PART II

Solution of Integral Equations

Chapter 3

Boundary element approach of solving Fredholm and Volterra integral equations

1. Introduction

In the present chapter we applied boundary element method (BEM) to solve Fredholm and Volterra integral equations of second kind. As mentioned apriori, in this method the integral equation is reduced to a system of algebraic equation by discretizing the range of integration and the domain of definition of the integral equation into same number of intervals, assuming the unknown function to be constant in each small intervals. The unknown function is then evaluated on each line element by solving the system of linear algebraic equations.

To the best of our knowledge, this method has not been used in the literature to solve integral equation although Gray(1991), Guiggiani et al. (1992) developed an algorithm to study hypersingular boundary integral equation and evaluation of hypersingular integrals in the boundary element method in three-dimensional crack problems. The

† The content of this chapter is based on the paper " Boundary element approach of solving Fredholm and Volterra integral equations ", *Int. J. Mathematical Modelling and Numerical Optimisation*, 9(1) (2019) 1-11.

advantage of this method is that computationally it is very simple method as compared to other techniques like use of Bernstein polynomials, Galerkin method and quite accurate results are obtained.

2. Mathematical Formulation:

2.1 Solution of Fredholm integral equation:

Let us consider the following Fredholm integral equation of second kind

$$\phi(x) = f(x) + \lambda \int_a^b K(x,t)\phi(t)dt, a < x < b. \tag{3.1}$$

The function $f(x)$ and the constant λ are known while $\phi(x)$ is the unknown function to be determined by using boundary element method described below.

We divide the range of integration $[a,b]$ into n line elements where a_{j-1} and a_j are the end points of j^{th} line element, $j = 1,...n$. Thus the range of integration becomes $[a,b] = \bigcup_{j=1}^{n}[a_{j-1}, a_j]$ with $a_0 = a$ and $a_n = b$. Here we take

$$a_j = a_0 + jh,\ h = \frac{a_n - a_0}{n},\ j = 1,...n.$$

Consequently the integral equation (3.1) can be written as follows

$$\phi(x) = f(x) + \lambda \sum_{j=1}^{n} \int_{a_{j-1}}^{a_j} K(x,t)\phi(t)dt. \tag{3.2}$$

Now for t belonging to j^{th} line element joining the points a_{j-1} and a_j, we write $t = t_j$, so that

$$t_j = \eta a_j + (1-\eta)a_{j-1},\quad 0 \le \eta \le 1.$$

Hence equation (3.2) becomes

$$\phi(x) = f(x) + \lambda \sum_{j=1}^{n} \int_0^1 K(x, t_j)\phi(t_j)(a_j - a_{j-1})d\eta. \tag{3.3}$$

Now, for x belonging to the line element joining the points a_{i-1} and a_i, where $i = 1, ...n$ we write $x = x_i$, so that equation (3.3) becomes

$$\phi(x_i) = f(x_i) + \lambda \sum_{j=1}^{n} \int_0^1 K(x_i, t_j)\phi(t_j)(a_j - a_{j-1})d\eta, \ i = 1, ...n. \tag{3.4}$$

Assuming $\phi_j = \phi(x_j)$ as unknown constant in j^{th} line element [cf. Pozrikidis(2002)], equation (3.4) becomes

$$\phi_i = f_i + \lambda \sum_{j=1}^{n} k_{ij}\phi_j, \quad i = 1, ...n \tag{3.5}$$

where,

$$k_{ij} = \int_0^1 K(x_i, t_j)(a_j - a_{j-1})d\eta, \quad f(x_i) = f_i. \tag{3.6}$$

The equation (3.5) is a system of linear equation which can be written in alternate form as

$$\sum_{j=1}^{n} H^{ij}\phi_j = f_i, \qquad i = 1, ...n \tag{3.7}$$

where

$$H^{ij} = \delta_{ij} - \lambda k_{ij}. \tag{3.8}$$

We write

$$x_i = \zeta a_i + (1 - \zeta)a_{i-1}, \quad 0 \le \zeta \le 1.$$

so that for a particular value of ζ we get a value of x_i in $i^{th}, i = 1..n$ line element and thus solving (3.7) for a particular value of ζ, we get the unknown values of $\phi_i's$ for $x_i's$, on each line element. It may be noted here that for numerical computation we take $\zeta = 0.5$.

2.2 Solution of Volterra integral equation:

Here we consider Volterra integral equation of the second kind as follows

$$\phi(x) = f(x) + \lambda \int_a^x K(x,t)\phi(t)dt, \qquad x > a. \tag{3.9}$$

We shall apply Boundary Element Method (BEM) to solve (3.9) for $\phi(x)$ for different values of x. First we shall obtain $\phi(x)$ for $x = a_1$ where $a_1 = a_0 + h, a_0 = a$ and h is a small positive number chosen. In order to obtain $\phi(x)$ at $x = a_1$, we write

$$t_1 = \eta a_1 + (1-\eta)a_0, \ 0 \le \eta \le 1$$

where t_1 is a point on the line element joining a_0 and a_1. Consequently the integral equation (3.9) becomes

$$\phi(a_1) = f(a_1) + \lambda \int_0^1 K(a_1,t_1)\phi(t_1)(a_1-a_0)d\eta. \tag{3.10}$$

Here we assume that $\phi_1 = \phi(t_1)$ is a constant (unknown) for $t_1 \epsilon [a_0, a_1]$ (cf. Pozrikidis(2002)) so that equation (3.10) can be written as

$$\phi_1 = f(a_1) + \lambda\phi_1 \int_0^1 K(a_1,t_1)(a_1-a_0)d\eta \tag{3.11}$$

or alternately

$$(1-\lambda K_{11})\phi_1 = f_1, \tag{3.12}$$

where

$$K_{11} = \int_0^1 K(a_1,t_1)(a_1-a_0)d\eta, \quad f_1 = f(a_1). \tag{3.13}$$

Hence

$$\phi_1 = \frac{f_1}{1-\lambda K_{11}}. \tag{3.14}$$

Next to obtain $\phi(x)$ at $x = a_2$ where $a_i = a_0 + ih, i = 1, 2$ we proceed as follows. At

$x = a_2$, equation (3.9) becomes

$$\phi(a_2) = f(a_2) + \lambda \int_{a_0}^{a_1} K(a_2, t)\phi(t)dt + \lambda \int_{a_1}^{a_2} K(a_2, t)\phi(t)dt. \tag{3.15}$$

Writing $t_j = \eta a_j + (1-\eta)a_{j-1},\ j = 1, 2$ where t_j is a point on the line element joining points $[a_{j-1}, a_j]$ equation (3.15) becomes

$$\phi(a_2) = f_2 + \lambda \int_0^1 K(a_2, t_1)\phi(t_1)(a_1 - a_0)d\eta + \lambda \int_0^1 K(a_2, t_2)\phi(t_2)(a_2 - a_1)d\eta, \tag{3.16}$$

where $\phi_2 = \phi(t_2), \quad f_2 = f(a_2)$.
As before assuming that $\phi_j = \phi(t_j), j = 1, 2$ are constants (unknown) for $t_j \in [a_{j-1}, a_j]$, and noting that ϕ_1 satisfies equation (3.12), the equations (3.16) and (3.12) can be written as

$$(1 - \lambda K_{11})\phi_1 = f_1 \tag{3.17}$$

$$-\lambda K_{21}\phi_1 + (1 - \lambda K_{22})\phi_2 = f_2 \tag{3.18}$$

where

$$K_{2j} = \int_0^1 K(a_2, t_j)(a_j - a_{j-1})d\eta \tag{3.19}$$

and K_{11} is given by equation (3.13).

It may be noted that the matrix associated with the system of equations (3.17) and (3.18) is a lower triangular matrix. Hence solving equations (3.18) we obtain

$$\phi_2 = \frac{f_2 + \lambda K_{21}\phi_1}{1 - \lambda K_{22}}$$

where ϕ_1 is given by equation (3.14).

In a similar way to obtain $\phi(x)$ at $x = a_i$, we write

$$t_i = \eta a_i + (1 - \eta)a_{i-1}, \phi_i = \phi(t_i), \quad f_i = f(a_i). \tag{3.20}$$

Here t_i is the value of t in the i^{th} line element. We assume that ϕ_i is constant for $t_i \in [a_{i-1}, a_i]$ ([cf. Pozrikidis(2002)]).Hence from equation (3.9) we obtain the following system of linear equations.

$$\sum_{j=1}^{i} G_{ij}\phi_j = f_i, i = 1, 2, ...n. \tag{3.21}$$

where

$$G_{ij} = (\delta_{ij} - \lambda K_{ij}),\ j = 1, 2.....i, \quad i = 1, 2.....n.$$

is a lower triangular matrix. Thus solving the system of equation (3.21) we obtain

$$\phi_1 = \frac{f_1}{1 - \lambda K_{11}} \quad \phi_i = \frac{f_i + \lambda \sum_{j=1}^{i-1} K_{ij}\phi_j}{1 - \lambda K_{ii}},\ i = 2, ..n. \tag{3.22}$$

3. Examples:

To illustrate the method of solution of integral equation by BEM we consider the following five examples.

Example 1:

First we a second kind Fredholm integral equation

$$\phi(x) = \frac{11x}{6} + \frac{1}{4}\int_0^1 xt\phi(t)dt, 0 < x < 1. \tag{3.23}$$

Here $\phi(x) = 2x$ is the exact solution.
Following the procedure discussed in section 2.1 we discretize the domain of the integral equation in to 40 line segments and the values of the unknown functions, $\phi(x)$ is obtained for $x_i = a_i\zeta + (1 - \zeta)a_{i-1}, i = 1, ..., 40, \quad \zeta = 0.5$. Some representative values of $\phi(x)$ are given in Table 3.1. It is observed from the Table 3.1 that the relative error in each case is 1.4×10^{-5}. This shows that the error in the approximate value of $\phi(x)$

with respect to its exact value is same for all values of x.

Table 3.1: Comparative study of the exact result and present result.

values of x	**Solution**		**Error**	
	ϕ_{exact}	ϕ_{approx}	Absolute error	Relative error
0.0125	0.025000	0.025000	0.000000	0.000014
0.1875	0.375000	0.374995	0.000005	0.000014
0.3875	0.775000	0.774989	0.000011	0.000014
0.5875	1.175000	1.174983	0.000017	0.000014
0.7875	1.575000	1.574978	0.000022	0.000014
0.9875	1.975000	1.974972	0.000028	0.000014

Example 2:

We consider a second kind Fredholm integral equation

$$\phi(x) = 1 + \int_{-1}^{1} (xt + x^2t^2)\phi(t)dt - 1 < x < 1. \tag{3.24}$$

Here $\phi(x) = 1 + \frac{10}{9}x^2$ is the exact solution.
Following the procedure discussed in section 2.1 we discretize the domain of the integral equation in to 40 line segments and the values of the unknown functions, $\phi(x)$ is obtained for $x_i = a_i\zeta + (1-\zeta)a_{i-1}, i = 1, ..., 40, \quad \zeta = 0.5$. The results are given in Table 3.2. It may be noted here that the values of $\phi(x)$ are symmetric and some represented values of $\phi(x)$ are presented in Table 3.2. It is observed that for 40 line elements the relative error in $\phi(x)$ for small values of x is very small and increases as x increases. For values of x near ±1, the relative error is of order 10^{-4} and for small values of x, the relative error is of order 10^{-5} or 10^{-4}. We may mention here that this example was illustrated in Mandal and Bhattacharyya (2007) by the method based on approximating the unknown function by Bernstein polynomials and the absolute/relative error is of order 10^{-5}. However, computationally the method used in the present paper is simpler than the method used in Mandal and Bhattacharyya (2007).

Table 3.2: Comparative study of the exact result and present result.

values of x	**Solution**		**Error**	
	ϕ_{exact}	ϕ_{approx}	Absolute error	Relative error
±0.025	1.000694	1.000694	0.000000	0.000000
±0.175	1.034028	1.033988	0.000039	0.000038
±0.375	1.156250	1.156250	0.000180	0.000156
±0.575	1.367361	1.366937	0.000424	0.000310
±0.775	1.667361	1.666590	0.000771	0.000463
±0.975	2.056250	2.055029	0.001221	0.000594

Example 3:

We consider a second kind Fredholm integral equation

$$\phi(x) = 1 + \int_0^1 k(x,t)\phi(t)dt 0 < x < 1 \tag{3.25}$$

where

$$k(x,t) = t(1-x), \quad t \le x$$

$$= x(1-t), \quad t > x.$$

Here $\phi(x) = \sin x / \sin 1$ is the exact solution.

Following the procedure discussed in section 2.1 we discretize the domain of the integral equation in to 40 line segments and the values of the unknown functions, $\phi(x)$ is obtained for $x_i = a_i\zeta + (1-\zeta)a_{i-1}, i = 1, ..., 40, \quad \zeta = 0.5$. It may be noted here that the function H^{ij} in equation (3.8) is given by

$$H^{ij} = -\int_0^1 K_1(x_i, t_j)(a_j - a_{j-1})d\eta, \quad j < i,$$

$$H^{ij} = 1 - \int_0^1 K_1(x_i, t_{i1})(x_i - a_{i-1})d\eta - \int_0^1 K_2(x_i, t_{i2})(a_i - x_i)d\eta, \quad i = j,$$

$$H^{ij} = -\int_0^1 K_2(x_i, t_j)(a_j - a_{j-1})d\eta, \quad j > i,$$

where

$$k(x,t) = K_1(x,t) = t(1-x), \quad t \le x,$$

$$k(x,t) = K_2(x,t) = t(1-x), \quad t > x,$$

and $a_{i-1} \le t_{i1} \le x_i, \;\; x_i \le t_{i2} \le a_i$. The results are presented in Table 3.3. It is observed that for 40 line elements the relative error in $\phi(x)$ is of order 10^{-6}.

Table 3.3: Comparative study of the exact result and present result.

values of x	**Solution**		**Error**	
	ϕ_{exact}	ϕ_{approx}	Absolute error	Relative error
0.0375	0.044554	0.044554	0.0000000000	0.0000000000
0.1375	0.162890	0.162889	7.45×10^{-7}	4.57×10^{-6}
0.2375	0.279598	0.279597	1.23×10^{-6}	4.41×10^{-6}
0.3375	0.393512	0.393511	1.63×10^{-6}	4.15×10^{-6}
0.4375	0.503495	0.503493	1.92×10^{-6}	3.81×10^{-6}
0.5375	0.608447	0.608444	2.05×10^{-6}	3.37×10^{-6}
0.6375	0.707319	0.707317	2.01×10^{-6}	2.84×10^{-6}
0.7375	0.799124	0.799122	1.76×10^{-6}	2.20×10^{-6}
0.8375	0.882944	0.882943	1.28×10^{-6}	1.46×10^{-6}
0.9375	0.957943	0.957942	5.73×10^{-7}	5.9×10^{-7}

Example 4:

We consider the Volterra integral equation of the second kind given by,

$$\phi(x) = (1+x) + \int_0^x (x-t)\phi(t)dt, x > 0. \tag{3.26}$$

Here $\phi(x) = e^x$ is the exact solution. Following the procedure discussed in section 2.2

we discretize the domain of the integral equation in to 40 line segments and the values of the unknown functions, $\phi(x)$ is obtained for $x_i = a_i\zeta + (1-\zeta)a_{i-1}, i = 1, ..., 40, \;\; \zeta = 0.5$. Some representative values of $\phi(x)$ are given in Table 3.4 . For values of x near zero relative error is very small. But for $x \ge 0.2$. the relative error is of order 10^{-4}.

Table 3.4: Comparative study of the exact result and present result.

values of x	**Solution**		**Error**	
	ϕ_{exact}	ϕ_{approx}	Absolute error	Relative error
0.0125	1.012578	1.012579	0.000001	0.000001
0.0500	1.051271	1.051280	0.000009	0.000008
0.1000	1.105171	1.105205	0.000034	0.000030
0.1500	1.161834	1.161911	0.000076	0.000066
0.2000	1.221403	1.221540	0.000138	0.000113
0.2500	1.284025	1.284244	0.000218	0.000170
0.3000	1.349859	1.350178	0.000319	0.000237
0.3500	1.419068	1.419510	0.000443	0.000312
0.4000	1.491825	1.492414	0.000589	0.000395
0.4500	1.568312	1.569074	0.000761	0.000485
0.5000	1.648721	1.649680	0.000959	0.000582

Example 5:

We consider the Volterra integral equation of the second kind given by,

$$\phi(x) = (1 + xe^x) - \int_0^x t\phi(t)dt, x > 0. \tag{3.27}$$

Here $\phi(x) = e^x$ is the exact solution.

Following the procedure discussed in section 2.2 we discretize the domain of the integral equation in to 40 line segments and the values of the unknown functions, $\phi(x)$ is obtained for $x_i = a_i\zeta + (1-\zeta)a_{i-1}, i = 1, ..., 40, \quad \zeta = 0.5$. Some representative values of $\phi(x)$ are given in Table 3.5 . For values of x near zero relative error is very small. But for $x \geq 0.2$, the relative error is of order 10^{-4}.

3. Discussion and Conclusion:

Table 3.5: Comparative study of the exact result and present result.

values of x	**Solution**		**Error**	
	ϕ_{exact}	ϕ_{approx}	Absolute error	Relative error
0.0125	1.012578	1.012578	0.000000	0.000000
0.0500	1.051271	1.051264	0.000008	0.000009
0.1000	1.105171	1.105139	0.000032	0.000030
0.1500	1.161834	1.161759	0.000075	0.000065
0.2000	1.221403	1.221264	0.000139	0.000114
0.2500	1.284025	1.283801	0.000224	0.000175
0.3000	1.349859	1.349526	0.000333	0.000247
0.3500	1.419068	1.418601	0.000466	0.000329
0.4000	1.491825	1.491199	0.000626	0.000419
0.4500	1.568312	1.567500	0.000813	0.000518
0.5000	1.648721	1.647693	0.001028	0.000624

A simple numerical technique, namely boundary element method is employed here to solve Fredholm and Volterra integral equations of second kind. For Both types of integral equation, the discretization of range of integration in to line elements yields a system of linear equations. For Volterra integral equation, the matrix associated with the system of linear equations is a lower triangular matrix from which it is very simple to obtain the solution. For Fredholm integral equation, the matrix associated with the system of linear equations is a normal dense matrix whose inversion can be obtained by standard procedure. It is observed from the Tables 3.1, 3.2 and 3.3 that dividing the range of integration of Fredholm integral equation into 40 line elements, quite good accuracy in the results are obtained. From Tables 3.4 and 3.5, it is observed that for Volterra integral equation very accurate results are obtained for values of x near zero. The advantages of this method is that, this is very simple, time saving, accurate and efficient numerical technique as compared to other numerical techniques.

Chapter 4

Line element method of solving singular integral equations

1. Introduction

In the present chapter we have applied *boundary element method* described in chapter 3, to solve integral equations i) of first kind with weakly singular kernel, viz, Abel integral equation and integral equation with log kernel, ii) of first and second kind with hypersingular kernel.

Boundary value problems arising in Mathematical physics, particularly in solid mechanics and theory of water waves can be reduced to singular integral equation like Abel integral equations, integral equations with log kernel and hypersingular integral equation.The most general form of Abel Integral Equation of first kind is given by Mandal and Chakrabarti (2011).

$$\int_a^x \frac{K(x,t)\phi(t)}{(h(x)-h(t))^{\alpha}}dt = f(x), a < x < b, \tag{4.1}$$

where $f(a) = 0,\ 0 < \alpha < 1,$ K(x,t) is a continuous function, $K(x,x) \neq 0$ and $h(x)$ is strictly monotone increasing and differentiable function of x on $[a,b]$ and $h'(x) \neq 0$

† The content of this chapter is based on the paper " Line element method of solving singular integral equations ", *Indian journal of pure and applied mathematics*, 53(2), (2022), 528-541.

in $[a, b]$. It may be noted here that Abel integral equations are often referred to as Volterra integral equation.
A simple form of integral equation with log kernel is given by

$$\int_0^1 \phi(t) \ln\left|\frac{t-x}{t+x}\right| dt = f(x), \ 0 < x < 1 \tag{4.2}$$

where, $f(x)$ is a known function and

$$\phi(t) \sim O(|t-1|^{-\frac{1}{2}}) \ as \ t \to 1. \tag{4.3}$$

The integral equation (4.2) arises in the problem of scattering of water waves by a thin vertical barrier present in deep water [cf. Mandal and Chakrabarti (2000), Banerjea and Dutta (2008)]. The condition (4.3) satisfied by the unknown function $\phi(t)$ arises from the physics of the problem. This condition is necessary for the uniqueness of the solution [cf. Mandal and Chakrabarti (2000)].

Hypersingular integral equations serve as an important tool in solving a large class of mixed boundary value problems arising in mathematical physics[cf. Kaya and Erdogom (1987), Chan et. al. (2003)]. The simplest form of hypersingular integral equation is given by

$$\int_{-1}^{1} \frac{\phi(t)}{(t-x)^2} \, dt = f(x), \quad -1 \leq x \leq 1 \tag{4.4}$$

with

$$\phi(t) \sim O(|1-t^2|^{\frac{1}{2}}) \quad \text{as} \ \ |t| \to 1. \tag{4.5}$$

so that $\phi(\pm 1) = 0$. Here the integral in equation (4.4) is defined in the sense of Hadamard finite part integral.

The analytical solutions of integral equation(4.1) with $K(x,t) = 1$ and integral equation (4.2) and (4.4) are well known [cf. Mandal and Chakrabarti (2011)]. However if the kernel of the integral equation involves singularity with complicated form, the exact solution may not be easy to obtain in which case numerical methods are

helpful. Moreover, the integral equations (4.1) and (4.2) involve weakly singular kernel while the kernel of the integral equation (4.4) involves strong singularity. It is alredy mentioned in Chapter 1 that the integrals with weak singularity are amenable to the numerical techniques as the integrals can be defined in ordinary Riemann sense. However the integrals with strong singularity has to be defined in a special manner and for that reason the numerical evaluation of integrals with strong singularity needs special attention. In this chapter we shall adopt a very simple method viz Line Element Method to solve the integral equations (4.1), (4.2) and (4.4) as described in chapter 3. The line element method (LEM) used here is based on boundary element method. The application of line element method (LEM) in solving integral equations was initiated by Banerjea et. al. (2019) . They illustrated with examples, the application of LEM to obtain the solutions of Fredholm and Volterra integral equations of second kind as described in chapter 3. In their work, the convergence analysis of the method was not discussed. They applied LEM to reduce the integral equations to a system of linear algebraic equations. In the present approach, following Banerjea et. al. (2019), we applied line element method to find numerical solutions of integral equations with weakly singular kernel and hypersingular kernel. The error analysis of the line element method is discussed here.

2. Method of solution:

2.1 Solution of the Abel integral equation:

Most general form of Abel integral equation is given by equation (4.1). To find the unknown function $\phi(x)$ satisfying the integral equation (4.1) for different x in the region of definition, we shall apply here Line Element Method(LEM). We first consider the small line element joining the points a_0 and a_1 where $a_0 = a$ and $a_1 = a_0 + \gamma$, where γ is a very small positive number. If t_1 is a point on this line element, then t_1 can be written as

$$t_1 = \eta a_1 + (1 - \eta)a_0, \quad 0 \leq \eta \leq 1.$$

Consequently equation (4.1) becomes

$$\int_0^1 \frac{\gamma\ K(a_1,t_1)\ \phi(t_1)}{(h(a_1)-h(t_1))^\alpha} d\eta = f(a_1). \tag{4.6}$$

According to LEM discussed in Chapter 3 [cf. Pozrikidis (2002)], we consider the function $\phi(t)$ as constant throughout the very small line element joining the points a_0 and a_1 and write $\phi_1 = \phi(t_1)$. Then equation (4.6) reduces to

$$\phi_1 \int_0^1 \frac{\gamma\ K(a_1,t_1)}{(h(a_1)-h(t_1))^\alpha} d\eta. = f(a_1). \tag{4.7}$$

Alternately we can write as,

$$H_{11}\ \phi_1 = f_1, \tag{4.8}$$

where

$$H_{11} = \int_0^1 \frac{\gamma\ K(a_1,t_1)}{(h(a_1)-h(t_1))^\alpha} d\eta, \quad f_1 = f(a_1). \tag{4.9}$$

Hence,

$$\phi_1 = \frac{f_1}{H_{11}}. \tag{4.10}$$

Again taking $x = a_2$ where $a_2 = a_1 + \gamma$, the equation (4.1) becomes

$$\int_{a_0}^{a_1} \frac{K(a_2,t)\ \phi(t)}{(h(a_2)-h(t))^\alpha} dt + \int_{a_1}^{a_2} \frac{K(a_2,t)\ \phi(t)}{(h(a_2)-h(t))^\alpha} dt\ =\ f(a_2). \tag{4.11}$$

If t_j is a point on the line element joining the points a_{j-1} and a_j, $j = 1, 2$, then we can write t_j as

$$t_j = \eta a_j + (1-\eta) a_{j-1}, \quad j = 1, 2, \quad 0 \le \eta \le 1.$$

Then equation (4.11) becomes

$$\int_0^1 \frac{\gamma\ K(a_2,t_1)\ \phi(t_1)}{(h(a_2)-h(t_1))^\alpha} d\eta + \int_0^1 \frac{\gamma\ K(a_2,t_2)\ \phi(t_2)}{(h(a_2)-h(t_2))^\alpha} d\eta = f(a_2), \tag{4.12}$$

According to the assumption of LEM , we choose $\phi_j = \phi(t_j),\ j = 1, 2$ as constants

(unknown) for $t_j \in [a_{j-1}, a_j]$. Using this assumption, equation (4.12) can be written as

$$\sum_{j=1}^{2} H_{2j}\ \phi_j \ = \ f_2 \tag{4.13}$$

where

$$H_{2j} = \int_0^1 \frac{\gamma\ K(a_2, t_j)}{(h(a_2) - h(t_j))^{\alpha}} d\eta,\ \ j = 1, 2; \qquad f_2 = f(a_2). \tag{4.14}$$

It is noted that the matrix associated with the system of linear equations (4.8) and (4.13) is a lower triangular matrix. Hence solving equation (4.13), we obtain

$$\phi_2 = \frac{f_2 - H_{21}\phi_1}{H_{22}} \tag{4.15}$$

where ϕ_1 is known from equation (4.10). Proceeding similarly, $\phi(x)$ can be found numerically at $x = a_i$ where $a_i = a_0 + i\gamma,\ \ i = 1, 2, ..n$. At i-th step,with all the previous assumptions, equation (4.1) takes the form

$$\sum_{j=1}^{i} H_{ij}\ \phi_j \ = \ f_i, \quad i = 1, 2, ..., n \tag{4.16}$$

where

$$H_{ij} = \int_0^1 \frac{\gamma K(a_i, t_j)}{(h(a_i) - h(t_j))^{\alpha}} d\eta,\ \ i = 1, 2, ..., n;\ \ j = 1, 2, ...i; \qquad f_i = f(a_i). \tag{4.17}$$

with $\phi_i = \phi(t_i)$ as constant through the line element $[a_{i-1}, a_i]$ and

$$t_i = \eta a_i + (1 - \eta) a_{i-1}, \quad 0 \le \eta \le 1.$$

Equation (4.16) is a system of linear equations which forms a lower triangular matrix. Thus solving equation (4.16), we obtain

$$\phi_1 = \frac{f_1}{H_{11}}; \qquad \phi_i = \frac{f_i - \sum_{j=1}^{i-1} H_{ij}\phi_j}{H_{ii}} \tag{4.18}$$

2.2 Solution of integral equation with log kernel :

A simple form of integral equation with log kernel is given by equation (4.2) and (4.3). In order to find the unknown function $\phi(x)$ for different x in the region of definition numerically, we apply the Line Element Method(LEM). According to the method, we divide the range of integration $[a, b]$ into n line elements, where the end points of j-th line element is a_{j-1} and a_j, j=1,2,.....n, with $a_0 = 0$, $a_n = 1$, $a_j = a_0 + j\xi$, $j = 1, 2, ...n$ and $\xi = \frac{a_n - a_0}{n}$. Thus $[a, b] = \bigcup_{j=1}^{n}[a_{j-1}, a_j]$. Consequently integral equation (4.2) can be written as follows

$$\sum_{j=1}^{n} \int_{a_{j-1}}^{a_j} \phi(t) \ln\left|\frac{t-x}{t+x}\right| dt = f(x), 0 < x < 1 \tag{4.19}$$

If $t = t_j$ is a point on the line joining the points a_{j-1} and a_j, then t_j can be written as

$$t_j = \eta a_j + (1-\eta)a_{j-1}, \quad 0 \leq \eta \leq 1.$$

Hence equation (4.19) becomes

$$\sum_{j=1}^{n} \int_{0}^{1} \xi \ \phi(t_j) \ln\left|\frac{t_j - x}{t_j + x}\right| d\eta, = f(x), 0 < x < 1 \tag{4.20}$$

Writing $x = x_i$, i=1,2,...,n, for i-th line element joining the points a_{i-1}, a_i, the equation (4.20) becomes

$$\sum_{j=1}^{n} \int_{0}^{1} \xi \ \phi(t_j) \ln\left|\frac{t_j - x_i}{t_j + x_i}\right| d\eta, = f(x_i) \tag{4.21}$$

According to LEM, we assume that the value of $\phi(t)$ is constant throughout the small line element joining the points a_{j-1} and a_j, so that $\phi_j = \phi(t_j)$, a constant [cf. Pozrikidis (2002)]. Then equation(4.21) reduces to

$$\sum_{j=1}^{n} H_{ij} \ \phi_j \ = \ f_i, \quad i = 1, 2, ..., n \tag{4.22}$$

where

$$H_{ij} = \int_0^1 \xi \ \ln\left|\frac{t_j - x_i}{t_j + x_i}\right| d\eta, \qquad f_i = f(x_i), i = 1, 2, ..., n; j = 1, 2, ..., n \tag{4.23}$$

It may be noted here that the integral in equation (4.23) is a weakly singular integral and it can be evaluated numerically. The equation (4.22) is a system of linear equation solving which we get the numerical values of $\phi(x_i),\ i = 1, 2...n$.

2.3 Solution of hypersingular integral equation :

Hypersingular integral equation of first kind :

We consider the simple hypersingular integral equation of first kind of the form

$$\int_{-1}^{1} \frac{\phi(t)}{(t-x)^2}\, dt \ = \ f(x), \qquad -1 \leq \ x \leq \ 1 \tag{4.24}$$

with condition (4.5) so that $\phi(\pm 1) = 0$. The exact solution of equation (4.24) is given by [cf. Martin (1992)]

$$\phi(x) = \int_{-1}^{1} f(t) \log\Big[\frac{|x-t|}{1 - xt + \sqrt{\{(1-x^2)(1-t^2)\}}}\Big]\, dt. \tag{4.25}$$

Noting the condition (4.5), we assume

$$\phi(t) = \sqrt{1-t^2}\ \psi(t) \tag{4.26}$$

where $\psi(t)$ is a regular function. Now replacing (4.26) in equation (4.24), we get

$$\int_{-1}^{1} \frac{\sqrt{1-t^2}\ \psi(t)}{(t-x)^2}\, dt \ = \ f(x), \qquad -1 \leq \ x \leq \ 1 \tag{4.27}$$

Now we subdivide the range of integration $[-1, 1]$ into n number of line elements.i.e.,

$[-1,1] = \bigcup_{j=1}^{n}[a_{j-1}, a_j]$ with $a_0 = -1$ and $a_n = 1$. Here we take

$$a_j = a_0 + jh,\ h = \frac{a_n - a_0}{n},\ j = 1, ...n.$$

Consequently equation (4.27) can be written as follows.

$$\sum_{j=1}^{n} \int_{a_{j-1}}^{a_j} \frac{\sqrt{1-t^2}\ \psi(t)}{(t-x)^2}\ dt\ =\ f(x), \quad -1 \le\ x \le\ 1 \tag{4.28}$$

Now for t belonging to j^{th} line element joining the points a_{j-1} and a_j, we write $t = t_j$, so that

$$t_j = \eta a_j + (1-\eta)a_{j-1}, \quad 0 \le \eta \le 1.$$

Hence equation (4.28) becomes

$$\sum_{j=1}^{n} \int_{0}^{1} \frac{h\ \sqrt{1-t_j^2}\ \psi(t_j)}{(t_j-x)^2}\ d\eta\ =\ f(x), \quad -1 \le\ x \le\ 1 \tag{4.29}$$

Now, for x belonging to the line element joining the points a_{i-1} and a_i, where $i = 1, ...n$ we write $x = x_i$, so that equation (4.29) becomes

$$\sum_{j=1}^{n} \int_{0}^{1} \frac{h\ \sqrt{1-t_j^2}\ \psi(t_j)}{(t_j-x_i)^2}\ d\eta\ =\ f(x_i) \tag{4.30}$$

Here we assume that $\psi(t_j) = \psi_j$ as constant in j^{th} line element joining the points $a_{j-1},\ a_j$, the equation (4.30) reduces to

$$\sum_{j=1}^{n} K_{ij}\ \psi_j = f_i, \quad i = 1, 2, 3....., n \tag{4.31}$$

where,

$$K_{ij} = \int_{0}^{1} \frac{h\ \sqrt{1-t_j^2}}{(t_j-x_i)^2}\ d\eta\ , \qquad f(x_i) = f_i. \tag{4.32}$$

For $i = j$, the integral in K_{ii} has strong singularity and so it is not amenable to numerical techniques. However to evaluate K_{ii}, can be evaluated analytically and for

this we write

$$K_{ii} = \frac{d}{dx_i} G_{ii}$$

where

$$G_{ii} = \int_{a_{i-1}}^{a_i} \frac{\sqrt{1-t_i^2}}{(x_i - t_i)}\, dt_i.$$

It is easy to evaluate G_{ii} so that K_{ii} can be evaluated as

$$\begin{aligned} K_{ii} = {} & \frac{x_i}{\sqrt{1-x_i^2}} \times \left[\ln \left| \frac{\big(A_i x_i - p(x_i)\big)\big(A_{i-1}x_i - q(x_i)\big)}{\big(A_i x_i - q(x_i)\big)\big(A_{i-1}x_i - p(x_i)\big)} \right| \right] \\ & - \frac{1}{x_i} \times \left[\frac{p(x_i)}{A_i x_i - p(x_i)} + \frac{q(x_i)}{A_i x_i - q(x_i)} - \frac{p(x_i)}{A_{i-1}x_i - p(x_i)} - \frac{q(x_i)}{A_{i-1}x_i - q(x_i)} \right] \\ & - \sin^{-1} a_i + \sin^{-1} a_{i-1} \end{aligned} \tag{4.33}$$

where

$$A_i = \frac{a_i}{\sqrt{1+\sqrt{1-a_i^2}}} \;;\quad p(x) = 1 + \sqrt{1-x^2} \;;\quad q(x) = 1 - \sqrt{1-x^2} \tag{4.34}$$

Thus knowing K_{ii}, the system of linear equation (4.31) can be solved to obtain the unknown values of $\psi_i' s$ for each $x_i \epsilon [a_{i-1}, a_i]$. Finally from equation (4.26), the function $\phi(x)$ can be known.

Hypersingular integral equation of second kind :

A simple hypersingular integral equation of second kind is given by

$$\phi(x) - \int_{-1}^{1} \frac{\phi(t)\; s(x,t)}{(t-x)^2}\, dt \;=\; f(x), \qquad -1 \leq\; x \leq\; 1 \tag{4.35}$$

with $\phi(\pm 1) = 0$ and $s(x,t)$ is a known well behaved function. Noting the condition $\phi(\pm 1) = 0$, we assume

$$\phi(t) = \sqrt{1-t^2}\; \psi(t) \tag{4.36}$$

where $\psi(t)$ is a regular function. Following the same procedure for solving first kind hypersingular integral equation, the second kind hypersingular integral equation (4.35) can be reduced to a system of algebraic equations. The solution of the system of algebraic equations produces the solution of the hypersingular integral equation (4.35). In the next section we shall illustrate the method described through some examples.

3. Numerical results :

We now consider some examples to illustrate the Line element method.

3.1 Abel integral equation:

Example 1:

We consider the Abel integral equation

$$\int_0^x \frac{\phi(t)}{\sqrt{x-t}}dt = \frac{4}{3}\, x^{\frac{3}{2}},\ 0 < x < 1 \tag{4.37}$$

Here $\phi(x) = x$ is the exact solution. Following the procedure discussed in section 2.1, taking $\gamma = .1$ and $\gamma = .01$ respectively, we obtain the values of $\phi(x)$. Some representative values of $\phi(x)$ are given in the table 4.1 and table 4.2 below.

Example 2:

We consider the following Abel integral equation which arises in connection with the problem of scattering of water waves by a vertical barrier partially immersed in deep water [cf. Chakrabarti et. al. (1995)].

$$\int_0^x \frac{t\ \phi(t)}{\sqrt{x^2-t^2}}dt = x,\ 0 < x < 1 \tag{4.38}$$

The exact solution of this Abel integral equation is $\phi(t) = 1$. Following the procedure

Table 4.1: Comparative study of the exact result and present result.

γ=**0.1**			
values of x	**Solution**		**Absolute Error**
	ϕ_{exact}	ϕ_{approx}	
0.1	0.1	0.0954336	4.56639×10^{-3}
0.2	0.2	0.1953010	4.69879×10^{-3}
0.3	0.3	0.2952450	4.75550×10^{-3}
0.4	0.4	0.395211	4.78890×10^{-3}
0.5	0.5	0.495189	4.81149×10^{-3}
0.6	0.6	0.595172	4.82812×10^{-3}
0.7	0.7	0.695153	4.84100×10^{-3}
0.8	0.8	0.795149	4.85136×10^{-3}
0.9	0.9	0.89514	4.85993×10^{-3}
1.0	1.0	0.995133	4.86717×10^{-3}

Table 4.2: Comparative study of the exact result and present result.

γ=**0.01**			
values of x	**Solution**		**Absolute Error**
	ϕ_{exact}	ϕ_{approx}	
0.1	0.1	0.0995133	4.86716×10^{-4}
0.2	0.2	0.199503	4.90624×10^{-4}
0.3	0.3	0.299508	4.92335×10^{-4}
0.4	0.4	0.399507	4.93355×10^{-4}
0.5	0.5	0.499506	4.94055×10^{-4}
0.6	0.6	0.599505	4.94639×10^{-4}
0.7	0.7	0.699505	4.9505×10^{-4}
0.8	0.8	0.799505	4.95375×10^{-4}
0.9	0.9	0.899504	4.95536×10^{-4}
1.0	1.0	0.999504	4.95757×10^{-4}

discussed in section 2.1, and taking the length of each line element γ = .1 and γ = .01 respectively, the unknown function $\phi(x)$ is obtained for different values of x where $x \in [0, 1]$. Some representative values of $\phi(x)$ are given in table 4.3 and table 4.4 respectively below.

From Tables 4.1 and 4.2 for example 1, and from Tables 4.3 and 4.4 for example 2, it is observed that as γ increases 10^{-1} times, the absolute error also increases by 10^{-1} times. However, for γ = 0.1, the absolute error in example 1 is of order 10^{-3} while in

Table 4.3: Comparative study of the exact result and present result.

γ=**0.1**			
values of x	**Solution**		**Absolute Error**
	ϕ_{exact}	ϕ_{approx}	
0.1	1	1.00000	6.49833×10^{-8}
0.2	1	1.00000	4.30718×10^{-8}
0.3	1	1.00000	3.14319×10^{-8}
0.4	1	1.00000	3.3801×10^{-8}
0.5	1	1.00000	4.13483×10^{-8}
0.6	1	1.00000	4.48594×10^{-8}
0.7	1	1.00000	4.07682×10^{-8}
0.8	1	1.00000	5.07618×10^{-8}
0.9	1	1.00000	6.13094×10^{-8}
1.0	1	1.00000	6.67634×10^{-8}

Table 4.4: Comparative study of the exact result and present result.

γ=**0.01**			
values of x	**Solution**		**Absolute Error**
	ϕ_{exact}	ϕ_{approx}	
0.1	1	1.00000	9.38194×10^{-9}
0.2	1	1.00000	2.75213×10^{-8}
0.3	1	1.00000	2.23096×10^{-8}
0.4	1	1.00000	2.73001×10^{-8}
0.5	1	1.00000	2.93306×10^{-8}
0.6	1	1.00000	2.29234×10^{-8}
0.7	1	1.00000	2.07567×10^{-8}
0.8	1	1.00000	2.11109×10^{-8}
0.9	1	1.00000	2.37410×10^{-8}
1.0	1	1.00000	2.42862×10^{-8}

example 2 it is of order 10^{-8}. Thus it is observed that line element method is simple and fairly accurate method.

3.2 Integral equation with log kernel:

We consider the integral equation (4.2, 4.3) with $f(x) = \pi x$ given by

$$\int_0^1 \phi(t) \ln \left|\frac{t-x}{t+x}\right| dt = \pi x, \ 0 < x < 1. \tag{4.39}$$

The above integral equation arises in connection with the problem of scattering of water waves by a vertical barrier partially immersed in deep water [cf. Banerjea Dutta (2008)] whose exact solution is $\phi(x) = -\frac{x}{\sqrt{1-x^2}}$. Since the unknown function $\phi(x)$ satisfies the condition (4.3), so we write

$$\phi(x) = \frac{\psi(x)}{\sqrt{1-x}},$$

where $\psi(x)$ is a regular function. Thus the given integral equation reduces to

$$\int_0^1 \ln\left|\frac{t-x}{t+x}\right| \frac{\psi(t)}{\sqrt{1-t}} dt = \pi x, \ 0 < x < 1. \tag{4.40}$$

The exact solution of the given integral equation is $\phi(x) = -\frac{x}{\sqrt{1-x^2}}$, [cf. Banerjea Dutta (2008)] so that $\psi(x) = -\frac{x}{\sqrt{1+x}}$. Following the procedure discussed in section 2.2, the domain $[0,1]$ is discretized into 10 and 100 line elements respectively, taking $\xi = 0.1,\ 0.01$, so that we get different values of $\psi(x)$ in different line segments. Some representative values of $\phi(x)$ are given in table 4.5 and table 4.6 for $\xi = 0.1$ and $\xi = 0.01$ respectively. It is observed from Table 4.5 that the order of absolute error is 10^{-4} for $\xi = 0.1$. This indicates that for 10 line elements, the results are fairly accurate. However it is observed from Table 4.6 that the order of absolute error is 10^{-6} for $\xi = 0.01$. This shows that the Line Element method gives fairly accurate results and as ξ is decreases by 10^{-1} times the absolute error decreases by 10^{-2} times.

Table 4.5: Comparative study of the exact result and present result.

ξ=0.1

Interval	values of x	**Solution**		**Absolute Error**
		ϕ_{exact}	ϕ_{approx}	
$[0,.1]$	0.05	-0.04795	-0.0489828	1.8775×10^{-4}
$[.1,.2]$	0.15	-0.139876	-0.140246	3.6984×10^{-4}
$[.2,.3]$	0.25	-0.223607	-0.233996	3.8875×10^{-4}
$[.3,.4]$	0.35	-0.301232	-0.301656	4.2373×10^{-4}
$[.4,.5]$	0.45	-0.373705	-0.374181	4.7631×10^{-4}
$[.5,.6]$	0.55	-0.441771	-0.442329	5.5872×10^{-4}
$[.6,.7]$	0.65	-0.506024	-0.506716	6.9189×10^{-4}
$[.7,.8]$	0.75	-0.566947	-0.567915	9.6860×10^{-4}
$[.8,.9]$	0.85	-0.624932	-0.625988	1.0552×10^{-3}
$[.9,1]$	0.95	-0.680309	-0.689418	9.1088×10^{-3}

Table 4.6: Comparative study of the exact result and present result.

ξ=0.01

Interval	values of x	**Solution**		**Absolute Error**
		ϕ_{exact}	ϕapprox	
$[0.05, 0.06]$	0.055	-0.0535472	-0.0535511	3.91519×10^{-6}
$[0.15, 0.16]$	0.155	-0.144225	-0.144229	3.91375×10^{-6}
$[0.25, 0.26]$	0.255	-0.227624	-0.227628	4.02584×10^{-6}
$[0.35, 0.36]$	0.355	-0.304971	-0.304975	4.30648×10^{-6}
$[0.45, 0.46]$	0.455	-0.377207	-0.377212	4.80107×10^{-6}
$[0.55, 0.56]$	0.555	-0.445069	-0.445075	5.61181×10^{-6}
$[0.65, 0.66]$	0.655	-0.509146	-0.509153	6.97712×10^{-6}
$[0.75, 0.76]$	0.755	-0.569913	-0.569922	9.5418×10^{-6}
$[0.85, 0.86]$	0.855	-0.627761	-0.627777	1.57518×10^{-5}
$[0.95, 0.96]$	0.955	-0.683015	-0.683065	4.99048×10^{-5}

3.3 Hypersingular Integral Equation:

Example 1:

Here we consider the hypersingular integral equation (4.24) when $f(x) = 1$

$$\int_{-1}^{1} \frac{\phi(t)}{(t-x)^2}\, dt \;=\; 1, \qquad -1 \leq \; x \leq \; 1 \tag{4.41}$$

with

$$\phi(t) \sim O(|1-t^2|^{\frac{1}{2}}) \qquad \text{as } |t| \to 1. \tag{4.42}$$

The exact solution of equation (4.41) is given by (equation (4.25) with $f(x) = 1$)

$$\phi(x) = -\frac{1}{\pi}\sqrt{1-x^2}. \tag{4.43}$$

According to the substitution used in equation (4.26), we obtain $\psi(x) = -\frac{1}{\pi}$. Following the procedure discussed in section 2.3, we discretise the domain $[-1, 1]$ into 20 and 200 line elements respectively so that the length of each subinterval $h = 0.1,\ 0.01$ respectively. Some representative values of $\psi(x)$ are given for both cases in Table 4.7 and Table 4.8 respectively.

Table 4.7: Comparative study of the exact result and present result.

h=0.1

Intervals	values of x	**Solution**		**Absolute Error**
		ϕ_{exact}	ϕ_{approx}	
$[.9, 1.0]$,$[-1, -.9]$	± 0.95	$-1/\pi$	-0.31831	1.77747×10^{-12}
$[.7, .8]$,$[-.8, -.7]$	± 0.75	$-1/\pi$	-0.31831	2.01006×10^{-12}
$[.5, .6]$,$[-.6, -.5]$	± 0.55	$-1/\pi$	-0.31831	2.16993×10^{-12}
$[.3, .4]$,$[-.4, -.3]$	± 0.35	$-1/\pi$	-0.31831	2.32203×10^{-12}
$[.1, .2]$,$[-.2, -.1]$	± 0.15	$-1/\pi$	-0.31831	2.54963×10^{-12}

Table 4.8: Comparative study of the exact result and present result.

h=0.01

Intervals	values of x	**Solution**		**Absolute Error**
		ϕ_{exact}	ϕ_{approx}	
$[.95, .96]$,$[-.96, -.95]$	± 0.955	$-1/\pi$	-0.31831	6.96221×10^{-14}
$[.75, .76]$,$[-.76, -.75]$	± 0.755	$-1/\pi$	-0.31831	8.24729×10^{-14}
$[.55, .56]$,$[-.56, -.55]$	± 0.555	$-1/\pi$	-0.31831	1.06742×10^{-13}
$[.35, .36]$,$[-.36, -.35]$	± 0.355	$-1/\pi$	-0.31831	1.50419×10^{-13}
$[.15, .16]$,$[-.16, -.15]$	± 0.155	$-1/\pi$	-0.31831	2.45437×10^{-13}

It is observed from table 4.7 that the error is of order 10^{-12} when $h = 0.1$, ie for 20 line elements. This shows the method adopted here is very simple, effective and produces quite accurate result. Table 4.8 shows that the error is of order 10^{-14} or 10^{-13} for $h = 0.01$, ie for 200 line elements. Hence it is observed that as h increases by 10^{-1} times, the absolute error increases by $10^{-2}/\ 10^{-1}$ times.

Example 2:

The hyper singular integral equation of second kind is given by

$$\phi(x) - \frac{\alpha(1-x^2)^{\frac{1}{2}}}{\pi} \int_{-1}^{1} \frac{\phi(t)}{(t-x)^2}\, dt \;=\; f(x), \qquad -1 \leq\; x \leq\; 1 \tag{4.44}$$

with $\phi(\pm 1) = 0$, which is known as the elliptic wing case of Prandtl's equation, for which $\alpha(> 0)$ is a known constant and $f(x) = (\frac{2\pi k}{\beta})(1-x^2)^{\frac{1}{2}}$, k , $\beta(> 0)$ are known constants [cf. Chakrabarti (1997)]. For simplicity we take $\beta = \pi$, $k = 1$, $\alpha = \frac{\pi}{2\beta}$ in (4.44)

so that $f(x) = 2(1-x^2)^{\frac{1}{2}}$.
Because of the condition $\phi(\pm 1) = 0$, we assume

$$\phi(t) = \sqrt{1-t^2}\ \psi(t) \tag{4.45}$$

where $\psi(t)$ is a regular function. Now replacing (4.45) in equation (4.44), we get

$$\psi(x) = 2 + \frac{1}{2\pi}\int_{-1}^{1} \frac{\sqrt{1-t^2}\ \psi(t)}{(t-x)^2}\ dt \tag{4.46}$$

Generalizing the procedure discussed in section 2.3 for 2nd kind hypersingular integral equation, we discretise the domain $[-1, 1]$ into 20 line elements.Some representative values of $\psi(x)$ are given in Table 4.9 .

Table 4.9: Numerical values.

values of x	ψ_{approx}
± 0.955	1.33333
± 0.755	1.33333
± 0.555	1.33333
± 0.355	1.33333
± 0.155	1.33333

A second method based on approximating the unknown function $\psi(t)$ in the equation (4.46) by Chebyshev polynomial is described below.

$$\psi(t) \cong \sum_{n=0}^{N} a_n\ U_n(t) \tag{4.47}$$

where U_n is Chebyshev polynomial of 2nd kind.

Now From Abramowitz and Stegun (1965), we know that

$$\int_{-1}^{1} \frac{\sqrt{1-t^2}\ U_n(t)}{x-t}\ dt = \pi\ T_{n+1}(x) \tag{4.48}$$

where T_n is Chebyshev polynomial of 1st kind.Now differentiating both side of equation (4.48) with respect to x , we get

$$\int_{-1}^{1} \frac{\sqrt{1-t^2}\ U_n(t)}{(x-t)^2}\ dt = \ -\pi(n+1)\ U_n(x) \tag{4.49}$$

Now substituting (4.47) in (4.46), and using the relations (4.48) and (4.49), we get

$$\sum_{n=0}^{N} a_n\ A_n(x)\ =\ 2,\ \ -1 < x < 1. \tag{4.50}$$

where $A_n(x) = \frac{n+3}{2} U_n(x)$. Now choosing $N+1$ values of x, we get a system of linear equation, solving which we get the coefficients a_n and then $\psi(x)$. To compare the result with solution obtained by boundary element method, here we take $N = 19$, and x_i same as the example (4.46). The results by Chebyshev polynomial approximation is given in Table 4.10.

Table 4.10: Numerical values.

values of x	ψ_{approx}
±0.955	1.33333
±0.755	1.33333
±0.555	1.33333
±0.355	1.33333
±0.155	1.33333

From Tables 4.9 and 4.10 it is observed that results obtained by two method agree with each other.

4. Convergence of the Line element method to solve integral equation with regular kernel :

In this section we shall establish the convergence [cf. Goldberg and Chen (1994)] of the line element method of solution of Fredholm integral equation of second kind. The proof of convergence for first kind integral equation follows similarly.

A second kind integral equation is given by

$$\phi(x) = f(x) + \lambda \int_a^b K(x,t)\phi(t)dt, a < x < b. \tag{4.51}$$

which can be alternately written as

$$\phi(x) = f(x) + \lambda(K\phi)(x), a < x < b, \tag{4.52}$$

where

$$(K\phi)(x) = \int_a^b K(x,t)\phi(t)dt \tag{4.53}$$

Following Banerjea et al. (2019), we approximate $(K\phi)(x)$ in equation (4.53) using line element method as $(K_n\phi)(x)$, given by

$$(K\phi)(x) \simeq (K_n\phi)(x) = \sum_{j=1}^{n} \int_0^1 K(x,t_j)\phi(t_j)(a_j - a_{j-1})d\eta \tag{4.54}$$

where $K_n : C[a,b] \to C[a,b]$ is a finite rank operator and

$$t_j = \eta a_j + (1-\eta)a_{j-1}, \quad 0 \le \eta \le 1.$$

where a_j and a_{j-1} are the end point of j-th line element.

Replacing $(K\phi)(x)$ from equation (4.54) into equation (4.51) we obtain n^{th} approximation $\phi_n(x)$ to $\phi(x)$ as

$$\phi_n(x) = \sum_{j=1}^{n} \int_0^1 K(x,t_j)\phi(t_j)(a_j - a_{j-1})d\eta + f(x) \tag{4.55}$$

To obtain $\{\phi_n(x)\}$ we evaluate $\phi_n(x)$ from (4.55) at $x = x_k$ where x_k belongs to the line element joining (a_{k-1}, a_k). Thus

$$\phi_n(x_k) = \sum_{j=1}^{n} \int_0^1 K(x_k,t_j)\phi_n(t_j)(a_j - a_{j-1})d\eta + f(x_k) \tag{4.56}$$

Considering $\phi_n(x_k) \equiv \phi_{nk}$ to be constant in k^{th} line element, the equation (4.56) can

be reduced to the following system of linear algebraic equations

$$\sum_{j=1}^{n} H_{ij}\phi_{nj} = f_i, i = 1, 2, ..., n \tag{4.57}$$

where $H_{ij} = \delta_{ij} - \int_0^1 K(x_i, t_j)(a_j - a_{j-1})d\eta$. If equation (4.57) has unique solution then equation (4.55) provides an interpolant

$$\phi_n(x) = \sum_{j=1}^{n} \int_0^1 K(x, t_j)\phi(t_j)(a_j - a_{j-1})d\eta + f(x) \tag{4.58}$$

of $\{\phi_m(x)\}_{m=1}^n$.
To prove the convergence of the $\{\phi_m(x)\}_{m=1}^n$, we use the Brakhage's lemma [cf. Goldberg and Chen (1994)] given as follows.

Brakhage's Lemma

Let $K : V \to V$ be a bounded linear operator and $K_n : V \to V$ be a sequence of finite rank operators such that $K_n(x) \to K(x), \ \forall x \epsilon V$. If $\| (K - K_n)K_n \| \to 0$ as $n \to \infty$ then $\forall n$ sufficiently large $(I - K_n)^{-1}$ exists and $\| (\phi - \phi_n) \|_\infty \ \leq \ \| K\phi - K_n\phi \|_\infty$.

Now $(K\phi)(x)$ and $(K_n\phi)(x)$ are defined by equations (4.54) and (4.53). Thus

$$\{(K - K_n)K_n\}\phi(x) = \sum_{j=1}^{n}(a_j - a_{j-1}) \int_0^1 E_n(x, t_j)\phi(t_j)d\eta, \tag{4.59}$$

where

$$E_n(x, t_j) = \int_a^b K(x, s)K(s, t_j)ds - \sum_{k=1}^{n}(a_k - a_{k-1}) \int_0^1 K(x, s_k)K(s_k, t_j)d\zeta. \tag{4.60}$$

where $s_k = (1 - \zeta)a_{k-1} + \zeta a_k$.

Now it is easy to see that

$$\| (K - K_n)K_n \|_\infty \leq \max_{x\varepsilon[a,b]} \sum_{j=1}^{n} (a_j - a_{j-1}) \int_0^1 |E_n(x, t_j)| d\eta. \tag{4.61}$$

Thus to show that $\| (K-K_n)K_n \|_\infty \to 0$ as $n \to \infty$ it is sufficient to show that $\{E_n(x,t)\}$ is a uniformly bounded equicontinuous set of functions which are pointwise convergent to zero so that by Ascoli Arzela's theorem it can be asserted that $\{E_n(x,t)\}$ uniformly to zero.

Now Equation (4.60) shows that $\{E_n(x,t)\}$ is point wise convergent and converges to zero.

We first show that $\{E_n(x,t)\}$ is uniformly bounded sequence. From equation (4.60) we have

$$|E_n(x,t_j)| \leq 2(b-a)|K(x,t|^2 \leq 2(b-a) \max_{(x,t)\epsilon[a,b]\times[a,b]} |K(x,t)|^2 \leq M \tag{4.62}$$

where M is a constant, showing that $\{E_n(x,t)\}$ is uniformly bounded. To show that $\{E_n(x,t)\}$ is equicontinuous we write

$$|E_n(x,t) - E_n(y,z)| \leq |E_n(x,t) - E_n(y,t)| + |E_n(y,t) - E_n(y,z)|. \tag{4.63}$$

Now, using equation (4.60) it can be easily shown that

$$|E_n(x,t) - E_n(y,t)| \leq 2(b-a)\kappa \max_{s\epsilon[a,b]} |K(x,s) - K(y,s)|. \tag{4.64}$$

where $\kappa = \max_{(x,t)\epsilon[a,b]\times[a,b]} |K(x,t)|$
Similarly

$$|E_n(y,t) - E_n(y,z)| \leq 2(b-a)\kappa \max_{s\epsilon[a,b]} |K(s,t) - K(s,z)|. \tag{4.65}$$

Since $K(x,t)$ is uniformly continuous, so for $\varepsilon > 0$, the following holds.
$|K(x,s) - K(y,s)| < \varepsilon/2\kappa(b-a)$ whenever $|x-y| < \delta_1$ and $|K(y,t) - K(y,z)| <$

$\varepsilon/2\kappa(b-a)$ whenever $|t-z| < \delta_2$. Thus choosing $\delta = min(\delta_1, \delta_2)$ we have

$$|E_n(x,t) - E_n(y,z)| \leq \varepsilon. \tag{4.66}$$

This shows that $\{E_n(x,t)\}$ is equicontinuous. Thus $\{E_n(x,t)\}$ satisfies all the conditions of Ascoli Arzela's theorem. Hence by Brakhage's Lemma the we can say that $\phi_n \to \phi$ as $n \to \infty$ [cf. Goldberg and Chen (1994)].

For the singular integral equations the dominant term can be evaluated exactly and the corresponding singular integral equations can be reduced to system of linear equations and proof of convergence of the method can be extended for singular integral equations also [cf. Goldberg and Chen (1994)].

5. Conclusion :

A simple numerical technique, viz, line element method is employed here to solve Abel integral equations, integral equation with log kernel and hypersingular integral equation of first kind. For all three types of integral equations, the discretization of range of integration as well as the interval of definition of the integral equations into small line elements, yields a system of linear equations. For Abel integral equation, the matrix associated with the system of linear equations is a lower triangular matrix from which it is very simple to obtain the solution. For log integral equation and hypersingular integral equation, the matrix associated with the system of linear equations is a normal dense matrix whose inversion can be obtained by standard procedure.

Some numerical examples are considered for all the integral equations. It is observed that in each example, that

i) the the method is very simple to implement numerically,

ii) the absolute error is fairly small even for 10 line elements. This shows the efficiency of the method.

iii) as the number of line elements increases by 10 times, the absolute error decreases by $10^{-2}/\ 10^{-1}$ times.

This shows that the Line Element Method is a very efficient method and yields very

accurate results for solving weakly singular integral equations as well as hypersingular integral equations.

PART III

Water wave scattering problems by thin barrier

Chapter 5

Hypersingular Integral Equation Formulation of the Problem of Water Wave Scattering by A Circular Arc Shaped Impermeable Barrier Submerged in Water of Finite Depth

1. Introduction

In this Chapter we study the problem of scattering of water waves by a thin impermeable circular arc shaped barrier submerged in ocean of finite depth under the assumption of linearised theory of water waves. As already mentioned in Chapter 1

† The content of this chapter is based on the paper " Hypersingular Integral Equation Formulation of the Problem of Water Wave Scattering by A Circular Arc Shaped Impermeable Barrier Submerged in Water of Finite Depth ", *The Quarterly Journal of Mechanics and Applied Mathematics*, 74(4) (2021) 491-505.

that breakwaters in the shape of a circular arc submerged in water was studied by many researchers because it is known that the increase in arc length of a circular arc-shaped rigid breakwater reduces the reflection of water waves.
The problem is formulated in terms of a hypersingular integral equation of first kind in terms of the unknown function representing the difference of potential function across the curved barrier. The hypersingular integral equation is then solved by using two numerical methods.

The first method is boundary element method (BEM) which is discussed in detail in chapters 3 and 4. The second method is collocation method where the unknown function is expanded in terms of Chebyshev polynomials of second kind. Choosing the collocation points suitably, the integral equation is reduced to a system of algebraic equations which is then solved to obtain the unknown function satisfying the hypersingular integral equation.

The physical quantities of interest viz, the reflection coefficient, transmission coefficients, which are expressed in terms of the solution of the hypersingular integral equation, are computed by both the methods and studied graphically. The comparison of the reflection coefficient by the two methods shows reasonably good agreement.
We now proceed to formulate the problem mathematically.

2. Mathematical Formulation:

Assuming linear theory we consider the two dimensional motion in water due to interaction of waves with a circular arc shaped thin impermeable barrier which is fully submerged in a water region of finite depth h. The configuration is described by a cartesian co-ordinate system with x-axis along the mean free surface of water and y-axis vertically downward passing through the center of the circle. The circular arc shaped barrier with radius b is placed such a way that it is symmetrical about the y-axis and the center of the circular arc is at the depth $(d+b)$ from the free surface and the radius through the end points of the barrier makes an angle θ with y-axis. Thus any point (x, y) on the plate can be expressed as $x = b\sin s\theta, \quad y = d + b - b\cos s\theta \quad -1 \leq s \leq 1.$

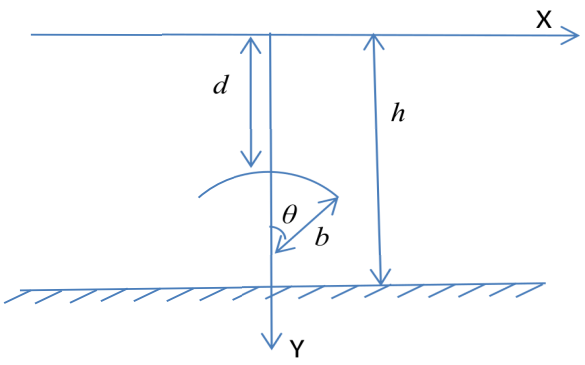

Figure 5.1: Geometry of the problem

We consider a time harmonic train of surface waves with velocity potential $Re(\phi^{inc}(x,y)e^{-i\sigma t})$ and angular frequency σ from $x \to -\infty$ is incident on the barrier and is partly reflected and partly transmitted over and below the barrier. Here,

$$\phi^{inc} = \frac{\cosh k_0(h-y)e^{ik_0x}}{\cosh k_0 h} \tag{5.1}$$

where k_0 is the unique real positive root of the transcendental equation

$$k \tanh kh = K \tag{5.2}$$

with $K = \sigma^2/g$.
Now the resulting motion can be described by velocity potential $Re(\phi(x,y)e^{-i\sigma t})$, $\phi(x,y)$ satisfies the following boundary value problem.

$$\nabla^2\phi = 0 \qquad \text{in the fluid region,} \tag{5.3}$$

$$K\phi + \phi_y = 0 \quad \text{on} \quad y = 0, \tag{5.4}$$

$$\frac{\partial\phi}{\partial y} = 0 \quad \text{on} \quad y = h, \tag{5.5}$$

$$r^{1/2}\ \nabla\phi \qquad \text{is bounded as } r \to 0, \tag{5.6}$$

where r is the distance of any point of the fluid region from the either sharp ends of the barrier. This is a well known condition which expresses the singular behaviour of velocity at the tips of the thin plate within the frame work of linearised theory of water waves. A detailed discussion on this condition is given in (cf. Mandal and Chakrabarti (2000)).

The boundary condition on the curved plate surface Γ is given by

$$\frac{\partial\phi_1}{\partial n} = \frac{\partial\phi_2}{\partial n} = 0 \quad \text{on} \quad \Gamma. \tag{5.7}$$

Here the potential functions $\phi_2(x,y)$ is in the region $x^2+(y-b-d)^2 > b^2$ and $\phi_1(x,y)$ is in the region $x^2+(y-b-d)^2 < b^2$ and $\frac{\partial}{\partial n}$ denotes the normal derivative at a point on Γ.
The far field condition is

$$\phi(x,y) \sim \begin{cases} \phi^{inc}(x,y) + R\phi^{inc}(-x,y) \text{ as } x \to -\infty, \\ T\phi^{inc}(x,y) \text{ as } x \to \infty, \end{cases} \tag{5.8}$$

where R and T are the reflection and transmission coefficients respectively, which are to be determined.

3. Method of solution:

In this section we will proceed to find the reflection and transmission coefficients using hypersingular integral equation formulation. Following Parson and Martin (1994), we shall reduce the boundary value problem (5.1) to (5.8) to a hypersingular integral equation of first kind over the barrier Γ using Green's integral theorem. Let $G(x,y;\xi,\eta)$ be the source potential which describes motion in water due to the presence of a line source at (ξ,η). The representation of $G(x,y;\xi,\eta)$ is given (cf. Mandal Chakrabarti

(2000)) below.

$$G(x,y;\xi,\eta) = \log\left(\frac{r}{r'}\right)$$

$$-2\int_0^\infty \left[\frac{\cosh k(h-y)\cosh k(h-\eta)}{k\sinh kh - K\cosh kh} + \frac{e^{-kh}\sinh k\eta \sinh ky}{k}\right]\frac{\cos k(x-\xi)}{\cosh kh}dk \qquad (5.9)$$

where $r, r' = \sqrt{(x-\xi)^2 + (y \mp \eta)^2}$ and the symbol $\int_0^\infty$ indicates that, along the path of integration, there is a small circular indentation below the unique real positive root k_0 of the transcendental equation $k\sinh kh - K\cosh kh = 0$.

Now applying Green's Integral theorem to the functions $\psi(x,y) = \phi(x,y) - \phi^{inc}(x,y)$ and $G(x,y;\xi,\eta)$ in the fluid region suitably, we obtain the integral representation of the potential function as

$$\phi(\xi,\eta) = \phi^{inc}(\xi,\eta) - \frac{1}{2\pi}\int_\Gamma [\phi](p)\frac{\partial}{\partial n_p}G(x,y;\xi,\eta)ds_p \qquad (5.10)$$

where $p \equiv (x,y)$ is a point on barrier Γ, $[\phi](p)$ is the discontinuity of potential function $\phi(x,y)$ across Γ and $\frac{\partial}{\partial n_p}$ is the normal derivative at the point p on Γ. It is very clear that the unknown function $[\phi](p)$ vanishes at the tips of the arc barrier and its derivative has square root singularity there.
Now taking normal derivative to both sides of equation (5.10) at another point $q \equiv (\xi,\eta)$ on the barrier, and using the boundary condition (5.7), we finally obtain the integro-differential equation

$$\frac{1}{2\pi}\frac{\partial}{\partial n_q}\int_\Gamma [\phi](p)\frac{\partial}{\partial n_p}G(p;q)ds_p = \frac{\partial \phi^{inc}}{\partial n_q}(\xi,\eta). \qquad (5.11)$$

Now the order of integration and differentiation in equation (5.11) can be interchanged provided the integral is interpreted as a Hadamard Finite part integral and finally we obtain the hypersingular integral equation

$$\frac{1}{2\pi}\int_\Gamma [\phi](p)\frac{\partial^2}{\partial n_q \partial n_p}G(p,q)ds_p = \frac{\partial \phi^{inc}}{\partial n_q}(\xi,\eta) \qquad (5.12)$$

where $[\phi(p)]$ vanishes at the tips of Γ.

Now to obtain the explicit form of the kernel of the integral equation (5.12), we write parametrically the coordinates of points $p(x,y)$ and $q(\xi,\eta)$ on the barrier Γ and the normal derivatives n_p and n_q at points p and q respectively as follows

$$x(s) = b\sin s\theta, \quad y(s) = d + b - b\cos s\theta; \quad -1 \le s \le 1, \tag{5.13}$$

$$\xi(t) = b\sin t\theta, \quad \eta(t) = d + b - b\cos t\theta; \quad -1 \le t \le 1, \tag{5.14}$$

$$n_p \equiv (-\sin s\theta, \cos s\theta); \quad n_q \equiv (-\sin t\theta, \cos t\theta), \tag{5.15}$$

$$X = x - \xi = b(\sin s\theta - \sin t\theta); \; Y = y + \eta = 2d + 2b - b(\cos s\theta + \cos t\theta). \tag{5.16}$$

Now using equations (5.13), (5.14) and (5.15) in equation (5.9), we get the simplified form of $\frac{\partial^2 G}{\partial n_q \partial n_p}(p;q)$ as

$$\frac{\partial^2 G}{\partial n_q \partial n_p}(p;q) = -\frac{1}{b^2\theta^2(s-t)^2} + L(s,t) \tag{5.17}$$

where

$$\begin{aligned}
L(s,t) = -\Big[&\frac{1}{4b^2\sin^2\frac{(s-t)\theta}{2}} - \frac{1}{b^2\theta^2(s-t)^2}\Big] \\
&-\frac{X^2-Y^2}{(X^2+Y^2)^2}\cos(s-t)\theta + \frac{2XY}{(X^2+Y^2)^2}\sin(t-s)\theta \\
&-2\sin t\theta\sin s\theta\int_0^\infty \mu(k)\sinh k\eta\sinh ky\cos kX\,dk \\
&+2\sin t\theta\cos s\theta\int_0^\infty \mu(k)\sinh k\eta\cosh ky\sin kX\,dk \\
&-2\cos t\theta\sin s\theta\int_0^\infty \mu(k)\cosh k\eta\sinh ky\sin kX\,dk \\
&-2\cos t\theta\cos s\theta\int_0^\infty \mu(k)\cosh k\eta\cosh ky\cos kX\,dk \\
-\sin t\theta\sin s\theta\Big[&\zeta i\cosh k_0(h-y)\cosh k_0(h-\eta)\; e^{ik_0|X|} \\
&-\sum_{n=1}^{\infty}\lambda_n\cos k_n(h-y)\cos k_n(h-\eta)\; e^{-k_n|X|} + \frac{2\pi}{h}\sum_{n=0}^{\infty}\alpha_n\sin\alpha_n y\sin\alpha_n\eta\; e^{-\alpha_n|X|}\Big]
\end{aligned}$$

$$
\begin{aligned}
&-\cos t\theta\cos s\theta\Big[\zeta i\sinh k_0(h-y)\sinh k_0(h-\eta)\ e^{ik_0|X|}\\
&\quad+\sum_{n=1}^{\infty}\lambda_n\sin k_n(h-y)\sin k_n(h-\eta)\ e^{-k_n|X|}-\frac{2\pi}{h}\sum_{n=0}^{\infty}\alpha_n\cos\alpha_n y\cos\alpha_n\eta\ e^{-\alpha_n|X|}\Big]\\
&-\sin t\theta\cos s\theta\Big[\zeta\sinh k_0(h-y)\cosh k_0(h-\eta)\ e^{ik_0|X|}\\
&\quad-\sum_{n=1}^{\infty}\lambda_n\sin k_n(h-y)\cos k_n(h-\eta)\ e^{-k_n|X|}+\frac{2\pi}{h}\sum_{n=0}^{\infty}\alpha_n\cos\alpha_n y\sin\alpha_n\eta\ e^{-\alpha_n|X|}\Big]\\
&+\cos t\theta\sin s\theta\Big[\zeta\cosh k_0(h-y)\sinh k_0(h-\eta)\ e^{ik_0|X|}\\
&-\sum_{n=1}^{\infty}\lambda_n\cos k_n(h-y)\sin k_n(h-\eta)\ e^{-k_n|X|}+\frac{2\pi}{h}\sum_{n=0}^{\infty}\alpha_n\sin\alpha_n y\cos\alpha_n\eta\ e^{-\alpha_n|X|}\Big] \qquad (5.18)
\end{aligned}
$$

where k_0 and ik_n are roots of the transcendental equations $k\tanh kh-K=0$; and $i\alpha_n$'s are roots of the equation $\cosh kh=0$. and

$$\mu(k)=\tfrac{k\ e^{-kh}}{\cosh kh};\quad \zeta=\tfrac{4\pi k_0^2}{2k_0h+\sinh(2k_0h)};\quad \lambda_n=\tfrac{4\pi k_n^2}{2k_nh+\sin(2k_nh)}.$$

Here $L(s,t)$ is the nonsingular part of the kernel .

From equation (5.1), we get

$$\frac{\partial\phi^{inc}(\xi,\eta)}{\partial n_q}=-\frac{k_0e^{ik_0\xi}}{\cosh k_0h}\ \sinh(k_0(h-\eta)+it\theta). \qquad (5.19)$$

Writing

$$f(s)=[\phi(p(s))],\quad -1\le s\le 1. \qquad (5.20)$$

and using equations (5.17) and (5.20), the hypersingular integral equation can be written as

$$\int_{-1}^{1}f(s)\Big[\frac{1}{(s-t)^2}-b^2\theta^2L(s,t)\Big]\,ds=2\pi b\theta\ \frac{k_0e^{ik_0\xi(t)}\sinh\left(k_0(h-\eta(t))+\imath t\theta\right)}{\cosh k_0h}. \qquad (5.21)$$

We will solve the above integral equation (5.21) by two methods, (i) Boundary element method ,(ii) Chebyshev Polynomial approximation method in the next section. Using the solution $f(s)$ of the hypersingular integral equation (5.21), the reflection and

transmission coefficients can be written in terms of $f(s)$ as described below.

Making $\xi \to -\infty$ in equation (5.10) and comparing it with far field condition for $\phi(\xi, \eta)$ in equation (5.8), we obtain

$$R = -\frac{2b\theta i k_0 \cosh k_0 h}{2k_0 h + \sinh 2k_0 h} \int_{-1}^{1} f(s) \sinh(k_0(h - y(s)) + is\theta)\ e^{ik_0 x(s)}\ ds. \tag{5.22}$$

Similarly making $\xi \to +\infty$ in equation (5.10) and using equation (5.8), we get

$$T = 1 - \frac{2b\theta i k_0 \cosh k_0 h}{2k_0 h + \sinh 2k_0 h} \int_{-1}^{1} f(s) \sinh(k_0(h - y(s)) - is\theta)\ e^{-ik_0 x(s)}\ ds. \tag{5.23}$$

In the next section we shall proceed to solve the integral equation (5.21) to find $f(s)$.

4. Solution of the Integral Equation:

We will use two methods to solve the integral equation (5.21) numerically.

Method I : Boundary Element Method

It is already known that $[\phi] = 0$ at the tips of the barrier, this asserts that $f(s) = 0$ at $s = \pm 1$.

Hence we construct

$$f(s) = \sqrt{1 - s^2}\ g(s) \tag{5.24}$$

where $g(s)$ is a regular function in $[-1, 1]$.

So substituting (5.24) in (5.21), the hypersingular integral equation can be rewritten as

$$\int_{-1}^{1} \sqrt{1 - s^2} \left\{ \frac{1}{(s - t)^2} + L(s, t) \right\} g(s) ds = \chi(t) \tag{5.25}$$

where $\chi(t) = 2\pi b\theta k_0 \frac{e^{ik_0 \xi(t)} \sinh(k_0(h - \eta(t)) + it\theta)}{\cosh k_0 h}$.

Now we divide the range of integration $[-1, 1]$ into m number of line elements i.e.

$[-1,1] = \bigcup_{j=1}^{m}[a_{j-1}, a_j]$, where a_{j-1} and a_j are the end points of jth line element and $a_0 = -1$, $a_m = 1$. and $a_j = a_0 + jr'$, $r' = \frac{a_m - a_0}{m}$.
Now we take $s = s_j$ where $s_j \in [a_{j-1}, a_j], j = 1, 2...., m$. So

$$s_j = (1-\tau)a_{j-1} + \tau a_j, \quad 0 \le \tau \le 1. \tag{5.26}$$

Also t belonging to line element joining a_{i-1} and a_i, we write $t = t_i = (1-\gamma)a_{i-1} + \gamma a_i,\ 0 \le \gamma \le 1\ ,\ i = 1, 2, ..., m$.
So, equation (5.25) can be rewritten as

$$\sum_{j=1}^{m} \int_0^1 \sqrt{1-s_j^2}\ \Big\{\frac{1}{(s_j - t_i)^2} + L(s_j, t_i)\Big\}\ g(s_j)\ r'\ d\tau = \chi(t_i)\ ,\ i = 1, 2, ..., m. \tag{5.27}$$

Now in this Boundary Element Method, we assume that the unknown function in the integral equation takes constant values in each small intervals, i.e. we take $g(s_j) = g_j$ as a constant for jth line element, $j = 1, 2, ..., m$. So, under this assumption Integral equation (5.27) is reduced to a system of linear equations which can be written as

$$\sum_{j=1}^{m}\ a_{ij}\ g_j = \chi_i\ ,\ i = 1, 2, ..., m \tag{5.28}$$

where

$$a_{ij} = \int_0^1 \sqrt{1-s_j^2}\{\frac{1}{(s_j - t_i)^2} + L(s_j, t_i)\}\ r'\ d\tau\ ,\ i = 1, 2, ..., m;\ \ j = 1, 2, ..., m, \tag{5.29}$$

$$\chi_i = \chi(t_i)\ ,\quad i = 1, 2, ..., m. \tag{5.30}$$

Now when $i = j$, the integral $\int_0^1 \frac{\sqrt{1-s_j^2}}{(s_j - t_i)^2}\ \ d\tau\ ,\ s_i, t_i\ \in [a_{i-1}, a_i]$ becomes hypersingular integral. It is difficult to find any quadrature formula to evaluate this hypersingular integral. However this can be evaluated exactly by simple algebraic manipulation and is given by

$$\int \frac{A(s)}{(s-t)^2}\ ds\ =\ \frac{t}{A(t)}\ \log\left|\frac{st - (1+A(t))(1+A(s))}{st - (1-A(t))(1+A(s))}\right|$$

$$- 2A(t)\left(\frac{\frac{s}{(1+A(s))A(t)} - \frac{t}{A(t)}}{(\frac{st}{1+A(s)} - 1)^2 - A(t)^2} \right) - \sin^{-1}(s) \tag{5.31}$$

where $A(s) = \sqrt{1-s^2}$.

Now choosing $t_i = \frac{a_i + a_{i-1}}{2}$, $i = 1, 2, ..., m$, the system of equation (5.28) is solved to obtain the unknown functions g_j, $j = 1, 2, ..m$ and hence $f(s_j)$ is approximated in each $[a_{j-1}, a_j]$. Hence $|R|$, $|T|$ can be evaluated as

$$R = -\frac{2\imath k_0 b\theta \cosh k_0 h}{2k_0 h + \sinh 2k_0 h} \sum_{j=1}^{m} g_j \int_0^1 \sqrt{1-s_j^2} \sinh\left(k_0(h - y(s_j)) + \imath s_j \theta\right) e^{\imath k_0 x(s_j)} \; r' \; d\tau. \tag{5.32}$$

$$T = 1 - \frac{2\imath k_0 b\theta \cosh k_0 h}{2k_0 h + \sinh 2k_0 h} \sum_{j=1}^{m} g_j \int_0^1 \sqrt{1-s_j^2} \sinh\left(k_0(h - y(s_j)) - \imath s_j \theta\right) e^{-\imath k_0 x(s_j)} \; r' \; d\tau. \tag{5.33}$$

Method II : Chebyshev polynomial approximation method

In this method we approximate $f(s)$ as

$$f(s) \;\approx\; \sqrt{1-s^2} \sum_{n=0}^{N} c_n U_n(s) \tag{5.34}$$

where N is an integer, $U_n(s)$ is the nth order Chebyshev polynomial of 2nd kind and c_n are unknown complex constants for each $n = 0, 1, 2....., N$.

Substituting $f(s)$ from (5.34) in (5.21), we find that the hypersingular integral equation (5.21) reduces to the following system of linear algebraic equation in c_n s.

$$\sum_{n=0}^{N} c_n \; A_n(t) \;=\; v(t) \;, \quad -1 \le t \le 1, \tag{5.35}$$

where

$$\begin{aligned} A_n(t) &= \int_{-1}^{1} \frac{\sqrt{1-s^2}}{(s-t)^2} \; U_n(s) \; ds \;-\; b^2\theta^2 \int_{-1}^{1} \sqrt{1-s^2} \; U_n(s) \; L(s,t) \; ds \\ &= -\pi(n+1) \; U_n(t) \;-\; b^2\theta^2 \int_{-1}^{1} \sqrt{1-s^2} \; U_n(s) \; L(s,t) \; ds, \end{aligned} \tag{5.36}$$

$$v(t) \;=\; 2\pi b\theta k_0 \; \frac{e^{ik_0\xi(t)}\sinh\left(k_0(h-\eta(t))+it\theta\right)}{\cosh k_0 h}. \tag{5.37}$$

Now to find the unknown coefficients c_n, we choose the collocation points $t = t_j$ as

$$t = t_j = \cos\Big(\frac{2j+1}{2N+2}\Big)\pi \;, \quad j = 0, 1, 2, ..., N. \tag{5.38}$$

Substituting t_j s from (5.38) in (5.35) , we get a system of $(N+1)$ linear equations in $(N+1)$ unknowns c_n s given by

$$\sum_{n=0}^{N} c_n \; A_n(t_j) \;=\; v(t_j) \;, \quad j = 0, 1, 2, ..., N. \tag{5.39}$$

Solving the above system equations, we can evaluate the constants $c_n,\ n = 0, 1, 2, ..., N$, and using these we can find the Reflection and Transmission coefficients as

$$R = -\frac{2\imath k_0 b\theta\cosh k_0 h}{2k_0 h+\sinh 2k_0 h}\sum_{n=0}^{N} c_n \int_{-1}^{1}\sqrt{1-s^2}\; U_n(s)\; \sinh\left(k_0(h-y(s))+\imath s\theta\right)e^{\imath k_0 x(s)}\; ds. \tag{5.40}$$

$$T = 1 - \frac{2\imath k_0 b\theta\cosh k_0 h}{2k_0 h+\sinh 2k_0 h}\sum_{n=0}^{N} c_n \int_{-1}^{1}\sqrt{1-s^2}\; U_n(s)\; \sinh\left(k_0(h-y(s))-\imath s\theta\right)e^{-\imath k_0 x(s)}\; ds. \tag{5.41}$$

5. Numerical Results:

The reflection coefficient $|R|$ and the transmission coefficient $|T|$ are computed numerically and depicted graphically against the wave number Kh after solving the hypersingular integral equations by boundary element method and the collocation method for various values of the non dimensional parameters $d/h,\ b/h$ and θ. The numerical values of $|R|$ and $|T|$ are evaluated from equations (5.32) and (5.33) respectively, once $f(y)$ satisfying the hypersingular integral equation is solved by boundary element method. In this method it is observed that the values of $|R|$ for fixed $Kh, d/h, b/h, \theta$ coincide up to four places of decimal if the system of linear equation (5.28) is solved for 25 to 30 line

elements for $\theta = \pi/10,\ 3\pi/10$ and 40 to 45 line elements for higher value of θ. Also the collocation method of solution of hypersingular integral equation gives the numerical values of $|R|$ and $|T|$ from equations (5.40) and (5.41). Here the values of $|R|$ coincide up to four decimal places for $N = 15$ and 20 in equation (5.35). The values of $|R|$ obtained from above mentioned two methods are presented for $d/h = 0.2,\ b/h = 0.2$ in the tables 5.1 to 5.5 and for various values of $\theta = \frac{(2n-1)\pi}{10};\ n = 1, 2, 3, 4, 5$ respectively. It is observed from the following tables that the difference between values of $|R|$ computed by two methods occur at fourth or fifth decimal places. This shows that $|R|$ obtained from two methods agree with each other reasonably well. However better accuracy can be achieved by increasing the number of line elements in equation (5.28) and N in equation (5.35) which requires very high speed computers. It may be mentioned here that the energy identity $|R|^2 + |T|^2 = 1$ is satisfied for various values of the parameter.

Table 5.1: Reflection coefficient for $\theta = \frac{\pi}{10};\ \frac{d}{h} = 0.2\ ;\ \frac{b}{h} = 0.2$

Kh	BEM	Collocation Method
0.2	0.000278079	0.000295432
0.8	0.00300751	0.003365431
1.6	0.0104197	0.01073812

Table 5.2: Reflection coefficient for $\theta = \frac{3\pi}{10};\ \frac{d}{h} = 0.2\ ;\ \frac{b}{h} = 0.2$

Kh	BEM	Collocation Method
0.2	0.000556401	0.00058391
0.8	0.013196	0.01328417
1.6	0.0515258	0.05149834

Table 5.3: Reflection coefficient for $\theta = \frac{5\pi}{10};\ \frac{d}{h} = 0.2\ ;\ \frac{b}{h} = 0.2$

Kh	BEM	Collocation Method
0.2	0.0130173	0.0131289
0.8	0.00429729	0.0043156
1.6	0.0435797	0.0438269

In the figure 5.2, the values of $|R|$ obtained by the present method for semicircular barrier are depicted against wave number and compared with the results of Liu and Li (2012) for $d/h = 0.5,\ b/h = 0.5\ \theta = \pi/2$. As mentioned in Chapter 1, the problem of wave

Table 5.4: Reflection coefficient for $\theta = \frac{7\pi}{10}$; $\frac{d}{h} = 0.2$; $\frac{b}{h} = 0.2$

Kh	BEM	Collocation Method
0.2	0.0339529	0.0338976
0.8	0.0470688	0.04734521
1.6	0.0493447	0.0495498

Table 5.5: Reflection coefficient for $\theta = \frac{9\pi}{10}$; $\frac{d}{h} = 0.2$; $\frac{b}{h} = 0.2$

Kh	BEM	Collocation Method
0.2	0.0552093	0.0556122
0.8	0.0540345	0.0539642
1.6	0.1341400	0.1343521

interaction with perforated semicircular barrier was considered by Liu and Li (2012) who used multipole expansion method to study the problem. In Table 1 of the work of Liu and Li (2012), numerical results for $|R|$ for impermeable semicircular barrier are presented. from figure 5.2, it is observed that $|R|$ for a semi-circular breakwater almost coincide with the data given in Table 1 of Liu and Li (2012). The figures 5.3 to 5.8 depicts $|R|$ against the wave number Kh for different values of arc length θ, depth of barrier below mean free surface d/h and radius of the circular barrier b/h. It is observed from the figures that

1. For fixed d/h and b/h, $|R|$ shows monotone increasing behaviour for $\theta = \pi/10,\ 3\pi/10$. However, for $\theta = \pi/2$, i.e., for semicircular barrier, $|R|$ shows oscillatory behaviour. This may be attributed to the fact that as the arc length of the barrier increases, there occurs a multiple reflections of waves between the bottom of the water region and the arcs of the semicircular barrier, as the two ends of the arc are nearer to the bottom of the water region. In fact this oscilatory behavior of $|R|$ occurs for semicircular barrier as d/h increases.

2. For fixed $\theta,\ d/h,\ |R|$ increases as radius increases.

3. For fixed $\theta, b/h, |R|$ decreases as d/h increases.

4. The work of Parsons and Martin (1994) shows that when the barrier is present in infinitely deep water region, $|R|$ decreases with increase of arc length of the barrier. However, in the present study, when the water region is of finite depth, such behaviour of the $|R|$ is not observed in general. It is seen from fig 5.4 that except for certain wave

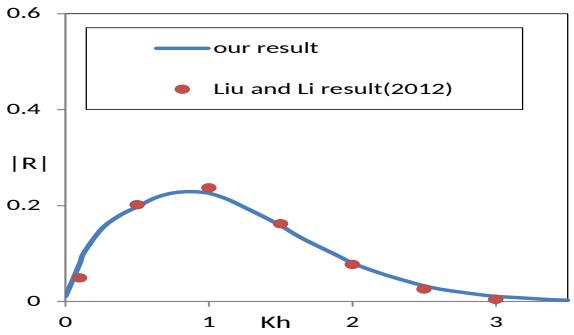

Figure 5.2: Comparison between our result and the results of Liu and Li for $d/h = 0.5$, $b/h = 0.5$ and $\theta = \frac{\pi}{2}$

number Kh, $|R|$ does not usually decrease with the increase of arc length of the barrier.

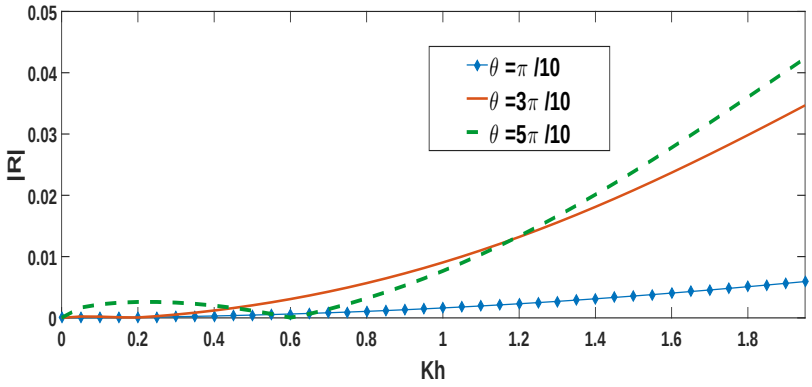

Figure 5.3: Reflection coefficient vs. wave number for different θ, $d/h = 0.1$, $b/h = 0.1$

6. Conclusion:

The problem of scattering of water waves by a impermeable curved barrier is studied by using first kind hypersingular integral equation based on judicious application of Green's integral theorem. The hyper singular integral equation is solved by two

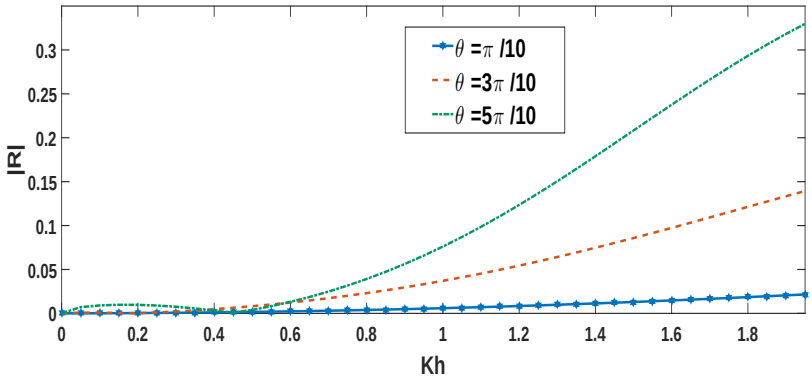

Figure 5.4: Reflection coefficient vs. wave number for different θ, $d/h = 0.1$, $b/h = 0.2$

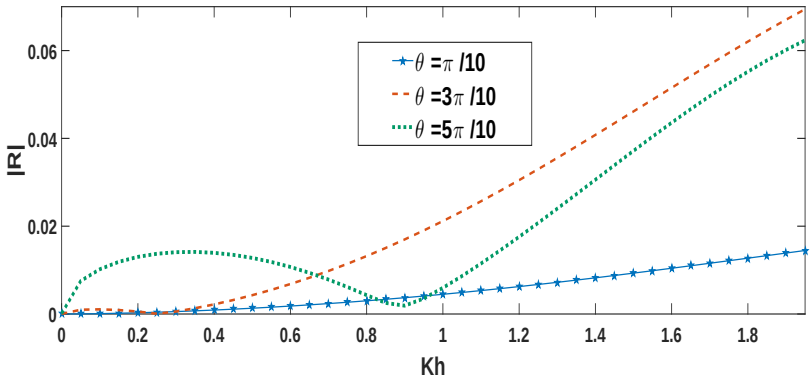

Figure 5.5: Reflection coefficient vs. wave number for different θ, $d/h = 0.2$, $b/h = 0.2$

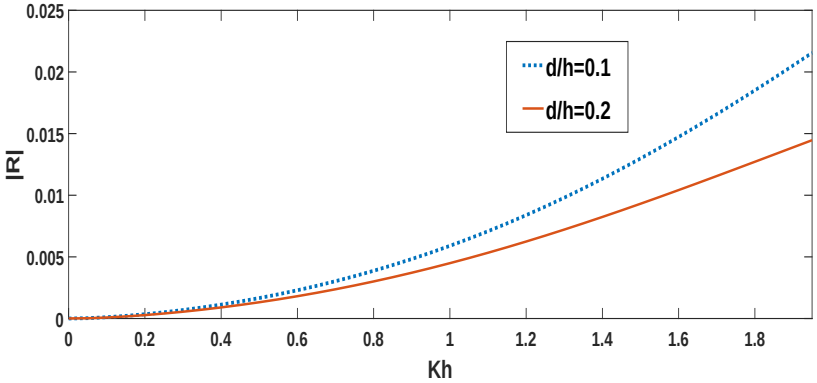

Figure 5.6: Reflection coefficient vs. wave number for different depth d/h where $b/h = 0.2$ and $\theta = \frac{\pi}{10}$

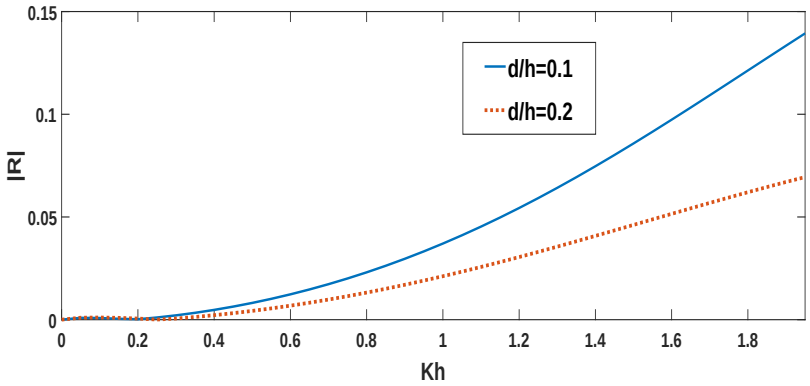

Figure 5.7: Reflection coefficient vs. wave number for different depth d/h where $b/h = 0.2$ and $\theta = \frac{3\pi}{10}$

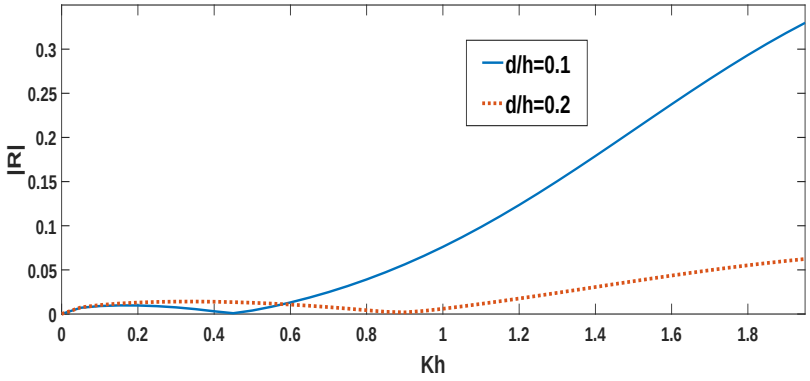

Figure 5.8: Reflection coefficient vs. wave number for different depth d/h where $b/h = 0.2$ and $\theta = \frac{5\pi}{10}$

methods viz, the Boundary Element Method and the Collocation Method. The collocation method based on Chebychef polynomial approximation is well known and widely used in numerical solution of the integral equations. However, the boundary element method is usually not very common in solving integral equation but it is a simple method which gives reasonably good results. The reflection coefficient, transmission coefficient are evaluated from the two method agrees reasonably well. Also the reflection coefficient evaluated by the present method are compared with the results in Liu Li (2012) and it was found that the results are in very good agreement with each other. From graphical results, the following conclusions are made.

1. For fixed radius of the barrier and for fixed depth of the barrier below the mean free

surface, it is observed that $|R|$ shows oscillatory behaviour for a semi circular barrier.

2. For fixed arc length of the barrier and for fixed depth of the barrier below the mean free surface, $|R|$ increases as radius of the barrier increases.

3. For fixed arc length and radius of the barrier, $|R|$ decreases as the depth of the barrier below the mean free surface increases.

4. It is observed from the literature that when the barrier is present in infinitely deep water region, $|R|$ decreases with increase of arc length of the barrier. However, in the present study, when the water region is of finite depth, it is observed that except for certain values of wave number, $|R|$ does not usually decrease with the increase of arc length of the barrier. This may be attributed to the interaction of the barrier with the depth of the water region.

Chapter 6

Water wave interaction with a circular arc shaped porous barrier submerged in a water of finite depth

1. Introduction

In this chapter we study the problem of scattering of water waves by a thin circular arc shaped porous barrier submerged in water of finite depth. It is already mentioned in chapter 1 that the problem of scattering of water waves by a porous coastal structure like rubble mound breakwater is important in coastal engineering as the pores in the barrier attenuates wave action by dissipating the wave energy and thereby protects the shore line or harbour. Many researchers used sophisticated mathematical techniques to study scattering problems involving porous barrier.

By judicious application of Green's integral theorem, the problem concerned is formu-

† The content of this chapter is based on the paper " Water wave interaction with a circular arc shaped porous barrier submerged in a water of finite depth ", *Journal of Engineering mathematics*, (Accepted for publication)

lated in terms of a hypersingular integral equation of second kind where the unknown function represents the difference of potential function across the curved barrier. The hypersingular integral equation is then solved by two methods viz, boundary element method (BEM) and the collocation method as decribed in Chapter 5. Using the solution of the hypersingular integral equation, obtained by both the methods, the reflection coefficient, transmission coefficient and energy dissipation coefficient are computed and depicted graphically against the wave number.

2. Problem Formulation:

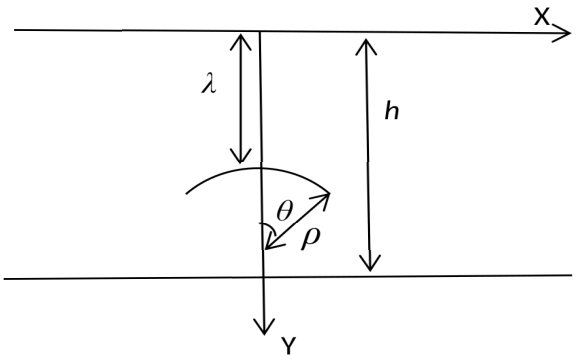

Figure 6.1: Geometry of the problem

We consider an irrotational motion in water due to the interaction of incident waves with a thin porous circular-arc shaped barrier Γ, submerged in water of finite depth h, as sketched in figure 6.1. A cartesian coordinate system is taken with x-axis along the undisturbed free surface and y-axis vertically downwards so that the water region is $0 < y < h$; $-\infty < x < \infty$. The barrier Γ is an arc of the circle of radius ρ and center at $(0, \lambda + \rho)$ and is placed such that it is symmetric about y-axis and the radius through end points make angle θ with y-axis, so that any point (x, y) on Γ is given by $x = \rho \sin \xi\theta, \quad y = \lambda + \rho - \rho \cos \xi\theta \ , \quad -1 \leq \xi \leq 1.$

Under the assumption of the linearised theory of water waves, a train of surface waves represented by the velocity potential $Re(\phi^{inc}(x, y)e^{-i\sigma t})$ and frequency σ is normally

incident from $x \to -\infty$ on the porous barrier Γ and is partially reflected by Γ and partially transmitted over and below Γ. Here

$$\phi^{inc} = \frac{\cosh k_0(h-y)e^{ik_0x}}{\cosh k_0 h} \tag{6.1}$$

where k_0 is the unique real positive root of the transcendental equation

$$k \tanh kh = K \tag{6.2}$$

with $K = \sigma^2/g$.
The scattered potential is described by $Re(\phi(x,y)e^{-i\sigma t})$ where $\phi(x,y)$ is the solution of the following boundary value problem.

$$\nabla^2\phi = 0; \qquad \text{in the fluid region,} \tag{6.3}$$

$$K\phi + \phi_y = 0 \quad \text{on} \quad y = 0, \tag{6.4}$$

$$\frac{\partial\phi}{\partial y} = 0 \quad \text{on} \quad y = h, \tag{6.5}$$

$$r^{1/2}\nabla\phi \qquad \text{is bounded as } r \to 0 \tag{6.6}$$

where r is the distance of any point of the fluid from the either sharp end of the barrier.

On the porous surface of the barrier Γ (cf. Yu (1995),Solitt and Cross (1972))

$$\frac{\partial\phi_{out}}{\partial n} = \frac{\partial\phi_{inn}}{\partial n} = \frac{\partial\phi}{\partial n} \quad \text{on} \quad \Gamma. \tag{6.7a}$$

$$\frac{\partial\phi}{\partial n} = -ik_0G\,[\phi](x,y) \quad \text{on} \quad \Gamma. \tag{6.7b}$$

Here the potential functions $\phi_{out}(x,y)$ is in the region $x^2+(y-\rho-\lambda)^2 > \rho^2$ and $\phi_{inn}(x,y)$ is in the region $x^2 + (y-\rho-\lambda)^2 < \rho^2$ and $\frac{\partial}{\partial n}$ denotes the normal derivative at a point on Γ and $[\phi](x,y) = \phi_{out}(x,y) - \phi_{inn}(x,y)$ is the potential difference across Γ and G is the porous-effect-parameter given by

$$G = G_r + iG_i \tag{6.8}$$

where G_r and G_i are related to the resistance coefficient and the inertial coefficient of the porous barrier Γ respectively (cf. Yu (1995)).
We note that the first equality in equation (6.7) indicates the continuity of normal fluxes at the perforated plate. The second equality indicates that the normal fluid velocity passing through the perforated plate is linearly proportional to the pressure difference between the both sides of the arc.
The far field condition is

$$\phi(x,y) \sim \begin{cases} \phi^{inc}(x,y) + R\phi^{inc}(-x,y) \text{ as } x \to -\infty, \\ T\phi^{inc}(x,y) \text{ as } x \to \infty \end{cases} \tag{6.9}$$

where R and T are the reflection and transmission coefficients respectively, which are to be determined.

3. Method of solution:

3.1 Reduction of the boundary value problem to a second kind hypersingular integral equation

In this section, following Parson and Martin (1994) we shall reduce the boundary value problem (6.1) to (6.9) to a hypersingular integral equation of second kind over the barrier Γ using Green's integral theorem. For this let us suppose that $\mathcal{G}(x,y;\alpha,\beta)$ be a source potential due to a line source at (α,β) in the fluid region. The $\mathcal{G}$ is given by (cf. Mondal et. al. (2021))

$$\mathcal{G}(x,y;\alpha,\beta) = \log\left(\frac{R}{R'}\right) - 2\int_0^\infty \left[\frac{\cosh k(h-y)\cosh k(h-\beta)}{k\sinh kh - K\cosh kh}\right.$$

$$+\frac{e^{-kh}\sinh k\beta\sinh ky}{k}\Big]\frac{\cos k(x-\alpha)}{\cosh kh}dk, \tag{6.10}$$

where $R, R' = \sqrt{(x-\alpha)^2+(y\mp\beta)^2}$.

Now applying Green's integral theorem to the function $\phi(x,y) - \phi^{inc}(x,y)$ and $\mathcal{G}(x,y;\alpha,\beta)$ in the fluid region suitably, we obtain the integral representation of potential function as

$$\phi(\alpha,\beta) = \phi^{inc}(\alpha,\beta) - \frac{1}{2\pi}\int_\Gamma [\phi](p)\frac{\partial}{\partial n_p}\mathcal{G}(x,y;\alpha,\beta)ds_p \tag{6.11}$$

where $p \equiv (x,y)$ is a point on barrier Γ, $[\phi](p)$ is the discontinuity of potential function $\phi(x,y)$ across Γ and $\frac{\partial}{\partial n_p}$ is the normal derivative at the point p on Γ. Since the unknown function $[\phi](p)$ vanishes at the tips of the arc barrier while its derivative has square root singularity there.

Now taking normal derivative of both sides of equation (6.11) at another point $q \equiv (\alpha,\beta)$ on the barrier, and using the boundary condition (6.7) given by

$$\frac{\partial\phi}{\partial n_q} = -ik_0G\,[\phi](q), \quad q \text{ on } \Gamma, \tag{6.12}$$

we finally obtain the integro-differential equation from equation (6.11) as

$$\frac{1}{2\pi}\frac{\partial}{\partial n_q}\int_\Gamma [\phi](p)\frac{\partial}{\partial n_p}\mathcal{G}(p;q)ds_p - ik_0G\,[\phi](q) = \frac{\partial\phi^{inc}}{\partial n_q}(\alpha,\beta), \quad q \text{ on } \Gamma. \tag{6.13}$$

Simplification of equation (6.13) produces the hypersingular integral equation of second kind for $[\phi]$ as

$$\frac{1}{2\pi}\int_\Gamma [\phi](p)\frac{\partial^2}{\partial n_q\partial n_p}\mathcal{G}(p,q)ds_p - ik_0G\,[\phi](q) = \frac{\partial\phi^{inc}}{\partial n_q}(\alpha,\beta), \quad q \text{ on } \Gamma \tag{6.14}$$

where

$$[\phi] = 0 \quad \text{at the two end points of } \Gamma. \tag{6.15}$$

In the equation (6.14) the hypersingular integral is understood in the sense of Hadamard finite part integral as given in Parsons and Martin (1994). To obtain the explicit form

of the kernel of (6.14), we parametrically represent the points $p \equiv (x, y)$ and $q \equiv (\alpha, \beta)$ as

$$x(\xi) = \rho \sin \xi\theta, \quad y(\xi) = \lambda + \rho - \rho \cos \xi\theta; \quad -1 \le \xi \le 1, \tag{6.16}$$

$$\alpha(\eta) = \rho \sin \eta\theta, \quad \beta(\eta) = \lambda + \rho - \rho \cos \eta\theta; \quad -1 \le \eta \le 1. \tag{6.17}$$

The unit normals n_p and n_q at the points p and q on barrier Γ are given by

$$n_p \equiv (-\sin \xi\theta, \cos \xi\theta); \quad n_q \equiv (-\sin \eta\theta, \cos \eta\theta). \tag{6.18}$$

Using relations (6.16) and (6.17) in (6.10), we simplified the kernel of integral equation (6.14) as

$$\frac{\partial^2 \mathcal{G}}{\partial n_q \partial n_p}(p; q) = -\frac{1}{\rho^2\ \theta^2\ (\xi - \eta)^2} + \mathcal{H}(\xi, \eta) \tag{6.19}$$

where the function $\mathcal{H}(\xi, \eta)$ represents the nonsingular part of the kernel. The expression for $\mathcal{H}(\xi, \eta)$ is given by

$$\begin{aligned}
\mathcal{H}(\xi, \eta) = &-\left[\frac{1}{4\rho^2 \sin^2 \frac{(\xi-\eta)\theta}{2}} - \frac{1}{\rho^2\theta^2(\xi-\eta)^2}\right] - \frac{X^2 - Y^2}{(X^2+Y^2)^2}\ \cos(\xi - \eta)\theta \\
&+ \frac{2XY}{(X^2+Y^2)^2}\ \sin(\eta - \xi)\theta - 2\sin\eta\theta \sin\xi\theta \int_0^\infty \mu(k) \sinh k\beta \sinh ky \cos kX\, dk \\
&+ 2\sin\eta\theta \cos\xi\theta \int_0^\infty \mu(k) \sinh k\beta \cosh ky \sin kX\, dk \\
&- 2\cos\eta\theta \sin\xi\theta \int_0^\infty \mu(k) \cosh k\beta \sinh ky \sin kX\, dk \\
&- 2\cos\eta\theta \cos\xi\theta \int_0^\infty \mu(k) \cosh k\beta \cosh ky \cos kX\, dk \\
&- \sin\eta\theta \sin\xi\theta \Bigg[\zeta i \cosh k_0(h-y) \cosh k_0(h-\beta)\ e^{ik_0|X|} \\
&- \sum_{n=1}^{\infty} \kappa_n \cos k_n(h-y) \cos k_n(h-\beta)\ e^{-k_n|X|} + \frac{2\pi}{h} \sum_{n=0}^{\infty} \epsilon_n \sin \epsilon_n y \sin \epsilon_n \beta\ e^{-\epsilon_n|X|}\Bigg] \\
&- \cos\eta\theta \cos\xi\theta \Bigg[\zeta i \sinh k_0(h-y) \sinh k_0(h-\beta)\ e^{ik_0|X|}
\end{aligned}$$

$$+\sum_{n=1}^{\infty}\kappa_n \sin k_n(h-y)\sin k_n(h-\beta)\ e^{-k_n|X|} - \frac{2\pi}{h}\sum_{n=0}^{\infty}\epsilon_n \cos\epsilon_n y \cos\epsilon_n\beta\ e^{-\epsilon_n|X|}\Bigg]$$
$$-\sin\eta\theta\cos\xi\theta\Bigg[\zeta\sinh k_0(h-y)\cosh k_0(h-\beta)\ e^{ik_0|X|}$$
$$-\sum_{n=1}^{\infty}\kappa_n \sin k_n(h-y)\cos k_n(h-\beta)\ e^{-k_n|X|} + \frac{2\pi}{h}\sum_{n=0}^{\infty}\epsilon_n \cos\epsilon_n y \sin\epsilon_n\beta\ e^{-\epsilon_n|X|}\Bigg]$$
$$+\cos\eta\theta\sin\xi\theta\Bigg[\zeta\cosh k_0(h-y)\sinh k_0(h-\beta)\ e^{ik_0|X|}$$
$$-\sum_{n=1}^{\infty}\kappa_n \cos k_n(h-y)\sin k_n(h-\beta)\ e^{-k_n|X|} + \frac{2\pi}{h}\sum_{n=0}^{\infty}\epsilon_n \sin\epsilon_n y \cos\epsilon_n\beta\ e^{-\epsilon_n|X|}\Bigg] \quad (6.20)$$

where k_0 and $\pm ik_n$ are roots of the trancendental equations $k\tanh kh - K = 0$; $i\epsilon_n$'s are roots of the equation $\cosh kh = 0$; $X = x-\alpha$; $Y = y+\beta$, and

$$\mu(k) = \tfrac{k\ e^{-kh}}{\cosh kh};\quad \zeta = \tfrac{4\pi k_0^2}{2k_0h+\sinh(2k_0h)};\quad \kappa_n = \tfrac{4\pi k_n^2}{2k_nh+\sin(2k_nh)}.$$

Also using relation (6.17) and equation (6.1), the expression for $\frac{\partial\phi^{inc}}{\partial n_q}(\alpha,\beta)$ in equation (6.14) can be simplified as

$$g(\eta) = \frac{\partial\phi^{inc}(\alpha,\beta)}{\partial n_q}$$
$$= -\frac{k_0 e^{ik_0\alpha(\eta)}}{\cosh k_0h}\sinh(k_0(h-\beta(\eta)) + i\eta\theta). \quad (6.21)$$

Writing $f(\xi) = [\phi(p(\xi))]$, where $[\phi(p(\xi))]$ represents the discontinuity of ϕ across the barrier at p, the simplified form of hypersingular integral equation (6.14) can be rewritten as

$$\int_{-1}^{1} f(\xi)\Bigg[\frac{1}{(\xi-\eta)^2} - \rho^2\theta^2\ \mathcal{H}(\xi,\eta)\Bigg]d\xi + 2\pi i\rho\theta k_0 G\ f(\eta) = 2\pi\rho\theta g(\eta),\quad -1\le\eta\le 1 \quad (6.22)$$

so that f satisfies the end conditions

$$f(\pm 1) = 0. \quad (6.23)$$

We will solve the above integral equation (6.22) by two method, (i) Boundary element

method, (ii) Collocation method.

3.2 Reflection and Transmission coefficient

The reflection and transmission coefficients can be obtained in terms of $f(\xi)$ in the following manner.
Making $\alpha \to -\infty$ in equation (6.11) and then comparing with far field condition (6.9) for $\phi(\xi, \eta)$, we obtain reflection coefficient as

$$R = -\frac{2\rho\theta i k_0 \cosh k_0 h}{2k_0 h + \sinh 2k_0 h} \int_{-1}^{1} f(\xi) \sinh(k_0(h - y(\xi)) + i\xi\theta)\ e^{ik_0 x(\xi)}\ d\xi. \tag{6.24}$$

Similarly, making $\alpha \to +\infty$ in equation (6.11), the transmission coefficient is given by

$$T = 1 - \frac{2\rho\theta i k_0 \cosh k_0 h}{2k_0 h + \sinh 2k_0 h} \int_{-1}^{1} f(\xi) \sinh(k_0(h - y(\xi)) - i\xi\theta)\ e^{-ik_0 x(\xi)}\ d\xi. \tag{6.25}$$

3.3 Solution of Integral Equation

We will use two method to solve the integral equation (6.22) numerically by the following two methods.

Method I : Boundary Element Method

To obtain the numerical solution of the hypersingular equation (6.22) along with the edge condition (6.23), we write $f(\xi)$ as

$$f(\xi) = \sqrt{1 - \xi^2}\ \psi(\xi), \tag{6.26}$$

where $\psi(\xi)$ is a regular function in $[-1, 1]$. The square root factor in (6.26) ensures that $f(\xi)$ has the correct behaviour at the ends of the porous barrier.

Noting $f(\xi)$ from equation (6.26), the hypersingular integral equation (6.22) can

be rewritten as

$$\int_{-1}^{1}\sqrt{1-\xi^2}\left[\frac{1}{(\xi-\eta)^2}-\rho^2\theta^2\ \mathcal{H}(\xi,\eta)\right]\psi(\xi)\ d\xi+2\pi i\rho\theta k_0 G\sqrt{1-\eta^2}\ \psi(\eta)$$
$$=2\pi\rho\theta g(\eta),\quad -1\le\eta\le 1. \tag{6.27}$$

Now we divide the domain of integration $[-1,1]$ into n number of line elements as $[-1,1]=\bigcup_{j=1}^{n}[a_{j-1},a_j]$ with end points $a_0=-1$ and $a_n=1$ and $a_j=a_0+jb$, where $b=\frac{a_n-a_0}{n}$.
Taking $\xi=\xi_j$ for $\xi_j\in[a_{j-1},a_j]$ i.e.

$$\xi_j=(1-\tau)a_{j-1}+\tau a_j,\quad 0\le\tau\le 1,\quad j=1,2,....,n \tag{6.28}$$

and $\eta=\eta_i\in[a_{i-1},a_i]$, for $\eta_i=(1-\gamma)a_{i-1}+\gamma a_i,\quad 0\le\gamma\le 1,\quad i=1,2,.....,n$, we rewrite equation (6.27) as

$$\sum_{j=1}^{n}\int_{0}^{1}\sqrt{1-\xi_j^2}\left[\frac{1}{(\xi_j-\eta_i)^2}-\rho^2\theta^2\ \mathcal{H}(\xi_j,\eta_i)\right]\psi(\xi_j)b\ d\tau+2\pi i\rho\theta k_0 G\sqrt{1-\eta_i^2}\psi(\eta_i)$$
$$=2\pi\rho\theta g(\eta_i),\quad i=1,2,....,n. \tag{6.29}$$

Now according to boundary element method approximation [cf. Banerjea et. al. (2019), Samanta et. al. (2022)], we assume that the unknown function in integral equation takes constant values in each small intervals i.e. we take $\psi(\xi_j)=\psi_j,\ j=1,2,...,n$ as a constant for j-th line element. So, the integral equation (6.29) is reduced to a system of linear equations

$$\sum_{j=1}^{n}c_{ij}\psi_j=2\pi\rho\theta g_i,\quad i=1,2,....,n \tag{6.30}$$

where

$$c_{ij}=\int_{0}^{1}\sqrt{1-\xi_j^2}\left[\frac{1}{(\xi_j-\eta_i)^2}-\rho^2\theta^2\ \mathcal{H}(\xi_j,\eta_i)\right]b\ d\tau+\delta_{ij}2\pi i\rho\theta k_0 G\sqrt{1-\eta_i^2}. \tag{6.31}$$

Here δ_{ij} is Kronecker delta and

$$g_i = g(\eta_i), \quad i = 1, 2, ..., n. \tag{6.32}$$

Now, for $i = j$, the integral $\int_0^1 \frac{\sqrt{1-\xi_i^2}}{(\xi_j-\eta_i)^2}\ d\tau$, $(\xi_i,\ \eta_i) \in [a_{i-1}, a_i]$ in the coefficient c_{ij} in (6.30) is hypersingular which can be evaluated exactly by simple algebraic manipulation as mentioned in chapter 5 and is given by [cf. Samanta et. al. (2022)]

$$\int \frac{A(\xi)}{(\xi-\eta)^2}\ d\xi = \frac{\eta}{A(\eta)} \log\left|\frac{\xi\eta - (1+A(\eta))(1+A(\xi))}{\xi\eta - (1-A(\eta))(1+A(\xi))}\right| - 2A(\eta)\left(\frac{\frac{\xi}{(1+A(\xi))A(\eta)} - \frac{\eta}{A(\eta)}}{(\frac{\xi\eta}{1+A(\xi)} - 1)^2 - A(\eta)^2}\right) - \sin^{-1}(\xi) \tag{6.33}$$

where $A(\xi) = \sqrt{1-\xi^2}$.

Now solving the system of linear equation (6.30), we obtain the unknown function ψ_j for $j = 1, 2, ..., n$, and $f(\xi_j)$ is approximated in each line intervals to evaluate R and T from equation (6.24) and (6.25) as

$$R = -\frac{2\rho\theta i k_0 \cosh k_0 h}{2k_0 h + \sinh 2k_0 h} \sum_{j=1}^{n} \psi_j \int_0^1 \sqrt{1-\xi_j^2} \sinh(k_0(h - y(\xi_j)) + i\xi_j\theta)\ e^{ik_0 x(\xi_j)} b\ d\tau, \tag{6.34}$$

$$T = 1 - \frac{2\rho\theta i k_0 \cosh k_0 h}{2k_0 h + \sinh 2k_0 h} \sum_{j=1}^{n} \psi_j \int_0^1 \sqrt{1-\xi_j^2} \sinh(k_0(h - y(\xi_j)) - i\xi_j\theta)\ e^{-ik_0 x(\xi_j)} b\ d\tau. \tag{6.35}$$

Method II : Collocation method

Here we approximate $f(\xi)$, keeping in mind the behavior of it at tips of barrier, as

$$f(\xi) \approx \sqrt{1-\xi^2} \sum_{n=0}^{N} d_n U_n(\xi) \tag{6.36}$$

where N is an integer, $U_n(\xi)$ is the nth order Chebyshev polynomial of 2nd kind and d_n are unknown complex constants for each $n = 0, 1, 2....., N$.

With $f(\xi)$ given by (6.36), the hypersingular part of equation (6.22) can be evaluated as

$$\int_{-1}^{1} \frac{\sqrt{1-\xi^2}\ U_n(\xi)}{(\xi-\eta)^2} d\xi \ = \ -\ \pi(n+1)U_n(\eta) \tag{6.37}$$

Substituting (6.36) in the hypersingular integral equation (6.22), and noting the relation (6.37) we obtain

$$\sum_{n=0}^{N} d_n\ B_n(\eta)\ = 2\pi\rho\theta\ g(\eta)\ , \quad -1 \le \eta \le 1 \tag{6.38}$$

where

$$B_n(\eta) = -\ \pi(n+1)U_n(\eta)\ -\ \rho^2\theta^2 \int_{-1}^{1} \sqrt{1-\xi^2}\ U_n(\xi)\ \mathcal{H}(\xi,\eta)\ d\xi$$
$$+2\pi i\rho\theta k_0 G\sqrt{1-\eta^2}\ U_n(\eta). \tag{6.39}$$

Choosing the collocation points $\eta = \eta_j, \quad j = 0, 1, ..., N$ as

$$\eta_j = \cos\Big(\frac{2j+1}{2N+2}\Big)\pi, \quad j = 0, 1, 2, ..., N \tag{6.40}$$

in (6.38), we obtain a system of linear equations

$$\sum_{n=0}^{N} d_n B_n(\eta_j)\ = 2\pi\rho\theta\ g(\eta_j), \quad j = 0, 1, 2, ..., N \tag{6.41}$$

for the determination of the constants d_ns.

The reflection and transmission coefficients are evaluated from equation (6.24) and (6.25) as

$$R = -\frac{2\rho\theta i k_0 \cosh k_0 h}{2k_0 h + \sinh 2k_0 h} \sum_{n=0}^{N} d_n \int_{-1}^{1} \sqrt{1-\xi^2}\ U_n(\xi) \sinh(k_0(h-y(\xi)) + i\xi\theta)\ e^{ik_0 x(\xi)}\ d\xi, \tag{6.42}$$

$$T = 1 - \frac{2\rho\theta i k_0 \cosh k_0 h}{2k_0 h + \sinh 2k_0 h} \sum_{n=0}^{N} d_n \int_{-1}^{1} \sqrt{1-\xi^2}\ U_n(\xi) \sinh(k_0(h-y(\xi)) - i\xi\theta)\ e^{-ik_0 x(\xi)}\ d\xi. \tag{6.43}$$

3.4 Energy Identity:

Porosity of the plate Γ causes the dissipation of wave energy, in which case $|R|^2 + |T|^2 < 1$. Mathematically we can justify this by using Green's Integral theorem to the functions ϕ and $\overline{\phi}$ in the region bounded by $-X \le x \le X,\ y = 0;\quad x = -X,\ 0 \le y \le h;\quad -X \le x \le X,\ y = h;\quad x = X,\ 0 \le y \le h$; and a closed contour enclosing the porous barrier Γ. Then making $X \to \infty$ we obtain the energy identity as

$$|R|^2 + |T|^2 = 1 - J \tag{6.44}$$

where

$$J = \frac{2KG_r\rho\theta\cosh k_0 h}{k_0 h + \frac{1}{2}\sinh 2k_0 h} \int_{-1}^{1} \left|f(\xi|)\right|^2 d\xi \tag{6.45}$$

is the energy dissipation coefficient. From the relation (6.44), it is clear that $|R|^2+|T|^2 < 1$ for $G_r \neq 0$ i.e., $G \neq 0$ i.e. wave energy-dissipation always occurs if the barrier is porous. It may be noted that $J = 0$ for $G = 0$.

4. Numerical Results

In this section, the numerical results for reflection and transmission coefficients and energy dissipation coefficient are depicted graphically against the dimensionless wave number Kh for various values of the non dimensional parameters $\theta,\ \frac{\lambda}{h},\ \frac{\rho}{h},\ G$. Here $\theta,\ \frac{\lambda}{h},\ \frac{\rho}{h},\ G$ represent arc length of the barrier, depth of submergence of the barrier below the mean free surface, radius of the circular barrier and the porosity parameter respectively. From equation (6.8) we have $G = G_r + iG_i$, where $G_r = Re[G]$ denotes the resistance coefficient of the porous barrier while $G_i = Im[G]$ denotes the inertial coefficient of the porous barrier. Large value of inertial coefficient denotes large pores in the barrier which allow the water to pass through it while large value of the resistance coefficient restricts the passage of water through the pores of the barrier. For a porous

medium where the resistance coefficient dominates the inertial coefficient, the porosity parameter G can be considered as real [cf. Yu (1995)]. Also $G = 0$ corresponds to rigid barrier.

In the Tables 6.1, 6.2 and 6.3, the reflection coefficients obtained by solving the hypersingular integral equation (6.22) by boundary element method and collocation method are compared for $\theta = \frac{\pi}{10}, \frac{3\pi}{10}, \frac{5\pi}{10}$ respectively and $\frac{\lambda}{h} = 0.2$; $\frac{\rho}{h} = 0.6$; $G = 1$. It is observed from the following tables that the reflection coefficients by both the method agree with each other till five places of decimal taking $N = 11$ in equation (6.41) and 35 line elements in equation (6.30). Better accuracy can be achieved by increasing the number of line element in equation (6.30) and increasing the number of collocation points N in equation (6.41).

Table 6.1: Reflection coefficient for $\theta = \frac{\pi}{10}$; $\frac{\lambda}{h} = 0.2$; $\frac{\rho}{h} = 0.6$; $G = 1$

Kh	BEM	Collocation Method
0.5	0.0095919	0.0095898
1.0	0.0318140	0.0318252
1.5	0.0614684	0.0614722
2.0	0.0886124	0.0886198

Table 6.2: Reflection coefficient for $\theta = \frac{3\pi}{10}$; $\frac{\lambda}{h} = 0.2$; $\frac{\rho}{h} = 0.6$; $G = 1$

Kh	BEM	Collocation Method
0.5	0.0083070	0.0083095
1.0	0.0339673	0.0339718
1.5	0.0519162	0.0519198
2.0	0.0543681	0.0543721

Table 6.3: Reflection coefficient for $\theta = \frac{5\pi}{10}$; $\frac{\lambda}{h} = 0.2$; $\frac{\rho}{h} = 0.6$; $G = 1$

Kh	BEM	Collocation Method
0.5	0.2232330	0.2232391
1.0	0.2129352	0.2129402
1.5	0.1695932	0.1695996
2.0	0.1344371	0.1344427

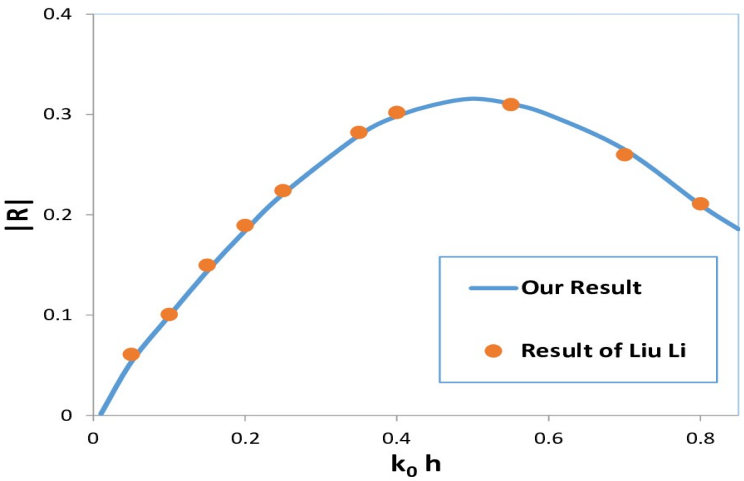

Figure 6.2: Comparison of $|R|$ between the results obtained by Liu and Li ? and our results with $\lambda/h = 0.1$, $\rho/h = 0.9$, $\theta = \pi/2$ and $G_0 = Gk_0h = 0.5$

In fig 6.2, the reflection coefficient obtained by using the methods in the present paper is compared with the results obtained by Liu and Li (2012) in 'fig.2'. This figure depicts $|R|$ against k_0h for $\lambda/h = 0.1$, $\rho/h = 0.9$, $\theta = \pi/2$, $G_0 = Gk_0h = 0.5$. This result corresponds to the problem of wave interaction with semicircular bottom standing porous barrier which was considered earlier by Liu and Li (2012) using a different method. From fig 6.2 it is observed that the reflection coefficients obtained in the present paper are in good agreement with 'fig.2' in Liu and Li (2012) for $\lambda/h = 0.1$, $\rho/h = 0.9$, $\theta = \pi/2$, $G_0 = Gk_0h = 0.5$.

In figures 6.3a and 6.3b, $|R|$ is depicted against the wave number Kh for different porosity parameter $G = 0,\ 1,\ 1 + i/2$, $\lambda/h = 0.1$, $\rho/h = 0.1$, $\theta = \frac{\pi}{10}$ and $\frac{3\pi}{10}$ respectively. The graph of $|R|$ for $G = 0$ corresponds to the rigid barrier which coincides with the results in Mondal et. al. (2021). For $G = 1$ it is already mentioned that the resistance coefficient dominated the porous coefficient. It is observed from both the figures 6.3a and 6.3b that as G changes from 0 to 1 and then $1 + i/2$ the value of $|R|$ decreases for a particular Kh. This shows that larger the value of inertial coefficient smaller is the value of $|R|$. So porosity of the barrier reduces the reflection of the surface waves. From figure 6.2a it is observed that for small values of the wave number Kh, $|R|$ almost

coincides for $G = 0, 1, 1 + i/2$. This is plausible because the barrier is near the surface ($\lambda/h = 0.1$) and so the long waves which are near the sea bottom are unaffected by the porosity of the barrier.

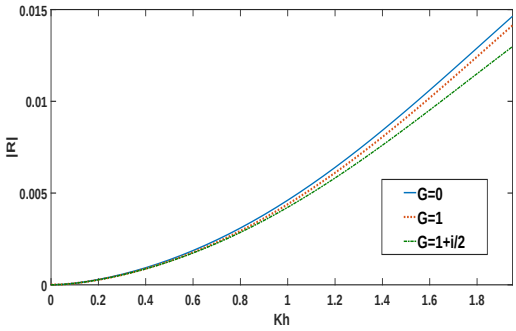

6.3a

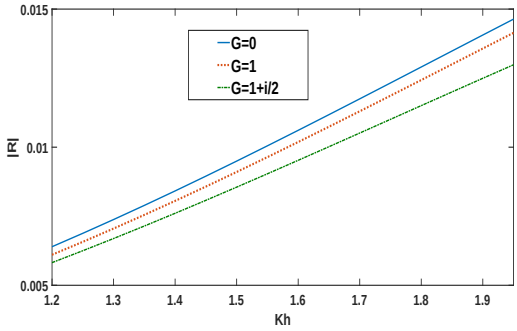

6.3b

Figure 6.3: Reflection coefficient against wave number for different porosity parameter . where (2a) $\lambda/h = 0.1,\ \rho/h = 0.1,\ \theta = \frac{\pi}{10}$; (2b) $\lambda/h = 0.1,\ \rho/h = 0.1,\ \theta = \frac{3\pi}{10}$

In Figures 6.4 and 6.5, $|R|,\ |T|$, and J are plotted against the wave number Kh for $\lambda/h = 0.1$, and $\theta = \frac{\pi}{10}$ for different radius ρ/h of the circular barrier and for the porosity parameter $G = 1,\ 1 + i/2$ respectively.

Now, from figures 6.4 and 6.5 it is observed for a fixed Kh, $|R|$, and J increases while $|T|$ decreases as the radius of the barrier ρ/h increases. This shows that an increase in the length of the radius induces more reflection and dissipation of wave energy. Also for a fixed radius, as Kh increases, $|R|$ and J increases and $|T|$ decreases showing that more energy dissipation and reflection of the short waves occur. Also for any fixed values of $\lambda/h,\ \rho/h$ and θ; $|R|,\ J$ decreases while $|T|$ increases as G changes from $G = 1$ to $G = 1 + i/2$. This shows that as the inertial coefficient G_i of the porosity parameter G increases, the reflection and energy dissipation coefficient decrease while transmission coefficient increases. This is plausible since the increase in inertial coefficient of the porosity parameter G implies that the pores in the barrier are bigger in size which allow the water to pass through them and thereby increasing the transmission and decreasing the reflection. This phenomena is also observed in figures 6.3a and 6.3b.

Figures 6.6 and 6.7 depict $|R|,\ |T|,\ J$ against Kh for different depths of the barrier below the mean free surface for $G = 1$ and $G = 1 + i/2$ respectively. From figures 6.6 and

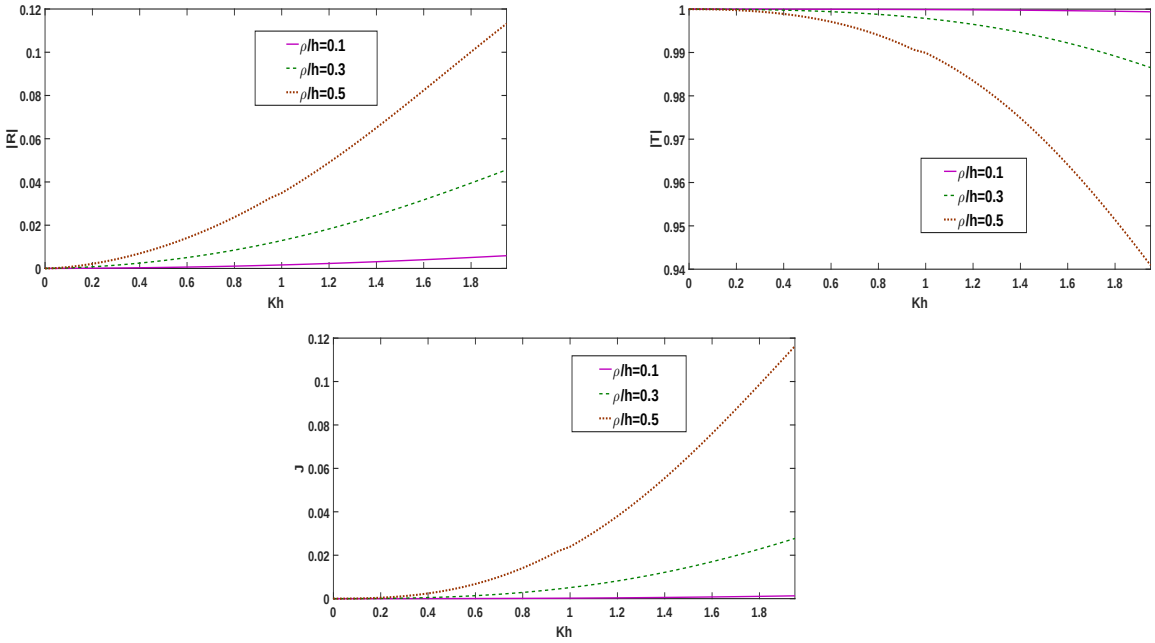

Figure 6.4: Reflection and Transmission coefficient and energy dissipation vs. wave number for different radius ρ, for $\lambda/h = 0.1$, $G = 1$, $\theta = \frac{\pi}{10}$

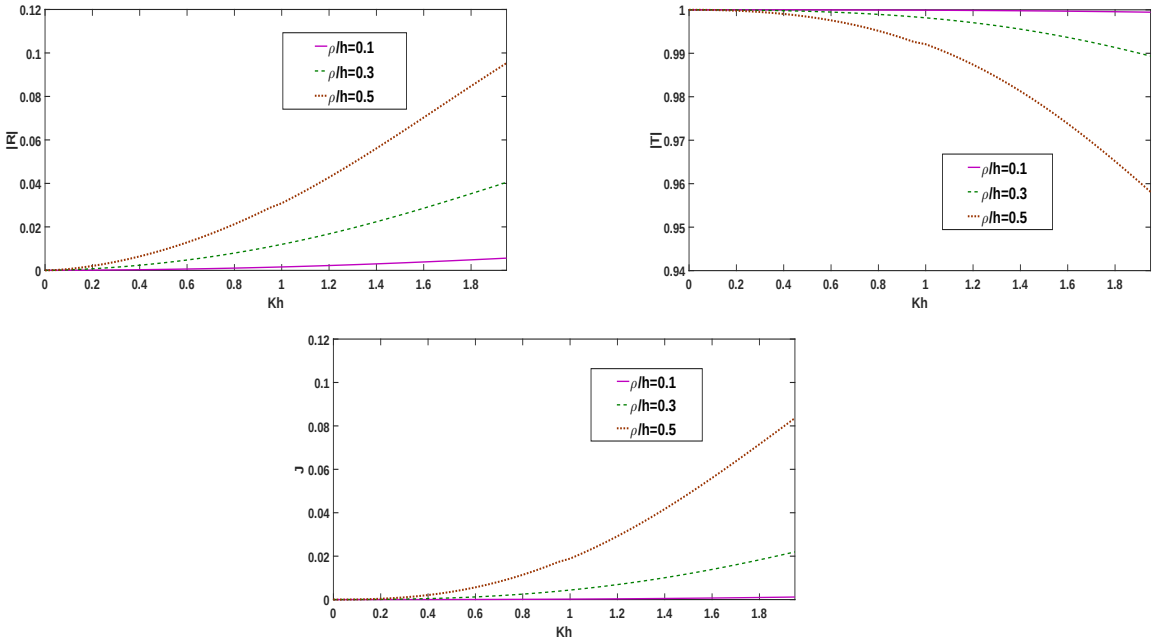

Figure 6.5: Reflection and Transmission coefficient and energy dissipation vs. wave number for different radius ρ, for $\lambda/h = 0.1$, $G = 1 + \frac{i}{2}$, $\theta = \frac{\pi}{10}$

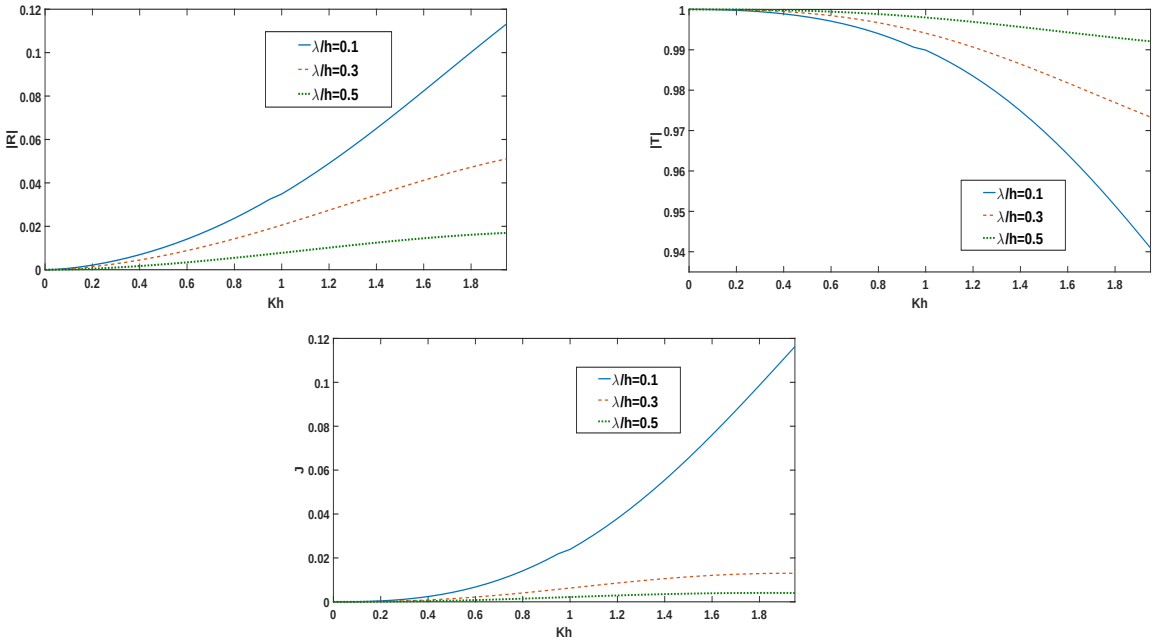

Figure 6.6: Reflection and Transmission coefficient and energy dissipation against wave number for different depth λ. where $\rho/h = 0.5$, $G = 1$, $\theta = \frac{\pi}{10}$

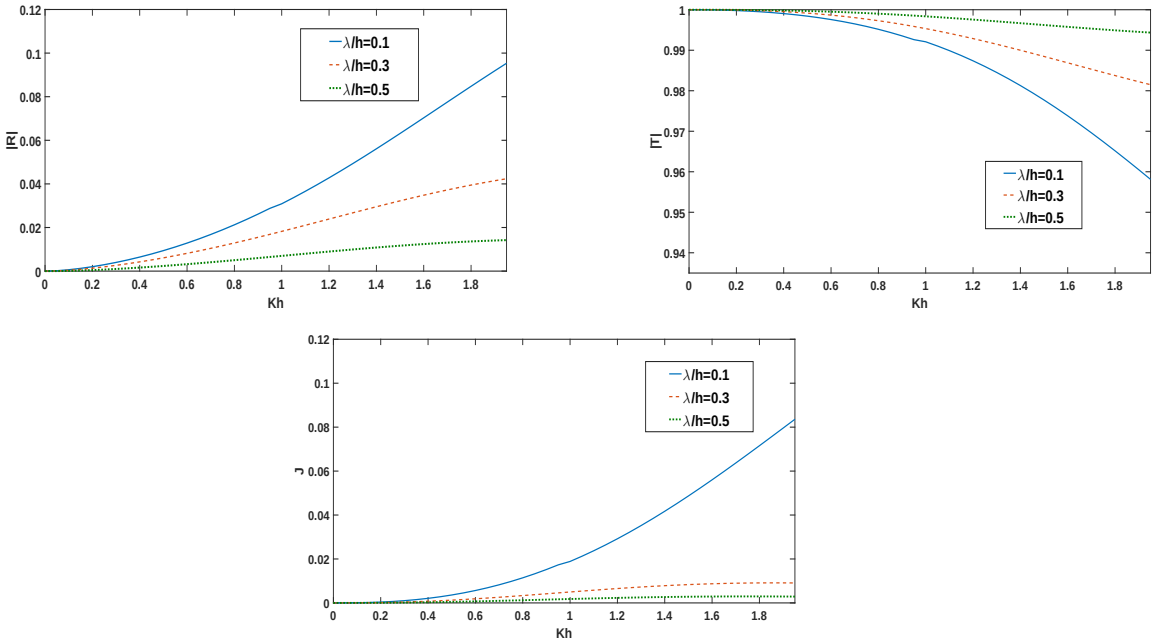

Figure 6.7: Reflection and Transmission coefficient and energy dissipation against wave number for different depth λ. where $\rho/h = 0.5$, $G = 1 + \frac{i}{2}$, $\theta = \frac{\pi}{10}$

6.7 it is observed that for fixed value of G, θ, ρ/h, and Kh, $|R|$, J decreases while $|T|$ increases as λ/h increases. This is plausible because as the depth of the barrier below the mean free surface increases, more wave energy is transmitted above the barrier reducing the reflection thereby.

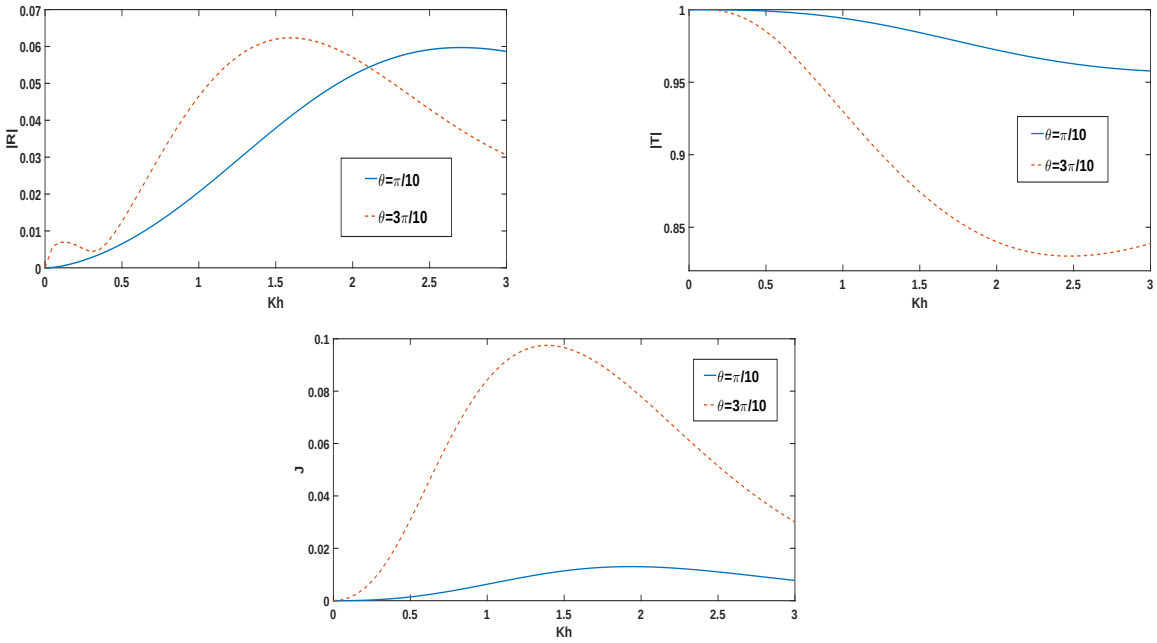

Figure 6.8: Reflection and Transmission coefficient and energy dissipation against wave number for different arc length where $\lambda/h = 0.3$, $\rho/h = 0.5$, $G = 1$

Figure 6.8 and 6.9 depicts $|R|$, $|T|$, J for various values of θ. A small oscillation in $|R|$ is observed from Fig 6.9, as the arc length θ increases. For fixed values of ρ/h, λ/h, G, it is observed that after a certain value of the wave number Kh, $|R|$ decreases rapidly with Kh as θ increases. This shows that the reflection of the short waves which are near the free surface decrease as the arc length of the barrier increases. However, as the arc length of the barrier increases, J increases while $|T|$ decreases. For a fixed arc length, J increases with Kh, reaches a maximum and then decrease with Kh.

5. Conclusion

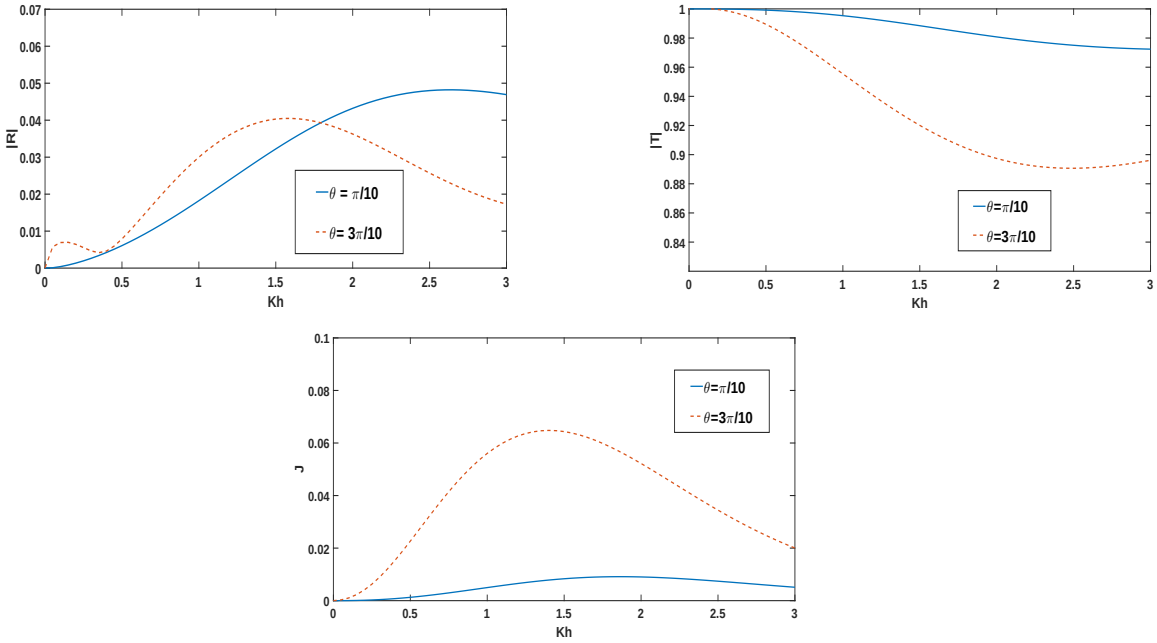

Figure 6.9: Reflection and Transmission coefficient and energy dissipation against wave number for different arc length where $\lambda/h = 0.3$, $\rho/h = 0.5$, $G = 1 + \frac{i}{2}$

The problem of scattering of water waves by a thin circular arc shaped porous barrier submerged in finite depth ocean is studied by using hypersingular integral equation formulation. Using Green's integral theorem suitably, the corresponding boundary value problem is reduced to a hypersingular integral equation of second kind in an unknown function representing the difference of potential function across the curved barrier. The hypersingular integral equation is then solved by two methods viz, the boundary element method and the collocation method. Using the solution of the hypersingular integral equation, the reflection coefficient, transmission coefficient and energy dissipation coefficient are computed and depicted graphically against the wave number. It was observed that the reflection, transmission and energy dissipation coefficients obtained by using the solution by both the methods, of the second kind hypersingular integral equation are in good agreement. The collocation method is a well known method which is usually used for solving hypersingular integral equation but the boundary element method used here is a simple method and is relatively less known method for solving hypersingular integral equation. Also the reflection coeffi-

cients corresponding to the problem of water wave scattering by a semicircular bottom standing barrier, obtained by using the methods described in the present paper is compared with the known results given by Liu and Li (2012). It was observed that the results are in good agreement.

From the graphical result the following observations are made:

1. The reflection and energy dissipation coefficient decrease while transmission coefficient increases as inertial coefficient of the porosity parameter G increases.

2. An increase in the length of the radius induces more reflection and dissipation of wave energy for fixed values of porosity parameter, arc length and the depth of submergence of the barrier below the mean free surface.

3. For fixed values of porosity parameter, arc length and radius of the barrier, as the depth of submergence of the barrier below the mean free surface increases, more wave energy is transmitted above the barrier reducing the reflection.

4. The reflection of the short waves which are near the free surface decrease as the arc length of the barrier increases.

This method based on hypersingular integral equation formulation is an efficient method which can be used for other suitable configurations of the circular arc shaped porous or rigid barrier.

PART IV

Water wave scattering problems by thick barrier

Chapter 7

Scattering of water waves by thick rectangular barrier in presence of ice cover

1. Introduction

Assuming linear theory, the two dimensional problem of water wave scattering by thick rectangular barrier in presence of thin ice cover, is investigated in this chapter. As mentioned in chapter 1, breakwaters in form of a thick vertical barrier with rectangular cross sections present in water with free surface has been studied by many researchers. When the water is covered with a thin sheet of ice which is modelled as a thin elastic plate, the corresponding water wave propagation problems in presence of thick rectangular barrier are of some interest to oceanographers. In this chapter, four types of thick barrier configurations are considered, viz, partially immersed, bottom standing, fully submerged upto a finite depth in water and in form of a thick rectangular wall with a submerged gap.

† The content of this chapter is based on the paper " Scattering of water waves by thick rectangular barriers in presence of ice cover", *Journal of Ocean Engineering and Science*, 5(3) (2020) 279-293.

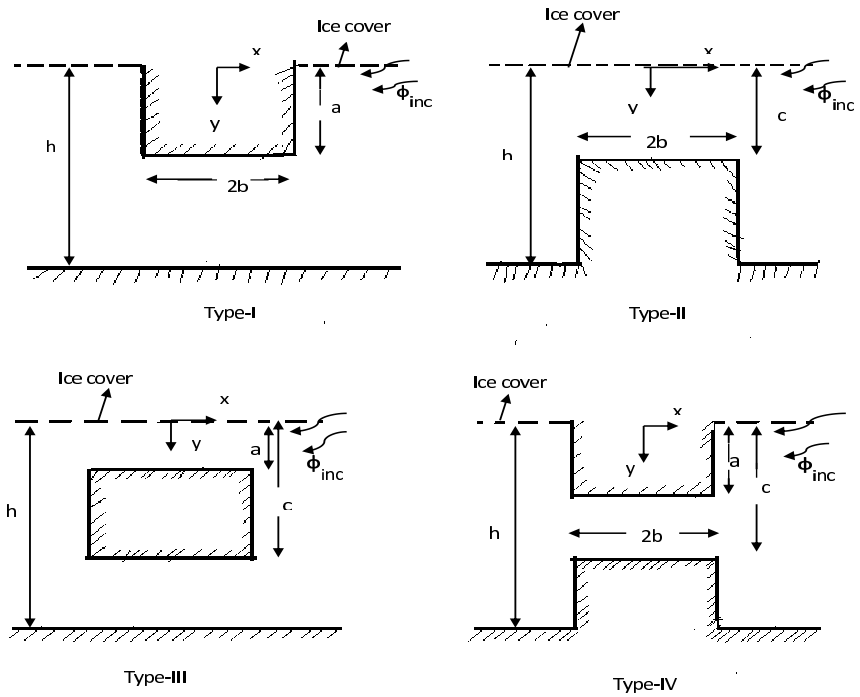

Figure 7.1: Figures of thick barriers

2. Problem Construction

We consider two dimensional irrotational motion due to presence of a thick barrier of uniform rectangular cross section, in water with a thin layer of ice cover on its upper surface. We choose a rectangular cartesian coordinate system in which the x axis is along the mean ice cover surface and y axis vertically downward so that the water occupies the region $0 < y < h$. The rectangular thick barrier of uniform thickness $2b$ is present in the water symmetrically about y axis. Four different configurations of the barrier are considered as shown in fig 7.1, so that the wetted part of barrier occupies the region $-b \leq x \leq b$ and $y \in L = L_j, j = 1, 2, 3, 4$. Here $L_1 = (0, a)$ for partially immersed barrier (type-I); $L_2 = (c, h)$ for bottom standing barrier (type-II); $L_3 = (a, c)$ for barrier which is fully submerged upto a finite depth in water (type-III) and $L_4 = (0, a) + (c, h)$, $0 \leq a \leq c \leq h$ for corresponding for thick rectangular wall with a submerged gap (type-IV).

Considering ice cover as an elastic plate, we study the motion due to interaction of a train of normally incident surface wave from positive infinity with the ice cover and the barrier. The the normally incident wave train is represented by the velocity potential $Re(\phi^{inc}(x,y)e^{-i\sigma t})$, where

$$\phi^{inc} = \frac{2\cosh\lambda_0(h-y)e^{-i\lambda_0(x-b)}}{\cosh\lambda_0 h} \tag{7.1}$$

and λ_0 is the unique real positive root of the transcendental equation

$$k(1-\epsilon K+Dk^4)\tanh kh = K. \tag{7.2}$$

Here $K = \sigma^2/g$, σ is the circular frequency of incoming wave train, g is gravitational acceleration and $D = \frac{Eh_0^3}{12(1-\upsilon^2)\rho_1 g}$, $\varepsilon = \frac{\rho_0 h_0}{\rho_1}$, ρ_0 is the density of ice, ρ_1 is the density of water, h_0 is the small thickness of the ice-cover and E, υ respectively are the Youngs modulus and Poissons ratio of the ice. Let the resulting motion in the fluid be described by the velocity potential $Re[\phi^{inc}(x,y)e^{-i\sigma t}]$ where $\phi(x,y)$ satisfies the following boundary value problem.

$$\nabla^2\phi = 0; \qquad \text{in the fluid region,} \tag{7.3}$$

$$(D\frac{\delta^4}{\delta x^4}+1-\varepsilon K)\phi_y + K\phi = 0; \qquad \text{on } y=0, \begin{cases} |x|>b & \text{for type I, IV barrier,} \\ |x|<\infty & \text{for type II, III barrier,} \end{cases} \tag{7.4}$$

$$\phi_x = 0, \qquad \text{on x=± b,} \qquad y \,\epsilon\, L_j \text{ for j=1,2,3,4,} \tag{7.5}$$

$$r^{1/3}\nabla\phi \quad \text{is bounded as r} \to 0 \tag{7.6}$$

where r is the distance of submerged edge of the thick barrier,

$$\phi_y = 0, \qquad \text{on } y=l_j,\ |x|<b \text{ for } j-th \text{ barrier type, j=1,2,3,4,} \tag{7.7}$$

$$\phi_y = 0, \qquad \text{on y=h,} \begin{cases} |x| > b & \text{for type II,IV barrier,} \\ |x| < \infty & \text{for type I,III barrier} \end{cases} \tag{7.8}$$

and finally,

$$\phi(x,y) \sim \begin{cases} \phi^{inc}(x,y) + R\phi^{inc}(-x,y) \text{ as } x \to \infty, \\ T\phi^{inc}(x,y) \text{ as } x \to -\infty. \end{cases} \tag{7.9}$$

Here R and T are the reflection and transmission coefficients and are to be determined for each barrier configuration. In equation(7.7), $l_1 = a$; $l_2 = c$; $l_3 = a, c$; $l_4 = a, c$ corresponding to type I, II, III and IV barrier configurations as depicted in Figure 7.1.

3. Method of solution

Due to the geometrical symmetry of the rectangular barrier about $x = 0$; $\phi(x,y)$ can be split into symmetric and antisymmetric parts, $\phi^{sm}(x,y)$ and $\phi^{ansm}(x,y)$, respectively, so that

$$\phi(x,y) = \phi^{sm}(x,y) + \phi^{ansm}(x,y) \tag{7.10}$$

where

$$\phi^{sm}(-x,y) = \phi^{sm}(x,y), \qquad \phi^{ansm}(-x,y) = -\phi^{ansm}(x,y). \tag{7.11}$$

Therefore, we consider only the region $x \geq 0$. Now $\phi^{sm,ansm}(x,y)$ satisfy equations (7.3) to (7.8) together with

$$\phi^{sm}_x(0,y) = 0 \qquad \phi^{ansm}(0,y) = 0 \qquad 0 < y < h. \tag{7.12}$$

Let the behavior of $\phi^{sm,ansm}(x,y)$ for large x be represented by

$$\phi^{sm,ansm}(x,y) \sim \frac{\cosh\lambda_0(h-y)}{\cosh\lambda_0 h}[e^{-i\lambda_0(x-b)} + R^{sm,ansm}e^{i\lambda_0(x-b)}], \text{ as } x \to \infty \tag{7.13}$$

where R^{sm} and R^{ansm} are unknown constants. These constants are related to R and T by

$$R, T = \frac{1}{2}(R^{sm} \pm R^{ansm})\ e^{-2ib\lambda_0}. \tag{7.14}$$

Now the eigen function expansions of $\phi^{sm,ansm}(x,y)$ satisfying equations (7.3), (7.4), (7.5), (7.7), (7.8), (7.12) for $x > 0$ in the different regions for each barrier configuration are given below.

Region I $(x > b,\ 0 < y < h)$:

$$\phi^{sm,ansm}(x,y) = \frac{\cosh\lambda_0(h-y)}{\cosh\lambda_0 h}\left[e^{-i\lambda_0(x-b)} + R^{sm,ansm}e^{i\lambda_0(x-b)}\right] + \sum_{n=1}^{\infty} A_n^{sm,ansm}\cos\lambda_n(h-y)\ e^{-\lambda_n(x-b)} \tag{7.15}$$

where λ_n $(n = 1, 2, ...)$ are the real positive roots of the equation

$$k(1 - \epsilon K + Dk^4)\tan kh + K = 0 \tag{7.16}$$

and $R^{sm,ansm}$, $A_n^{sm,ansm}$ are unknown constants to be determined.

Region II $(0 < x < b,\ y \in \bar{L} \equiv \bar{L_j} = (0,h) - L_j,\ \ j = 1,2,3,4)$.

For barrier configuration of Type I, $y \in \bar{L_1} = (a,h)$, $\phi^{sm}(x,y)$ and $\phi^{ansm}(x,y)$ are given by

$$\left\{\begin{array}{l}\phi^{sm}(x,y)\\ \phi^{ansm}(x,y)\end{array}\right\} = \left\{\begin{array}{l}0\\ B_0^{ansm}\ x\end{array}\right\} + \sum_{n=1}^{\infty}\left\{\begin{array}{l}B_n^{sm}\cosh\frac{n\pi x}{h-a}\\ B_n^{ansm}\sinh\frac{n\pi x}{h-a}\end{array}\right\}\cos\frac{n\pi(y-a)}{h-a}. \tag{7.17}$$

Here $B_n^{sm,ansm}$ are unknown constants to be determined.

For barrier configuration of Type II, $y \in \bar{L_2} = (0,c)$, $\phi^{sm}(x,y)$ and $\phi^{ansm}(x,y)$

are given by

$$\left\{ \begin{array}{l} \phi^{sm}(x,y) \\ \phi^{ansm}(x,y) \end{array} \right\} = \left\{ \begin{array}{l} C_0^{sm} \ \cos\alpha_0 x \\ C_0^{ansm} \ \sin\alpha_0 x \end{array} \right\} \frac{\cosh\ \alpha_0(c-y)}{\cosh\ \alpha_0 c} + \sum_{n=1}^{\infty} \left\{ \begin{array}{l} C_n^{sm} \ \cosh\ \alpha_n x \\ C_n^{ansm} \ \sinh\ \alpha_n x \end{array} \right\} \cos\alpha_n(c-y) \tag{7.18}$$

where $\pm\alpha_0$, $\pm i\alpha_n$, $(n = 1, 2, ...)$ are the roots of the equation

$$\alpha(1 - \epsilon K + D\alpha^4)\tanh\ \alpha c = K \tag{7.19}$$

and $C_n^{sm,ansm}$ are unknown constants to be determined.

For barrier configuration of Type III, $y \ \epsilon \ \bar{L_3} = (0,a) + (c,h)$, $\phi^{sm,ansm}(x,y)$ are given by

$$\left\{ \begin{array}{l} \phi^{sm}(x,y) \\ \phi^{ansm}(x,y) \end{array} \right\} = \left\{ \begin{array}{l} D_0^{sm} \ \cos\beta_0 x \\ D_0^{ansm} \ \sin\beta_0 x \end{array} \right\} \frac{\cosh\ \beta_0(a-y)}{\cosh\ \beta_0 a} + \sum_{n=1}^{\infty} \left\{ \begin{array}{l} D_n^{sm} \ \cosh\ \beta_n x \\ D_n^{ansm} \ \sinh\ \beta_n x \end{array} \right\} \cos\beta_n(a-y), \quad 0 < y < a, \tag{7.20}$$

where $\pm\beta_0, \pm i\beta_n, (n = 1, 2, ...)$ are the roots of equation

$$\beta(1 - \epsilon K + D\beta^4)\tanh\ \beta a = K \tag{7.21}$$

and

$$\left\{ \begin{array}{l} \phi^{sm}(x,y) \\ \phi^{ansm}(x,y) \end{array} \right\} = \left\{ \begin{array}{l} 0 \\ E_0^{ansm} \ x \end{array} \right\} + \sum_{n=1}^{\infty} \left\{ \begin{array}{l} E_n^{sm} \cosh\frac{n\pi x}{h-c} \\ E_n^{ansm} \sinh\frac{n\pi x}{h-c} \end{array} \right\} \cos\frac{n\pi(y-c)}{h-c} \ c < y < h. \tag{7.22}$$

Here $D_n^{sm,ansm}$ and $E_n^{sm,ansm}$ are unknown constants to be determined.

For barrier configuration of Type IV, $y \epsilon \bar{L_4} = (a, c)$, the expressions of $\phi^{sm,ansm}(x, y)$ are given by

$$\left\{ \begin{array}{l} \phi^{sm}(x,y) \\ \phi^{ansm}(x,y) \end{array} \right\} = \left\{ \begin{array}{l} 0 \\ H_0^{ansm}\ x \end{array} \right\} + \sum_{n=1}^{\infty} \left\{ \begin{array}{l} H_n^{sm} \cosh \frac{n\pi x}{c-a} \\ H_n^{ansm} \sinh \frac{n\pi x}{c-a} \end{array} \right\} \cos \frac{n\pi(y-a)}{c-a} \tag{7.23}$$

where $H_n^{sm,ansm}$ are unknown constants to be determined.

Now let us define

$$\phi_x^{sm,ansm}(b+0, y) = f^{sm,ansm}(y), \quad 0 < y < h. \tag{7.24}$$

Then

$$f^{sm,ansm}(y) = 0 \quad for\ y \epsilon L \equiv L_j, \quad and \quad x = b + 0. \tag{7.25}$$

Noting the continuity of $\phi_x^{sm,ansm}(x, y)$ across $x = b,\ y \epsilon \bar{L} \equiv \bar{L_j} = (0, h) - L_j$ we have

$$\phi_x^{sm,ansm}(b \pm 0, y) = f^{sm,ansm}(y) \quad for\ y \epsilon \bar{L} \equiv \bar{L_j} = (0, h) - L_j \tag{7.26}$$

so that $f^{sm,ansm}(y)$ is an unknown function for $y \epsilon \bar{L} \equiv \bar{L_j} = (0, h) - L_j,\ j = 1, 2, 3, 4.$ Also due to the edge condition described in equation (7.6) we must have the requirement that

$$f^{sm,ansm}(y) = O(|y - l|^{-1/3}) \quad as\ y \rightarrow l \equiv l_j\ (j = 1, 2, 3, 4). \tag{7.27}$$

Substituting $\phi_x^{sm,ansm}(x, y)$ from equation (7.15) into equation (7.24) and using Havelock inversion formula we obtain the constants $R^{sm,ansm}$, $A_n^{sm,ansm}$ in terms of the unknown function $f^{sm,ansm}(y)$ as

$$1 - R^{sm,ansm} = \frac{4i\ \cosh\ \lambda_0 h}{\delta_0} \int_{\bar{L}} f^{sm,ansm}(y) \cosh\ \lambda_0(h - y)\ dy \tag{7.28}$$

and

$$A_n^{sm,ansm} = -\frac{4}{\delta_n}\int_{\bar{L}} f^{sm,ansm}(y)\cos\lambda_n(h-y)\ dy \tag{7.29}$$

with

$\delta_0 = 2\lambda_0 h + \sinh\ 2\lambda_0 h\ ; \quad \delta_n = 2\lambda_n h + \sin\ 2\lambda_n h\ \ (n = 1, 2, ...).$

Next we shall proceed to evaluate the constants $B_n^{sm,ansm}, C_n^{sm,ansm}, D_n^{sm,ansm}, E_n^{sm,ansm}, H_n^{sm,a}$ appearing in the expressions for $\phi^{sm,ansm}(x,y)$ for Region II.

Barrier configuration of Type I:

Substituting the equation (7.17) in condition (7.26) and using Fourier cosine inversion, we get that $f^{sm}(y)$ for type-I barrier satisfy the condition

$$\int_a^h f^{sm}(y)\ dy = 0 \tag{7.30}$$

and the constants are obtained as

$$B_0^{ansm} = \frac{1}{h-a}\int_a^h f^{ansm}(y)\ dy, \tag{7.31}$$

$$B_n^{sm,ansm} = \frac{2}{n\pi}\left(\frac{1}{\sinh\ \frac{n\pi b}{h-a}}, \frac{1}{\cosh\ \frac{n\pi b}{h-a}}\right)\int_a^h f^{sm,ansm}(y)\cos\frac{n\pi(y-a)}{h-a}\ dy. \tag{7.32}$$

Barrier configuration of Type II:

Substituting the equation (7.18) in the condition (7.26), and using Havelock inversion formula, we get

$$C_0^{sm,ansm} = \frac{4\cosh\alpha_0 c}{\gamma_0}\left(-\frac{1}{\sin\alpha_0 b},\ \frac{1}{\cos\alpha_0 b}\right)\int_0^c f^{sm,ansm}(y)\cosh\alpha_0(c-y)\ dy, \tag{7.33}$$

$$C_n^{sm,ansm} = \frac{4}{\gamma_n}\left(\frac{1}{\sinh\alpha_n b},\ \frac{1}{\cosh\alpha_n b}\right)\int_0^c f^{sm,ansm}(y)\cos\alpha_n(c-y)\ dy \tag{7.34}$$

with

$\gamma_0 = 2\alpha_0 c + \sinh\ 2\alpha_0 c; \quad \gamma_n = 2\alpha_n c + \sin\ 2\alpha_n c.$

Barrier configuration of Type III:

Similarly we can derive the constants $D_n^{sm,ansm}$ as

$$D_0^{sm,ansm} = \frac{4\cosh\beta_0 a}{\epsilon_0}\left(-\frac{1}{\sin\beta_0 b},\ \frac{1}{\cos\beta_0 b}\right)\int_0^a f^{sm,ansm}(y)\cosh\beta_0(a-y)\ dy, \quad (7.35)$$

$$D_n^{sm,ansm} = \frac{4}{\epsilon_n}\left(\frac{1}{\sinh\beta_n b},\ \frac{1}{\cosh\beta_n b}\right)\int_0^a f^{sm,ansm}(y)\cos\beta_n(a-y)\ dy \quad (7.36)$$

with $\epsilon_0 = 2\beta_0 a + \sinh\ 2\beta_0 a; \quad \epsilon_n = 2\beta_n a + \sin\ 2\beta_n a,$ and

$$E_0^{ansm} = \frac{1}{h-c}\int_c^h f^{ansm}(y)\ dy, \quad (7.37)$$

$$E_n^{sm,ansm} = \frac{2}{n\pi}\left(\frac{1}{\sinh\ \frac{n\pi b}{h-c}}, \frac{1}{\cosh\ \frac{n\pi b}{h-c}}\right)\int_c^h f^{sm,ansm}(y)\cos\frac{n\pi(y-c)}{h-c}\ dy \quad (7.38)$$

and $f^{sm}(y)$ for type III barrier must satisfy the condition

$$\int_c^h f^{sm}(y)\ dy = 0. \quad (7.39)$$

Barrier configuration of Type IV:

In this case the constants H_n^{sm} is derived as

$$H_0^{ansm} = \frac{1}{c-a}\int_a^c f^{ansm}(y)\ dy, \quad (7.40)$$

$$H_n^{sm,ansm} = \frac{2}{n\pi}\left(\frac{1}{\sinh\ \frac{n\pi b}{c-a}}, \frac{1}{\cosh\ \frac{n\pi b}{c-a}}\right)\int_a^c f^{sm,ansm}(y)\cos\frac{n\pi(y-a)}{c-a}\ dy \quad (7.41)$$

and in this case $f^{sm}(y)$ must satisfy

$$\int_a^c f^{sm}(y)\ dy = 0. \tag{7.42}$$

3.2 Reduction to integral equation

Now $\phi^{sm,ansm}(x,y)$ is continuous across the line $x = b \quad y \in \bar{L} \equiv \bar{L_j}\ (j = 1,2,3,4)$, so that

$$\phi^{sm,ansm}(b+0,y) = \phi^{sm,ansm}(b-0,y), \quad y \in \bar{L} \equiv \bar{L_j}\ (j = 1,2,3,4) \tag{7.43}$$

which produces the integral equation

$$\int_{\bar{L}} F^{sm,ansm}(u)\ M^{sm,ansm}(y,u)\ du = \frac{\cosh\lambda_0(h-y)}{\cosh\lambda_0 h}, \quad y \in \bar{L} \equiv \bar{L_j}\ (j = 1,2,3,4) \tag{7.44}$$

where

$$F^{sm,ansm}(y) = \frac{4\cosh^2\lambda_0 h}{\delta_0(1+R^{sm,ansm})}\ f^{sm,ansm}(y), \quad y \in \bar{L} \equiv \bar{L_j}\ (j = 1,2,3,4) \tag{7.45}$$

and $M^{sm,ansm}(y,u)$ $(y,u \in \bar{L})$ are real and symmetric in y and u, and their expressions for each type of barrier configurations are given below.

Barrier configuration of Type I:

For $y,\ u \in \bar{L_1} = (a,h)$

$$M^{sm}(y,u) = \frac{\delta_0}{\cosh^2\lambda_0 h}\Bigg[\sum_{n=1}^{\infty}\Bigg(\frac{\cos\ \lambda_n(h-y)\cos\ \lambda_n(h-u)}{\delta_n} + \frac{1}{2n\pi}\coth\frac{n\pi b}{h-a}\cos\frac{n\pi(y-a)}{h-a}\cos\frac{n\pi(u-a)}{h-a}\Bigg)\Bigg], \tag{7.46}$$

$$M^{ansm}(y,u) = \frac{\delta_0}{\cosh^2\lambda_0 h}\Bigg[\frac{b}{4(h-a)} + \sum_{n=1}^{\infty}\Bigg(\frac{\cos\ \lambda_n(h-y)cos\ \lambda_n(h-u)}{\delta_n} + \frac{1}{2n\pi}\tanh\frac{n\pi b}{h-a}\cos\frac{n\pi(y-a)}{h-a}\cos\frac{n\pi(u-a)}{h-a}\Bigg)\Bigg]. \tag{7.47}$$

Barrier configuration of Type II:

For $y,\ u \in \bar{L}_2 = (0,c)$

$$M^{sm}(y,u) = \frac{\delta_0}{\cosh^2\lambda_0 h}\Bigg[\sum_{n=1}^{\infty}\Bigg(\frac{\cos\ \lambda_n(h-y)\cos\ \lambda_n(h-u)}{\delta_n} + \frac{\coth\alpha_n b\cos\alpha_n(c-y)\cos\alpha_n(c-u)}{\gamma_n}\Bigg) - \cot\alpha_0 b\ \frac{\cosh\alpha_0(c-y)\cosh\alpha_0(c-u)}{\gamma_0}\Bigg], \tag{7.48}$$

$$M^{ansm}(y,u) = \frac{\delta_0}{\cosh^2\lambda_0 h}\Bigg[\sum_{n=1}^{\infty}\Bigg(\frac{\cos\ \lambda_n(h-y)\cos\ \lambda_n(h-u)}{\delta_n} + \frac{\tanh\alpha_n b\cos\alpha_n(c-y)\cos\alpha_n(c-u)}{\gamma_n}\Bigg) + \tan\alpha_0 b\ \frac{\cosh\alpha_0(c-y)\cosh\alpha_0(c-u)}{\gamma_0}\Bigg]. \tag{7.49}$$

Barrier configuration of Type III:

For $y,\ u \in \bar{L}_3 = (0,a) + (c,h)$, we consider following three different cases.

Case-1 ($y,\ u \in (0,a)$):

$$M^{sm}(y,u) = \frac{\delta_0}{\cosh^2\lambda_0 h}\Bigg[\sum_{n=1}^{\infty}\Bigg(\frac{\cos\ \lambda_n(h-y)\ \cos\ \lambda_n(h-u)}{\delta_n} + \frac{\coth\beta_n b\cos\beta_n(a-y)\cos\beta_n(a-u)}{\epsilon_n}\Bigg) - \cot\beta_0 b\ \frac{\cosh\beta_0(a-y)\cosh\beta_0(a-u)}{\epsilon_0}\Bigg], \tag{7.50}$$

$$M^{ansm}(y,u) = \frac{\delta_0}{\cosh^2\lambda_0 h}\Bigg[\sum_{n=1}^{\infty}\Bigg(\frac{\cos\ \lambda_n(h-y)\cos\ \lambda_n(h-u)}{\delta_n} + \frac{\tanh\beta_n b\cos\beta_n(a-y)\cos\beta_n(a-u)}{\epsilon_n}\Bigg) + \tan\beta_0 b\ \frac{\cosh\beta_0(a-y)\cosh\beta_0(a-u)}{\epsilon_0}\Bigg]. \tag{7.51}$$

Case-2 ($y,\ u\ \epsilon\ (c,h)$):

$$M^{sm}(y,u) = \frac{\delta_0}{\cosh^2\lambda_0 h}\Bigg[\sum_{n=1}^{\infty}\Bigg(\frac{\cos\ \lambda_n(h-y)\cos\ \lambda_n(h-u)}{\delta_n} + \frac{1}{2n\pi}\coth\frac{n\pi b}{h-c}\cos\frac{n\pi(y-c)}{h-c}\cos\frac{n\pi(u-c)}{h-c}\Bigg)\Bigg], \tag{7.52}$$

$$M^{ansm}(y,u) = \frac{\delta_0}{\cosh^2\lambda_0 h}\Bigg[\frac{b}{4(h-c)} + \sum_{n=1}^{\infty}\Bigg(\frac{\cos\ \lambda_n(h-y)\cos\ \lambda_n(h-u)}{\delta_n} + \frac{1}{2n\pi}\tanh\frac{n\pi b}{h-c}\cos\frac{n\pi(y-c)}{h-c}\cos\frac{n\pi(u-c)}{h-c}\Bigg)\Bigg]. \tag{7.53}$$

Case-3 ($y\ \epsilon\ (0,a),\ u\ \epsilon\ (c,h)$ and $y\ \epsilon\ (c,h),\ u\ \epsilon\ (0,a)$):

$$M^{sm}(y,u) = M^{ansm}(y,u) = \frac{\delta_0}{\cosh^2\lambda_0 h}\sum_{n=1}^{\infty}\frac{\cos\ \lambda_n(h-y)\cos\ \lambda_n(h-u)}{\delta_n}. \tag{7.54}$$

Barrier configuration of Type IV:

For $y,\ u\ \epsilon\ \bar{L_4} = (a,c)$:

$$M^{sm}(y,u) = \frac{\delta_0}{\cosh^2\lambda_0 c}\Bigg[\sum_{n=1}^{\infty}\Bigg(\frac{\cos\ \lambda_n(c-y)\cos\ \lambda_n(c-u)}{\delta_n} + \frac{1}{2n\pi}\coth\frac{n\pi b}{c-a}\cos\frac{n\pi(y-a)}{c-a}\cos\frac{n\pi(u-a)}{c-a}\Bigg)\Bigg], \tag{7.55}$$

$$M^{ansm}(y,u) = \frac{\delta_0}{\cosh^2\lambda_0 c}\left[\frac{b}{4(c-a)} + \sum_{n=1}^{\infty}\left(\frac{\cos\ \lambda_n(c-y)\cos\ \lambda_n(c-u)}{\delta_n}\right.\right.$$
$$\left.\left. + \frac{1}{2n\pi}\tanh\frac{n\pi b}{c-a}\cos\frac{n\pi(y-a)}{c-a}\cos\frac{n\pi(u-a)}{c-a}\right)\right]. \tag{7.56}$$

If we now define the constants $C^{sm,ansm}$ by

$$C^{sm,ansm} = -i\frac{1-R^{sm,ansm}}{1+R^{sm,ansm}} \tag{7.57}$$

then by using the relations (7.28) and (7.45) , we get

$$\int_{\bar{L}} F^{sm,ansm}(y)\ \frac{\cosh\lambda_0(h-y)}{\cosh\lambda_0 h}\ dy = C^{sm,ansm}.\ \ \bar{L} \equiv\ \bar{L}_j,\ \ (j=1,2,3,4). \tag{7.58}$$

Thus if the integral equation (7.44) can be solved, then these solutions can be used to obtain $C^{sm,ansm}$ from equation (7.58). Also using equation (7.14) and (7.57), the reflection and transmission coefficients $|R|$ and $|T|$ can be produced by the following relations

$$|R| = \frac{|1+C^{sm}C^{ansm}|}{\Delta}\ ;\quad |T| = \frac{|C^{sm}-C^{ansm}|}{\Delta} \tag{7.59}$$

with

$$\Delta = [1+(C^{sm})^2+(C^{ansm})^2+(C^{sm}C^{ansm})^2]^{1/2}. \tag{7.60}$$

3.3 Galerkin approach to solve integral equation

In Galerkin approach we approximate the functions $F^{sm,ansm}(y)$ as

$$F^{sm,ansm}(y) \approx \mathcal{F}^{sm,ansm}(y),\quad y \in \bar{L} \equiv \bar{L}_j,\ \ (j=1,2,3,4) \tag{7.61}$$

where $\mathcal{F}^{sm,ansm}(y)$ have multi-term Galerkin expansions in terms of suitable basis func-

tions. We observe that $\bar{L}_1$, $\bar{L}_2$, $\bar{L}_4$ are single intervals, while $\bar{L}_3$ consists of two disjoint intervals. For the single intervals $\bar{L}_j$, $(j = 1, 2, 4)$, $\mathcal{F}^{sm,ansm}(y)$ are expressed as

$$\mathcal{F}^{sm,ansm}(y) = \sum_{n=0}^{N} a_n^{sm,ansm}\ t_n^{sm,ansm}(y), \quad y \in \bar{L}_j,\ (j = 1, 2, 4) \tag{7.62}$$

and for double interval $\bar{L}_3 = (0, a) + (c, h)$, $\mathcal{F}^{sm,ansm}(y)$ can be approximated as

$$\mathcal{F}^{sm,ansm}(y) = \begin{cases} \sum_{n=0}^{N} a_n^{sm,ansm}\ p_n^{sm,ansm}(y),\ 0 < y < a, \\ \sum_{n=0}^{N} b_n^{sm,ansm}\ q_n^{sm,ansm}(y),\ c < y < h, \end{cases} \tag{7.63}$$

where the basis functions $t_n^{sm,ansm}(y)$ for $y \in \bar{L}_j$ $(j = 1, 2, 4)$ and $p_n^{sm,ansm}(y)$ for $0 < y < a$, $q_n^{sm,ansm}(y)$ for $c < y < h$ are chosen in terms of ultraspherical Gegenbauer polynomials of order 1/6 with suitable weights [cf. Porter(1972), Evans and Fernyhough (1995)]. The basis functions in various intervals are given below.

3.4 Basis Functions

Barrier configuration of Type-I

As $\phi_y^{sm,asm} = 0$ on $y = h$ and hence

$$F^{sm,asm} \sim \phi_x^{sm,asm}(b, y)$$

can be continued as an even function of y across $y = h$. In this case the basis function is not explicitly depends on the upper surface condition because of the partially immersed barrier. The detailed is given in Kanoria (1999). We choose the basis function as follows

$$\begin{cases} t_m^{sm}(y) = g_{m+1}^{(1)}(y), \quad m = 0, 1, 2, ... \\ t_m^{ansm}(y) = g_m^{(1)}(y), \quad m = 0, 1, 2, ... \end{cases} \tag{7.64}$$

where

$$g_m^{(1)}(y) = \frac{2^{\frac{7}{6}}\ \Gamma(\frac{1}{6})(2m)!}{\pi\Gamma(2m+(1/3))(h-a)^{\frac{1}{3}}\ \{(h-a)^2-(h-y)^2\}^{\frac{1}{3}}} C_{2m}^{\frac{1}{6}}\left(\frac{h-y}{h-a}\right). \tag{7.65}$$

Barrier configuration of Type-II

For this type of fully submerged barrier, we have to take the ice cover condition and the behavior

$$F^{sm,asm} \sim (c-y)^{-1/3} \quad \text{as } y \to c-0$$

as derived by considering the flow field near the corner point (b,c). Thus $F^{sm,asm} \equiv F(y)$ satisfies

$$KF(y) + (1-\epsilon K)F'(y) = 0, \quad y = 0, \tag{7.66}$$

$$F(y) \sim (c-y)^{-1/3}, \quad \text{as} \quad y \to c-0. \tag{7.67}$$

Thus

$$t_m^{sm}(y) = t_m^{ansm}(y) = t_m(y) = -\frac{d}{dy}\left[e^{-\frac{K}{1-\epsilon K+Dk^4}y}\int_y^c e^{\frac{K}{1-\epsilon K+Dk^4}t}\ \hat{t}_m(t)\ dt\right], \quad 0<y<c. \tag{7.68}$$

We choose the basis function in terms of $\hat{t}_m(y)$, as follows

$$\hat{t}_m(y) = \frac{2^{\frac{7}{6}}\ \Gamma(\frac{1}{6})(2m)!}{\pi\Gamma(2m+\frac{1}{3})c^{\frac{1}{3}}(c^2-y^2)^{\frac{1}{3}}}\ C_{2m}^{\frac{1}{6}}\left(\frac{y}{c}\right), \quad 0<y<c. \tag{7.69}$$

Barrier configuration of Type-III

Here we choose two different basis functions for two disjoint intervals

$$p_m^{sm}(y) = p_m^{ansm}(y) = p_m(y) = -\frac{d}{dy}\left[e^{-\frac{K}{1-\epsilon K+Dk^4}y}\int_y^a e^{\frac{K}{1-\epsilon K+Dk^4}t}\ \hat{p}_m(t)\ dt\right], \quad 0<y<a \tag{7.70}$$

where

$$\hat{p}_m(y) = \frac{2^{\frac{7}{6}}\ \Gamma(\frac{1}{6})(2m)!}{\pi\Gamma(2m+\frac{1}{3})a^{\frac{1}{3}}(a^2-y^2)^{\frac{1}{3}}}\ C_{2m}^{\frac{1}{6}}\left(\frac{y}{a}\right), \quad 0<y<a \tag{7.71}$$

$$\begin{cases} q_m^{sm}(y) = g1_{m+1}^{(1)}(y), \quad m = 0,1,2,..... \\ q_m^{ansm}(y) = g1_m^{(1)}(y), \quad m = 0,1,2,..... \end{cases} \tag{7.72}$$

and

$$g1_m^{(1)}(y) = \frac{2^{\frac{7}{6}}\ \Gamma(\frac{1}{6})(2m)!}{\pi\Gamma(2m+(1/3))(h-c)^{\frac{1}{3}}\{(h-c)^2-(h-y)^2\}^{\frac{1}{3}}}\ C_{2m}^{\frac{1}{6}}\left(\frac{h-y}{h-c}\right), \quad c<y<h. \tag{7.73}$$

Barrier configuration of Type-IV

Here we choose basis function for $a<y<c$ as

$$\begin{cases} t_m^{sm}(y) = g_{m+1}^{(2)}(y), \quad m = 0,1,2,..... \\ t_m^{ansm}(y) = g_m^{(2)}(y), \quad m = 0,1,2,..... \end{cases} \tag{7.74}$$

where

$$g_m^{(2)}(y) = \frac{2^{\frac{1}{6}}\ \Gamma(\frac{1}{6})\ m!}{\pi\ \Gamma(m+\frac{1}{3})\left(\frac{c-a}{2}\right)^{\frac{1}{3}}\{(y-a)(c-y)\}^{\frac{1}{3}}} C_m^{\frac{1}{6}}\left(\frac{2y-a-c}{c-a}\right), \quad a<y<c. \tag{7.75}$$

3.5 Reduction of Integral equation to Linear system of equations

For single intervals $\bar{L} \equiv \bar{L}_j$, $(j = 1,2,4)$, we substitute the approximation (7.61) in equations (7.44) , and then multiplying both side by appropriate $t_m^{sm,ansm}(y)$ and

integrate over $\bar{L}$ to obtain the linear system of equations

$$\sum_{n=0}^{N} a_n^{sm,ansm}\ K_{mn}^{sm,ansm} = d_m^{sm,ansm}, \quad m = 0, 1, 2, ..., N \tag{7.76}$$

where

$$K_{mn}^{sm,ansm} = \int_{\bar{L}} \int_{\bar{L}} M^{sm,ansm}(y,u)\ t_n^{sm,ansm}(u)\ t_m^{sm,ansm}(y)\ du\ dy, \quad m, n = 0, 1, 2, ..., N, \tag{7.77}$$

$$d_m^{sm,ansm} = \int_{\bar{L}} \frac{\cosh \lambda_0(h-y)}{\cosh \lambda_0 h}\ t_m^{sm,ansm}(y)\ dy, \quad m = 0, 1, 2, ...N. \tag{7.78}$$

For each $\bar{L}_j$, $(j = 1, 2, 4)$, the integrals in the equations (7.77) and (7.78) can be evaluated explicitly. Thus the constants $a_n^{sm,ansm}$ $(n = 0, 1, ...N)$ are obtained by solving the linear equations (7.76) for each of type-I, type-II and type-IV barrier. The relation (7.58) produce

$$C^{sm,ansm} = \sum_{n=0}^{N} a_n^{sm,ansm}\ d_n^{sm,ansm} \tag{7.79}$$

and after knowing the values of $C^{sm,ansm}$, we can get the absolute values of reflection and transmission coefficient by equations (7.59) for each of type-I, type-II and type-IV barrier.

Now when $\bar{L} = \bar{L}_3 = (0, a) + (c, h)$, we substitute the expressions (7.63) in equation (7.44), and multiplying both side first by $p_m^{sm,ansm}(y)$ $(0 < y < a)$ and then by $q_m^{sm,ansm}(y)$ $(c < y < h)$ and then integrate over $(0, a)$ and (c, h) respectively, we get the linear system of equations

$$\sum_{n=0}^{N} a_n^{sm,ansm} \begin{pmatrix} G_{mn}^{sm,ansm} \\ P_{mn}^{sm,ansm} \end{pmatrix} + \sum_{n=0}^{N} \begin{pmatrix} H_{mn}^{sm,ansm} \\ Q_{mn}^{sm,ansm} \end{pmatrix} = \begin{pmatrix} d_m^{(1)sm,ansm} \\ d_m^{(2)sm,ansm} \end{pmatrix}, \quad m = 0, 1, ...N \tag{7.80}$$

where

$$G_{mn}^{sm,ansm} = \int_0^a \left\{ \int_0^a M^{sm,ansm}(y,u)\ p_n^{sm,ansm}(u)\ du \right\} p_m^{sm,ansm}(y)\ dy,$$

$$H_{mn}^{sm,ansm} = \int_0^a \left\{ \int_c^h M^{sm,ansm}(y,u)\ q_n^{sm,ansm}(u)\ du \right\} p_m^{sm,ansm}(y)\ dy, \tag{7.81}$$

$$P_{mn}^{sm,ansm} = \int_c^h \left\{ \int_0^a M^{sm,ansm}(y,u)\ p_n^{sm,ansm}(u)\ du \right\} q_m^{sm,ansm}(y)\ dy,$$

$$Q_{mn}^{sm,ansm} = \int_c^h \left\{ \int_c^h M^{sm,ansm}(y,u)\ q_n^{sm,ansm}(u)\ du \right\} q_m^{sm,ansm}(y)\ dy,$$

so that $P_{mn}^{sm,ansm} = H_{mn}^{sm,ansm}$, and

$$d_m^{(1)sm,ansm} = \int_0^a \frac{\cosh\lambda_0(h-y)}{\cosh\lambda_0 h}\ p_m^{sm,ansm}(y)\ dy,$$

$$d_m^{(2)sm,ansm} = \int_c^h \frac{\cosh\lambda_0(h-y)}{\cosh\lambda_0 h}\ q_m^{sm,ansm}(y)\ dy. \tag{7.82}$$

The integrals in the relations (7.81) and (7.82) can be evaluated explicitly and thus the constants for type-III $a_n^{sm,ansm}$ and $b_n^{sm,ansm}$ $(n = 0, 1, 2, ...N)$ from linear equations (7.80) are obtained. From equation (7.58), we approximate $C^{sm,ansm}$ as

$$C^{sm,ansm} = \sum_{n=0}^{N} \left\{ a_n^{sm,ansm}\ d_n^{(1)sm,ansm} + b_n^{sm,ansm}\ d_n^{(2)sm,ansm} \right\}. \tag{7.83}$$

3.6 Coefficients of Linear system of Equation

Here we shall calculate the coefficient matrix and forcing terms of the linear system of equations for each type of barrier configurations.

Barrier configuration of Type-I

In this case we get from equation (7.77) and (7.78)

$$K_{mn}^{sm} = \frac{\delta_0}{\cosh^2\lambda_0 h}\Bigg[(-1)^{m+n}\sum_{r=1}^{\infty}\Bigg(\frac{4J_{2n+\frac{13}{6}}\{\lambda_r(h-a)\}\,J_{2m+\frac{13}{6}}\{\lambda_r(h-a)\}}{\delta_r\{\lambda_r(h-a)\}^{\frac{1}{3}}} + \frac{2}{r\pi}\coth\frac{r\pi b}{h-a}\;\frac{J_{2n+\frac{13}{6}}(r\pi)J_{2m+\frac{13}{6}}(r\pi)}{(r\pi)^{\frac{1}{3}}}\Bigg)\Bigg], \tag{7.84}$$

$$K_{mn}^{ansm} = \frac{\delta_0}{\cosh^2\lambda_0 h}\Bigg[\Bigg(\frac{12\pi b}{h-a}\Bigg)\Bigg(\frac{2^{\frac{1}{3}}}{(\Gamma(\frac{1}{3})^4)}\Bigg)\delta_{0n}\delta_{0m} + (-1)^{m+n}\sum_{r=1}^{\infty}\Bigg(\frac{4J_{2n+\frac{1}{6}}\{\lambda_r(h-a)\}\,J_{2m+\frac{1}{6}}\{\lambda_r(h-a)\}}{\delta_r\{\lambda_r(h-a)\}^{\frac{1}{3}}} + \frac{2}{r\pi}\tanh\frac{r\pi b}{h-a}\;\frac{J_{2n+\frac{1}{6}}(r\pi)J_{2m+\frac{1}{6}}(r\pi)}{(r\pi)^{\frac{1}{3}}}\Bigg)\Bigg] \tag{7.85}$$

where $\delta_{0n} = 1$ for $n = 0$, and $\delta_{0n} = 0$ for $n \geq 1$ and $J_m{}'s$ are Bessel functions of first kind of order m.

$$d_m^{sm} = \frac{1}{\cosh\lambda_0 h}\;\frac{I_{2m+\frac{13}{6}}}{(\lambda_0(h-a))^{\frac{1}{6}}}, \tag{7.86}$$

$$d_m^{ansm} = \frac{1}{\cosh\lambda_0 h}\;\frac{I_{2m+\frac{1}{6}}}{(\lambda_0(h-a))^{\frac{1}{6}}}, \tag{7.87}$$

where $I_n{}'s$ are modified Bessel function of first kind of order n.

Barrier configuration of Type-II

In this case we get from equation (7.77) and (7.78)

$$K_{mn}^{sm} = \frac{\delta_0}{\cosh^2\lambda_0 h}\Bigg[4(-1)^{m+n}\sum_{r=1}^{\infty}\Bigg(\frac{\cos^2\lambda_r h\;J_{2n+\frac{1}{6}}(\lambda_r c)J_{2m+\frac{1}{6}}(\lambda_r c)}{\delta_r(\lambda_r c)^{\frac{1}{3}}}$$

$$+\frac{\coth\alpha_r b\cos^2\alpha_r c}{\gamma_r}\ \frac{J_{2n+\frac{1}{6}}(\alpha_r c)J_{2m+\frac{1}{6}}(\alpha_r c)}{(\alpha_r c)^{\frac{1}{3}}}\Bigg)$$

$$-\frac{\cot\alpha_0 b}{\gamma_0}\cosh^2\alpha_0 c\ \frac{I_{2n+\frac{1}{6}}(\alpha_0 c)I_{2m+\frac{1}{6}}(\alpha_0 c)}{(\alpha_0 c)^{\frac{1}{3}}}\Bigg], \tag{7.88}$$

$$K_{mn}^{ansm}=\frac{\delta_0}{\cosh^2\lambda_0 h}\Bigg[4(-1)^{m+n}\sum_{r=1}^{\infty}\Bigg(\frac{\cos^2\lambda_r h\ J_{2n+\frac{1}{6}}(\lambda_r c)J_{2m+\frac{1}{6}}(\lambda_r c)}{\delta_r(\lambda_r c)^{\frac{1}{3}}}$$

$$+\frac{\tanh\alpha_r b\cos^2\alpha_r c}{\gamma_r}\ \frac{J_{2n+\frac{1}{6}}(\alpha_r c)J_{2m+\frac{1}{6}}(\alpha_r c)}{(\alpha_r c)^{\frac{1}{3}}}\Bigg)$$

$$+\frac{\tan\alpha_0 b}{\gamma_0}\cosh^2\alpha_0 c\ \frac{I_{2n+\frac{1}{6}}(\alpha_0 c)I_{2m+\frac{1}{6}}(\alpha_0 c)}{(\alpha_0 c)^{\frac{1}{3}}}\Bigg], \tag{7.89}$$

$$d_m^{sm,ansm}=\frac{I_{2m+\frac{1}{6}}(\lambda_0 c)}{(\lambda_0 c)^{\frac{1}{6}}}. \tag{7.90}$$

Barrier configuration of Type-III

In this case we get from equation (7.81) and (7.82)

$$G_{mn}^{sm}=\frac{\delta_0}{\cosh^2\lambda_0 h}\Bigg[4(-1)^{m+n}\sum_{r=1}^{\infty}\Bigg(\frac{cos^2\lambda_r h\ J_{2n+\frac{1}{6}}(\lambda_r a)J_{2m+\frac{1}{6}}(\lambda_r a)}{\delta_r(\lambda_r a)^{\frac{1}{3}}}$$

$$+\frac{\coth\beta_r b\cos^2\beta_r a}{\epsilon_r}\ \frac{J_{2n+\frac{1}{6}}(\beta_r a)J_{2m+\frac{1}{6}}(\beta_r a)}{(\beta_r a)^{\frac{1}{3}}}\Bigg)$$

$$-\frac{\cot\beta_0 b}{\epsilon_0}\cosh^2\beta_0 a\ \frac{I_{2n+\frac{1}{6}}(\beta_0 a)I_{2m+\frac{1}{6}}(\beta_0 a)}{(\beta_0 a)^{\frac{1}{3}}}\Bigg], \tag{7.91}$$

$$G_{mn}^{ansm}=\frac{\delta_0}{\cosh^2\lambda_0 h}\Bigg[4(-1)^{m+n}\sum_{r=1}^{\infty}\Bigg(\frac{\cos^2\lambda_r h\ J_{2n+\frac{1}{6}}(\lambda_r a)J_{2m+\frac{1}{6}}(\lambda_r a)}{\delta_r(\lambda_r a)^{\frac{1}{3}}}$$

$$+\frac{\tanh\beta_r b\cos^2\beta_r a}{\epsilon_r}\ \frac{J_{2n+\frac{1}{6}}(\beta_r a)J_{2m+\frac{1}{6}}(\beta_r a)}{(\beta_r a)^{\frac{1}{3}}}\Bigg)$$

$$+\ \frac{\tan\beta_0 b}{\epsilon_0}\cosh^2\beta_0 a\ \frac{I_{2n+\frac{1}{6}}(\beta_0 a)I_{2m+\frac{1}{6}}(\beta_0 a)}{(\beta_0 a)^{\frac{1}{3}}}\Bigg], \tag{7.92}$$

$$H^{sm}_{mn} = \frac{4(-1)^{n+m+1}\delta_0}{\cosh^2\lambda_0 h}\ \sum_{r=1}^{\infty}\frac{\cos\lambda_r h}{\delta_r}\ \frac{J_{2n+\frac{13}{6}}\{\lambda_r(h-c)\}\,J_{2m+\frac{1}{6}}(\lambda_r a)}{\{\lambda_r(h-c)\}^{\frac{1}{6}}\,(\lambda_r a)^{\frac{1}{6}}}, \tag{7.93}$$

$$H^{ansm}_{mn} = H^{sm}_{m,n-1}, \tag{7.94}$$

$$P^{sm}_{mn} = H^{sm}_{nm}, \tag{7.95}$$

$$P^{ansm}_{mn} = P^{sm}_{m-1,n}, \tag{7.96}$$

$$Q^{sm}_{mn} = \frac{\delta_0}{\cosh^2\lambda_0 h}\Bigg[(-1)^{m+n}\sum_{r=1}^{\infty}\Bigg(\frac{4J_{2n+\frac{13}{6}}\{\lambda_r(h-c)\}\,J_{2m+\frac{13}{6}}\{\lambda_r(h-c)\}}{\delta_r\{\lambda_r(h-c)\}^{\frac{1}{3}}}$$

$$+\frac{2}{r\pi}\coth\frac{r\pi b}{h-c}\ \frac{J_{2n+\frac{13}{6}}(r\pi)J_{2m+\frac{13}{6}}(r\pi)}{(r\pi)^{\frac{1}{3}}}\Bigg)\Bigg], \tag{7.97}$$

$$Q^{ansm}_{mn} = \frac{\delta_0}{\cosh^2\lambda_0 h}\Bigg[\Bigg(\frac{12\pi b}{h-c}\Bigg)\Bigg(\frac{2^{\frac{1}{3}}}{(\Gamma(\frac{1}{3})^4)}\Bigg)\delta_{0n}\delta_{0m}$$

$$+(-1)^{m+n}\sum_{r=1}^{\infty}\Bigg(\frac{4J_{2n+\frac{1}{6}}\{\lambda_r(h-c)\}\,J_{2m+\frac{1}{6}}\{\lambda_r(h-c)\}}{\delta_r\{\lambda_r(h-a)\}^{\frac{1}{3}}}$$

$$+\frac{2}{r\pi}\tanh\frac{r\pi b}{h-c}\ \frac{J_{2n+\frac{1}{6}}(r\pi)J_{2m+\frac{1}{6}}(r\pi)}{(r\pi)^{\frac{1}{3}}}\Bigg)\Bigg], \tag{7.98}$$

where $\delta_{0n} = 1$ for $n = 0$, and $\delta_{0n} = 0$ for $n \geq 1$.

$$d_m^{(1)sm} = \frac{I_{2m+\frac{1}{6}}(\lambda_0 a)}{(\lambda_0 a)^{\frac{1}{6}}}, \tag{7.99}$$

$$d_m^{(1)ansm} = d_m^{(1)sm}, \tag{7.100}$$

$$d_m^{(2)sm} = \frac{1}{\cosh \lambda_0 h} \frac{I_{2m+\frac{7}{6}}\{\lambda_0(h-c))\}}{\{\lambda_0(h-c))\}^{\frac{1}{6}}}, \tag{7.101}$$

$$d_m^{(2)ansm} = d_{m-1}^{(2)sm}. \tag{7.102}$$

Barrier configuration of Type-IV

In this case we get from equation (7.77) and (7.78)

$$K_{mn}^{sm} = \frac{\delta_0}{\cosh^2 \lambda_0 h}\Bigg[\sum_{r=1}^{\infty}\Bigg\{\frac{4}{\delta_r(\lambda_r \frac{c-a}{2})^{\frac{1}{3}}} \times J_{n+\frac{7}{6}}\big(\lambda_r \frac{c-a}{2}\big) \times J_{m+\frac{7}{6}}\big(\lambda_r \frac{c-a}{2}\big) \times$$

$$\begin{pmatrix} (-1)^{n+\frac{1}{2}} \cos \lambda_r(h - \frac{c+a}{2}) \text{ if } n \text{ is odd} \\ (-1)^{\frac{n}{2}} \sin \lambda_r(h - \frac{c+a}{2}) \text{ if } n \text{ is even} \end{pmatrix} \times \begin{pmatrix} (-1)^{m+\frac{1}{2}} \cos \lambda_r(h - \frac{c+a}{2}) \text{ if } m \text{ is odd} \\ (-1)^{\frac{m}{2}} \sin \lambda_r(h - \frac{c+a}{2}) \text{ if } m \text{ is even} \end{pmatrix}\Bigg\}$$

$$+ \sum_{r=1}^{\infty}\Bigg\{\Big(\frac{2}{r\pi}\Big)^{\frac{4}{3}} \times \coth \frac{r\pi b}{c-a} \times J_{n+\frac{7}{6}}\big(\frac{r\pi}{2}\big) \times J_{m+\frac{7}{6}}\big(\frac{r\pi}{2}\big) \times$$

$$\begin{pmatrix} (-1)^{n+\frac{1}{2}} \cos(\frac{r\pi}{2}) \text{ if } n \text{ is odd} \\ (-1)^{\frac{n}{2}} \sin(\frac{r\pi}{2}) \text{ if } n \text{ is even} \end{pmatrix} \times \begin{pmatrix} (-1)^{m+\frac{1}{2}} \cos(\frac{r\pi}{2}) \text{ if } m \text{ is odd} \\ (-1)^{\frac{m}{2}} \sin(\frac{r\pi}{2}) \text{ if } m \text{ is even} \end{pmatrix}\Bigg\}\Bigg], \tag{7.103}$$

$$K_{mn}^{ansm} = \frac{\delta_0}{\cosh^2 \lambda_0 h}\Bigg[\frac{12\pi b}{c-a}\Big(\frac{2^{\frac{1}{3}}}{(\Gamma(\frac{1}{3})^4)}\Big)\delta_{0n}\delta_{0m}$$

$$+ \sum_{r=1}^{\infty}\Bigg\{\frac{4}{\delta_r(\lambda_r \frac{c-a}{2})^{\frac{1}{3}}} \times J_{n+\frac{1}{6}}\big(\lambda_r \frac{c-a}{2}\big) \times J_{m+\frac{1}{6}}\big(\lambda_r \frac{c-a}{2}\big) \times$$

$$\left(\begin{array}{l} (-1)^{n-\frac{1}{2}} \cos\lambda_r(h-\frac{c+a}{2}) \text{ if } n \text{ is odd} \\ (-1)^{\frac{n-1}{2}} \sin\lambda_r(h-\frac{c+a}{2}) \text{ if } n \text{ is even} \end{array} \right) \times \left(\begin{array}{l} (-1)^{m-\frac{1}{2}} \cos\lambda_r(h-\frac{c+a}{2}) \text{ if } m \text{ is odd} \\ (-1)^{\frac{m-1}{2}} \sin\lambda_r(h-\frac{c+a}{2}) \text{ if } m \text{ is even} \end{array} \right) \Bigg\}$$

$$+ \sum_{r=1}^{\infty} \Bigg\{ \left(\frac{2}{r\pi}\right)^{\frac{4}{3}} \times \tanh\frac{r\pi b}{c-a} \times J_{n+\frac{1}{6}}\left(\frac{r\pi}{2}\right) \times J_{m+\frac{1}{6}}\left(\frac{r\pi}{2}\right) \times$$

$$\left(\begin{array}{l} (-1)^{n-\frac{1}{2}} \cos\frac{r\pi}{2} \text{ if } n \text{ is odd} \\ (-1)^{\frac{n-1}{2}} \sin\frac{r\pi}{2} \text{ if } n \text{ is even} \end{array} \right) \times \left(\begin{array}{l} (-1)^{m-\frac{1}{2}} \cos\frac{r\pi}{2} \text{ if } m \text{ is odd} \\ (-1)^{\frac{m-1}{2}} \sin\frac{r\pi}{2} \text{ if } m \text{ is even} \end{array} \right) \Bigg\} \Bigg], \tag{7.104}$$

$$d_m^{sm} = \frac{(-1)^{m+1}\ e^{\lambda_0\left(h-(c+\frac{a}{2})\right)} + \ e^{-\lambda_0\left(h-(c+\frac{a}{2})\right)}}{2\cosh\lambda_0 h}\ \frac{I_{m+\frac{7}{6}}\left(\lambda_0\frac{c-a}{2}\right)}{\left(\lambda_0\frac{c-a}{2}\right)^{\frac{1}{6}}}, \tag{7.105}$$

$$d_m^{ansm} = d_{m-1}^{sm}\ . \tag{7.106}$$

4. Numerical Results

The numerical esimates of $|R|$ and $|T|$ are obtained from equation (7.59) after using the solution of the linear system (7.76) (for type I, II and IV barrier) and (7.80) (for type III barrier) for different values of wave numbers and other nondimensionalized parameters. In equations (7.76) and (7.80), we have taken $N = 30$ which gives five figure accuracy of the numerical values of unknowns a_{mn}. The energy identity relation $|R|^2 + |T|^2 = 1$ is numerically verified for various wave numbers for all types of barrier configurations. For Type I barrier configuration, the energy identity is presented in Table 7.1 where $|R|$ and $|T|$ are calculated for different values of the wave numbers and for $a/h = 0.2,\ b/h = 0.5,\ D/h^4 = 1,\ \epsilon/h = 0.1$

In Fig. 7.2 the reflection coefficients are depicted for four types of barrier configurations for very small values of ice cover parameters $\frac{D}{h^4} = 0.001$ and $\frac{\epsilon}{h} = 0.0001$ ie, when there is almost no ice cover. For Type I barrier configuration, we have taken $\frac{b}{h} = 0.1, \frac{a}{h} = 1.2$ and For Type II barrier configuration, $\frac{b}{h} = 2.0$ and $\frac{c}{h} = 0.5$; for Type III and Type IV

Table 7.1: Energy identity, Type I barrier for $\frac{a}{h} = 0.2$, $\frac{b}{h} = 0.5$, $\frac{D}{h^4} = 1$, $\frac{\epsilon}{h} = 0.1$

Kb	$\|R\|$	$\|T\|$	$\|R\|^2 + \|T\|^2 = 1$
0.1	0.666316	0.745669	1
0.5	0.914335	0.404958	1
1.0	0.951493	0.307672	1
1.5	0.964458	0.264236	1
2.0	0.971479	0.237124	1
2.5	0.976021	0.217677	1
2.9	0.978682	0.205381	1

barrier configurations $\frac{a}{h} = 0.2, \frac{c}{h} = 0.4, \frac{b}{h} = 1$ and $\frac{a}{h} = 0.2, \frac{c}{h} = 0.4, \frac{b}{h} = 0.1$ respectively. The graph of $|R|$ for Type I, Type II, Type III and Type IV barrier configurations in Fig.7.2 are compared with the curves of Figure 2 (a), Figure 3, Figure 4 and Figure 6 of Kanoria et. al. (1999). It is seen that the curves depicting $|R|$ in Fig.7.2 for very small values of ice cover parameters matches quite well with those figures of Kanoria et. al. (1999).

Also in table (Table 7.2), $|R|$ for Type I barrier configuration for $D/h^4 = 0.1\times10^{-4}$, $\epsilon/h = 0.1 \times 10^{-5}$ and for $\frac{a}{h} = 0.2$ and $\frac{b}{h} = 0.5$ are compared with the numerical data for $|R|$ from Kanoria et. al. (1999) (for $D/h^4 = 0$, $\epsilon/h = 0$. It is observed fron Table 7.2 that the results match up to 3 decimal places showing the correctness of results obtained in the present problem.

It is seen from Fig.7.2 that for barrier configuration of type IV ie, the barrier with a gap induces highest reflection $|R|$ as compared to other type of barrier configurations. Also the thick partially immersed barrier (Type I) produces more reflection than Type II and Type III barrier configuration. Also for Type II and Type III barrier configurations, $|R|$ shows oscillatory behaviour and for certain wave numbers $|R| = 0$. However this type of behaviour is not observed for Type I and Type IV barrier configurations. This type of behavior of the reflection coefficient $|R|$ for different types of thick rectangular barriers may be attributed to the nature of reflection and transmission of the incident wave train. The barriers of Type I and IV are surface piercing and as such an incident surface wave train undergoes more reflection than the Type II and III barriers which are submerged and not surface piercing. For Type I and Type IV barrier config-

urations there is not much scope for multiple reflections by the barrier and the bottom of water region, so that the oscillatory behavior of $|R|$ is not observed for these type of barrier configurations. For higher values of wave number, the incident wave train is confined near the upper surface and as such the incident wave is almost fully reflected by the barrier of Type I and IV. The fig. 7.2 precisely demonstrates this behaviour of reflected waves for type I and IV barriers. However, for type II and III barriers, there occurs multiple interactions of the waves with the upper surface of the barrier for Type II barrier configuration and upper and lower surface of the barrier for type III barrier configuration and the bottom of water region producing multiple reflection which results in exhibiting oscillatory behavior of $|R|$. These facts are well known in the theory of water waves (cf. Kanoria et. al. (1999)).

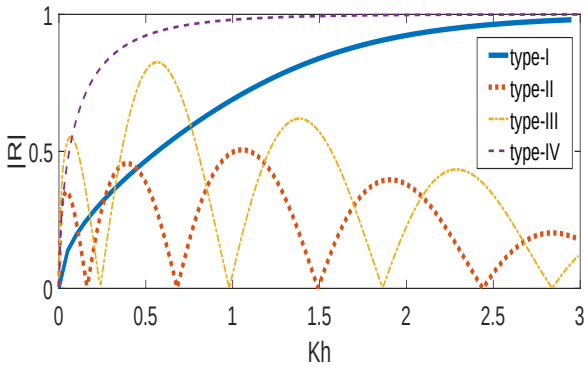

Figure 7.2: Reflection coefficients for four types of barriers without ice cover

Table 7.2: Reflection coefficient for $\frac{a}{h} = 0.2, \frac{b}{h} = 0.5, \frac{D}{h^4} = 1, \frac{\epsilon}{h} = 0.1$

Kh	$\|R\|$ **obtained from present result**	$\|R\|$ **obtained from Kanoria (1999)**
0.2	0.778132	0.778019
1.0	0.967543	0.967934
1.8	0.992729	0.992543

Fig. 7.3(a) to Fig. 7.6(a) show the behavior of $|R|$ and Fig. 7.3(b) to Fig. 7.6(b) show the behavior of $|T|$ against wave number for partially immersed thick barrier (Type I barrier configuration).

In Fig. 7.3(a), $|R|$ and in Fig. 7.3(b) $|T|$ are depicted for different values of $\frac{\epsilon}{h}$ =

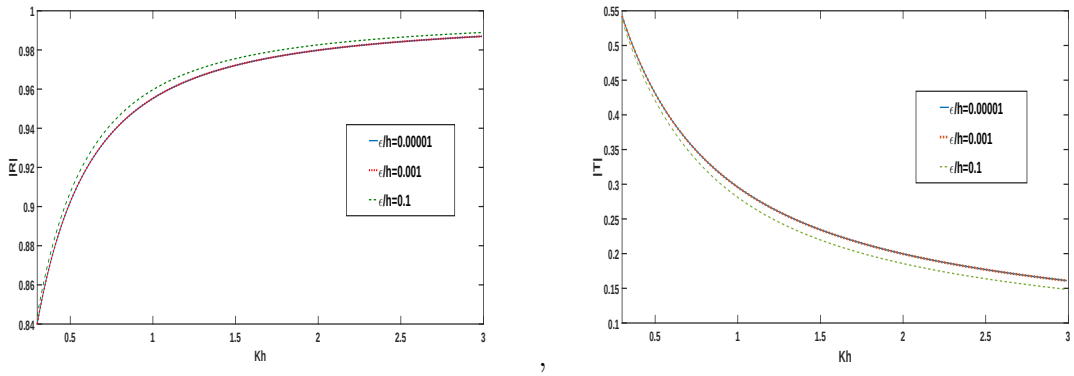

(a) (b)

Figure 7.3: (a) Reflection coefficient vs. wave number (b)Transmission coefficient vs. wave number for type-I barrier, for different ϵ/h, $D/h^4 = .1$, $a/h = 0.2$, $b/h = 0.5$

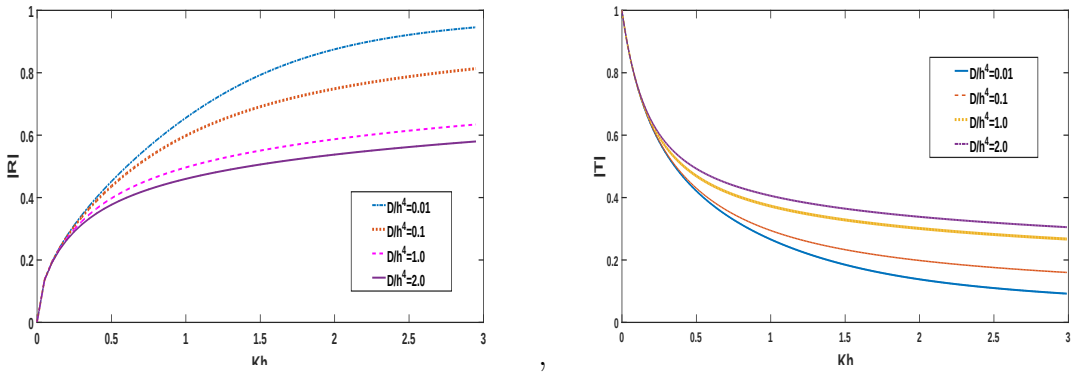

(a) (b)

Figure 7.4: (a)Reflection coefficient vs. wave number (b)Transmission coefficient vs. wave number for type-I barrier, for different $\frac{D}{h^4}$, $\epsilon/h = 0.01$, $a/h = 0.2$, $b/h = 0.5$

$0.00001, 0.001, 0.1$, and for $D/h^4 = 0.1$, $a/h = 0.2$, $b/h = 0.5$ .From the figures, it can be seen that as ϵ/h i.e., thickness of ice cover increases, $|R|$ increases while $|T|$ decreases although the change is not significant.

Figs. 7.4(a)and (b) depict the effect of elasticity of the ice cover on the reflection and transmission coefficients respectively. In Fig. 7.4(a) and in Fig. 7.4(b), $|R|$ and $|T|$ are plotted for four different values of $D/h^4 = 0.01, 0.1, 1, 2$ with fixed values of $\epsilon/h = 0.01$, $a/h = 0.2$ and $b/h = 0.5$. $|R|$ increases and $|T|$ decreases with decreasing values of $\frac{D}{h^4}$. This shows that large values of D induces more energy transmition and less wave reflection.

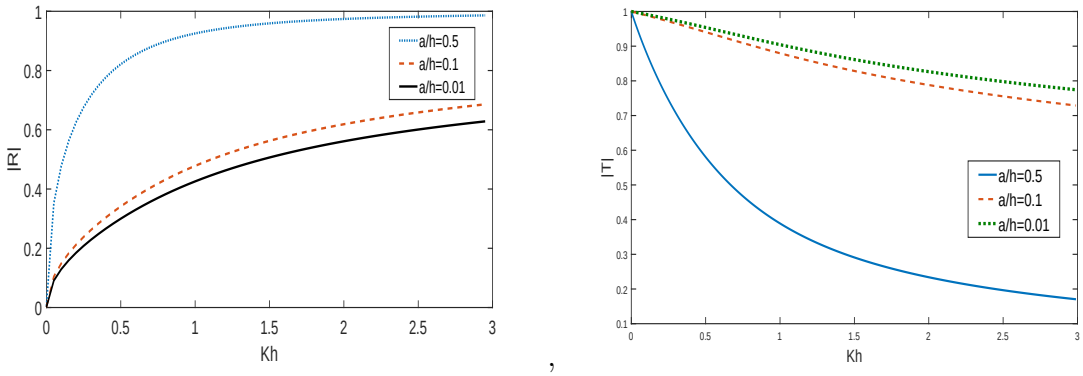

(a) , (b)

Figure 7.5: (a)Reflection coefficient vs. wave number (b)Transmission coefficient vs. wave number for type-I barrier, for different a/h, $\epsilon/h = 0.01, \frac{D}{h^4} = 0.1$, $b/h = 0.1$

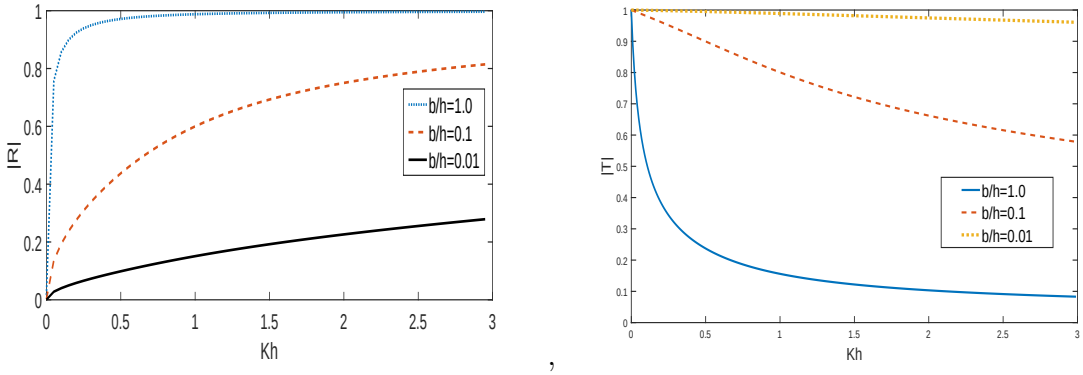

(a) , (b)

Figure 7.6: (a)Reflection coefficient vs. wave number (b)Transmission coefficient vs. wave number for type-I barrier, for different b/h, $\epsilon/h = 0.01, \frac{D}{h^4} = 0.1$, $a/h = 0.2$

In Figs. 7.5(a) and 7.5(b), $|R|$ and $|T|$ are depicted for various values of $\frac{a}{h} = 0.01, 0.1, 0.5$ and for fixed value of $D/h^4 = 0.1, \epsilon/h = 0.01, b/h = 0.1$ respectively. It is clear from the figure that increase in length of the barrier increases $|R|$ and decreases $|T|$.

In Fig. 7.6(a) and (b)depicts the effect of the width of the barrier ie, b/h on $|R|$ and $|T|$ for $D/h^4 = 0.1, \epsilon/h = 0.01, a/h = 0.2$. It is seen that large values of $\frac{b}{h}$ increases the values of $|R|$ and decreases $|T|$. Thus it can be remarked that gradually increasing values of width and length of the barrier induced more reflection and less transmission.

Fig. 7.7(a) to Fig. 7.9(a) depict $|R|$ and Fig. 7.7(b) to Fig. 7.9(b) depict $|T|$ for

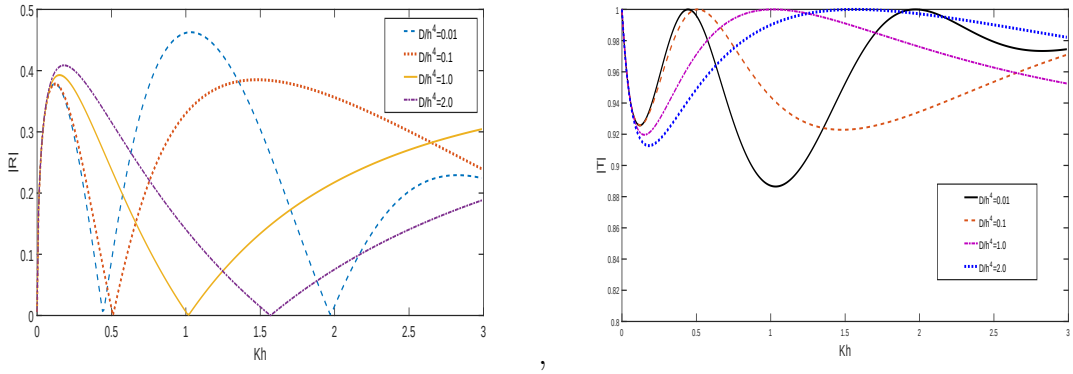

(a) (b)

Figure 7.7: (a)Reflection coefficient vs. wave number (b)Transmission coefficient vs. wave number for type-II barrier, for different D/h^4, $\epsilon/h = 0.1$, $b/h = 1.0$, $c/h = 0.5$

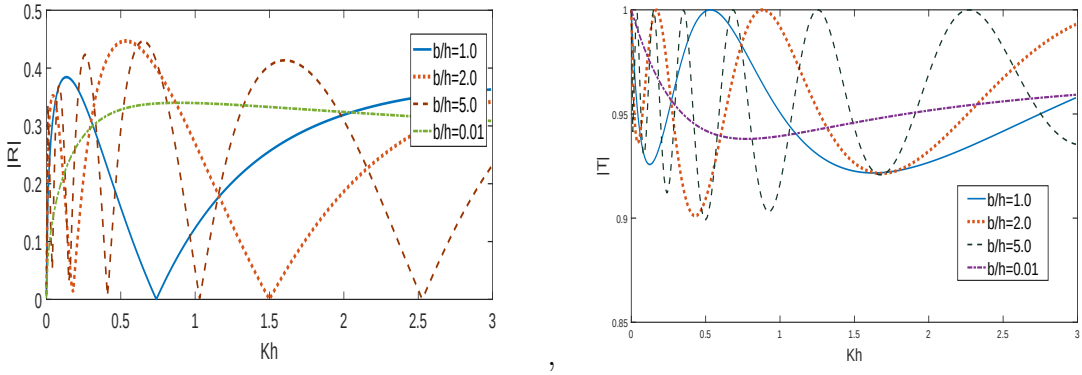

(a) (b)

Figure 7.8: (a)Reflection coefficient vs. wave number (b)Transmission coefficient vs. wave number for type-II barrier, for different b/h, $\epsilon/h = 0.01$, $\frac{D}{h^4} = .1$, $c/h = 0.5$

bottom standing thick barrier ie, Type-II barrier configuration. In Fig. 7.7(a) and 7.7(b), $|R|$ and $|T|$ are plotted respectively for different values of $\frac{D}{h^4} = 0.01, 0.1, 1.0, 2.0$ with fixed values of $\frac{\epsilon}{h} = 0.1$, $\frac{b}{h} = 1.0$, $\frac{c}{h} = 0.5$. It is seen from the graph that the elastic behaviour of the ice cover produces oscillations in $|R|$ and $|T|$.

Fig. 7.8(a), (b) depict $|R|$ and $|T|$ for different values of width of the barrier $\frac{b}{h} = 1.0, 2.0, 5.0, 0.01$ and $D/h^4 = 0.1$, $\epsilon/h = 0.01$, $c/h = 0.5$. It is observed that when the width of the barrier is very small there is hardly any oscillations in $|R|$ and $|T|$. However for a wide barrier oscillations in $|R|$ and $|T|$ are observed and for certain values of the wave number there occurs zero reflection and no transmission of wave energy.

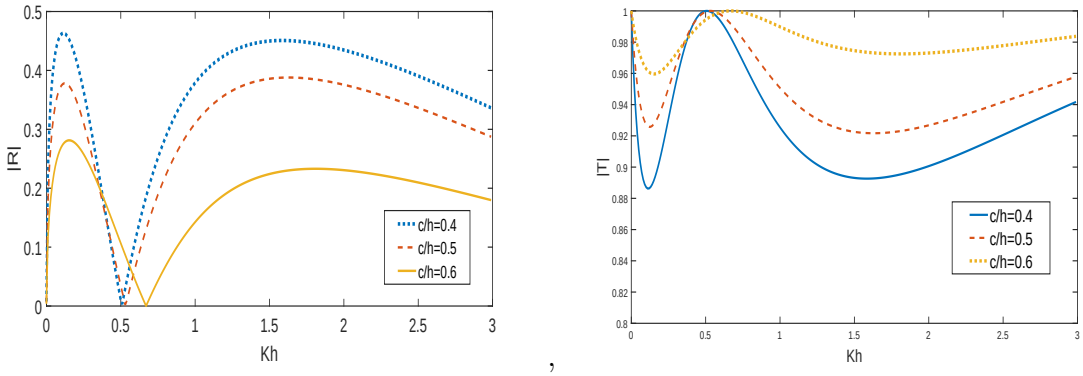

(a) , (b)

Figure 7.9: (a)Reflection coefficient vs. wave number (b)Transmission coefficient vs. wave number for type-II barrier, for different c/h, $\epsilon/h = 0.01$, $\frac{D}{h^4} = .1$, $b/h = 1.0$

Also as the width of the barrier increases the frequency of the oscillations in $|R|$ and $|T|$ inctreases.

In Fig. 7.9(a), (b) $|R|$ and $|T|$ are plotted against the wave number kh different values of $\frac{c}{h} = 0.4, 0.5, 0.6$ and $D/h^4 = 0.1$, $\epsilon/h = 0.01$, $b/h = 0.1$. Fig. 7.9(a), (b) exhibit oscillatory behaviour in $|R|$, $|T|$ and $|R| = 0$, $|T| = 0$ for certain values of wave number kh. It is also observed that as the values of $\frac{c}{h}$ decreases, ie, the length of the bottom standing thick barrier increases, the amplitude of $|R|, |T|$ gradually increases. This is plausible because long bottom standing barrier induces more reflection and less transmission of wave energy.

The behaviours of $|R|$ and $|T|$ for submerged thick rectangular block are exhibited in Fig. 7.10(a), Fig. 7.11(a) and in Figs. 7.10(b), 7.11(b) respectively for fully submerged barrier ie, for Type III barrier configuration.

Figs. 7.10(a) and 7.10(b) have shown the behavior of $|R|$ and $|T|$ respectively for different values of $D/h^4 = 0.01, 0.1, 1.0, 2.0$ with fixed values of $\frac{\epsilon}{h} = 0.01, \frac{b}{h} = 0.2, \frac{a}{h} = 0.6, \frac{c}{h} = 0.8$. The figures exhibit oscillatory behaviour of $|R|$ and $|T|$ and the frequecy of oscillation decrease with increase of D/h^4. These behaviors of $|R|$ and $|T|$ are due to the elastic behaviour of the ice cover.

Fig. 7.11(a) depicts $|R|$ and Fig. 7.11(b) depicts $|T|$ for different values of $\frac{b}{h} = 0.01, 1.0, 2.0$ with fixed values of $\frac{\epsilon}{h} = 0.01, \frac{a}{h} = 0.6, \frac{c}{h} = 0.8, \frac{D}{h^4} = 0.1$. From the figures

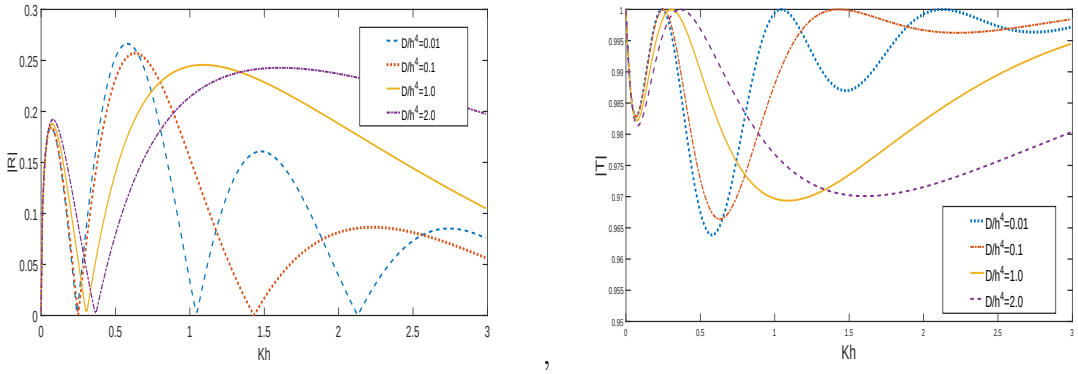

(a) (b)

Figure 7.10: (a)Reflection coefficient vs. wave number (b)Transmission coefficient vs. wave number for type-III barrier, for different D/h^4, $\epsilon/h = 0.01$, $b/h = 2.0$, $a/h = 0.6$, $c/h = 0.8$

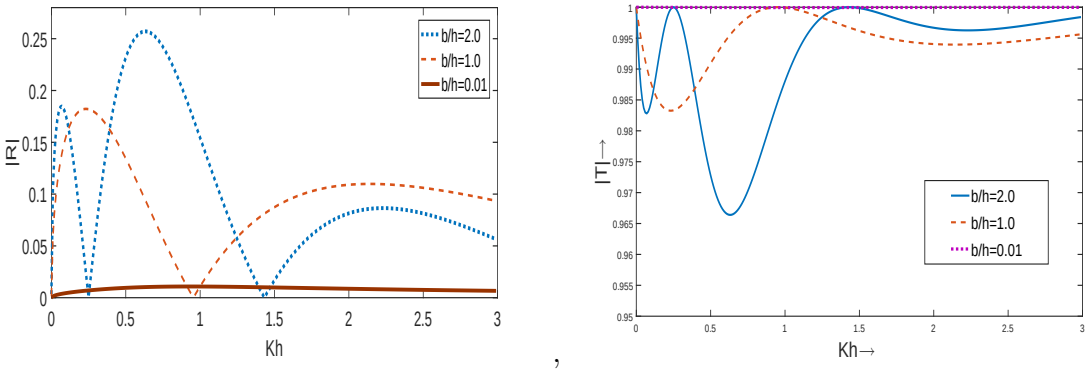

(a) (b)

Figure 7.11: (a)Reflection coefficient vs. wave number (b)Transmission coefficient vs. wave number for type-III barrier, for different b/h, $\epsilon/h = 0.01$, $\frac{D}{h^4} = .1$, $a/h = 0.6$, $c/h = 0.8$

it is observed that that $|R|$ and $|T|$ show oscillatory behaviour and the amplitude of oscillation increases as the width or the thickness of the barrier increases.

Finally, Fig. 7.12 to Fig. 7.14 depict the values of $|R|$ and $|T|$ for thick vertical wall with submerged gap ie, type-IV barrier configuration.

Fig. 7.12(a) and Fig. 7.12(b) show the behavior of $|R|$ and $|T|$ respectively for different values of $\frac{D}{h^4} = 0.01, 0.1, 1.0, 2.0$. with fixed $\epsilon/h = 0.01$, $b/h = 0.1$, $a/h = 0.2$, $c/h = 0.4$. It is observed that $|R|$ decreases and $|T|$ increases with increasing values of $\frac{D}{h^4}$. As observed by Kanoria et. al.(1999), in this case it is seen that $|R|$ asymptotically increases

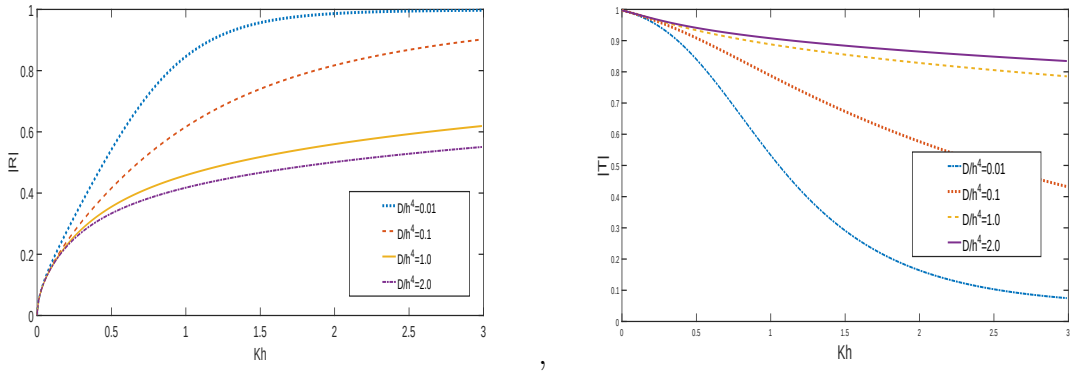

(a) (b)

Figure 7.12: (a)Reflection coefficient vs. wave number (b)Transmission coefficient vs. wave number for type-IV barrier, for different D/h^4, $\epsilon/h = 0.01$, $b/h = .1$, $a/h = 0.2$, $c/h = 0.4$

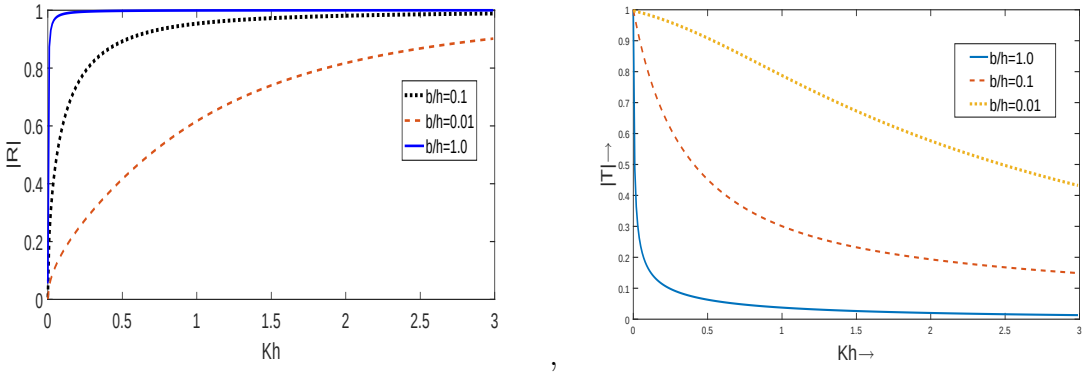

(a) (b)

Figure 7.13: (a)Reflection coefficient vs. wave number (b)Transmission coefficient vs. wave number for type-IV barrier, for different b/h, $\epsilon/h = 0.01$, $\frac{D}{h^4} = 0.1$, $a/h = 0.2$, $c/h = 0.4$

to unity and there is no oscillation for $|R|$. Similar qualitative behaviour is observed from Fig. 7.4, for Type I barrier configurations.

Fig. 7.13(a) and 7.13(b) express the behavior of $|R|$ and $|T|$ for different thickness of the barrier $\frac{b}{h} = 0.01, 0.1, 1.0$ with fixed values of $\frac{\epsilon}{h} = 0.01$, $\frac{a}{h} = 0.2$, $\frac{c}{h} = 0.4$, $\frac{D}{h^4} = 0.1$. From the figure it is clear that $|R|$ gradually increases with the increase of $\frac{b}{h}$. It is important to observe that, when the width of the barrier is almost same as the depth of water, $|R|$ is nearly equal to unity. But for the comparatively small values of $\frac{b}{h}$, $|R|$ asymptotically increases to unity and $|T|$ asymptotically decreases to zero as the

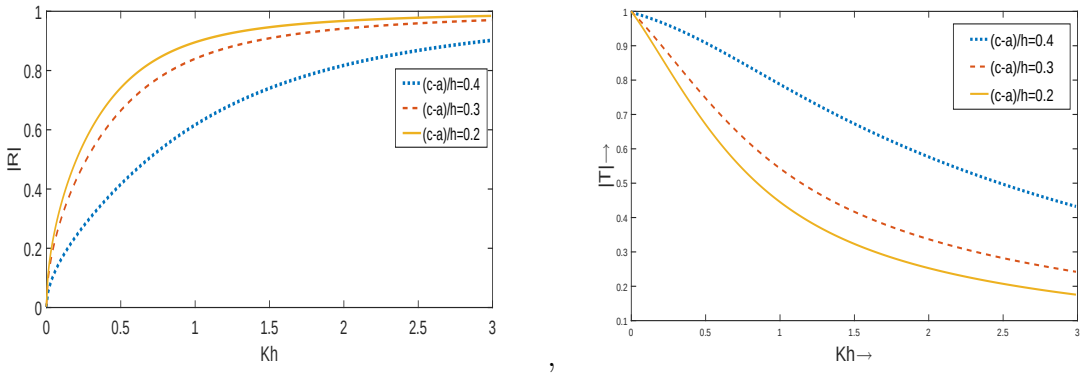

(a) , (b)

Figure 7.14: (a)Reflection coefficient vs. wave number (b)Transmission coefficient vs. wave number for type-IV barrier, for different gap i.e. $(c-a)/h$, $\epsilon/h = 0.01$, $\frac{D}{h^4} = 0.1$

wave number increases. This is plausible because with large wave number, the surface waves which are near the ice cover surface are reflected back by the barrier. The same qualitative feature can be observed in Figure 6 of Kanoria et. al.[1999] (in absence of ice cover over the rectangular barriers).

Fig. 7.14(a) and 7.14(b) are drawn for the Type IV barrier with different lengths of the submerged gap of the thick rectangular barrier $\frac{c-a}{h} = 0.2, 0.3, 0.4$ with $\epsilon/h = 0.01$, $D/h^4 = 0.1$. This figure shows that more wave energy reflected and less energy transmitted when the length of the gap decreases.

5. Conclusion

The problem of water wave scattering in a water body of uniform finite depth with a thin ice cover on its surface, in presence of thick rectangular barriers of four different geometrical configurations, are studied by employing the multiterm Galerkin approximation method involving ultraspherical Gegenbauer polynomials of order 1/6. Very accurate numerical results for reflection and transmission coefficient are obtained for different values of wave number and other parameters involving the physical problem.

They also satisfy the energy identity. The numerical results which agree quite well with the known results available in the literature in absence of ice cover. The thickness and depth of thick barriers affect the reflection and transmission coefficient which is quite evident from the figures. For partially immersed barrier(type-I), reflection increases with the increment of depth and thickness of barrier. For bottom standing (type-II) and fully immersed (type-III) barriers, there occurs zero reflection which depends on the width of barrier. Also in type-IV barrier configuration, the increment in the length of the submerged gap of the thick wall causes lesser reflection. Thus the breakwaters in form of rectangular thick barrier has some impact on the reflected and transmitted wave energy.

Chapter 8

Numerical approach to the problem of oblique wave scattering by a wide rectangular impediment with a vent placed under a finite depth water body with ice covered surface

1. Introduction

The problem of water wave diffraction by some obstacles of different geometrical shapes have been studied substantially by the researchers in last few decades with different mathematical techniques.

As mentioned in chapter 1, the problem of scattering of water waves by thin vertical barriers are studied by many researchers like, Ursell (1947) for a partially immersed vertical plate, Evans (1970) for a submerged vertical plate, Porter (1972) for a barrier

† The content of this chapter is based on the paper " Numerical approach on oblique wave scattering by a wide rectangular impediment with a vent placed under a finite depth water body with ice covered surface ", *Journal of offshore mechanics and arctic engineering*, 145(1) (2023) 011902.

with a submerged gap, Banerjea and Mandal (2009) for a surface piercing wall with multiple submerged gaps, Banerjea et. al. (1996) for a submerged wall with a gap, Kanoria and Mandal (1996) for two parallel vertical barriers with submerged gaps in water of uniform finite depth, Das et. al. (1997) for two parallel thin barriers with gaps and others. But now a days, due to the practical importance in marine engineering, the vertical barriers are chosen to be thick. Some researchers like Kanoria et. al. (1999), Mandal and Kanoria (2000), Xie et al. (2011) studied scattering problems by thick rectangular barriers placing them in different position under the finite depth water.
When ocean waves interact with floating sea ice, they are known to propagate as ice-coupled gravity waves at the interface between the floating sea ice and underlying water. Ice-coupled gravity waves are relevant in cold regions and in floating ice-cover platforms for vehicular usage. The basic characteristics of an ice sheet can be explained by modeling it as an elastic plate using the well-known Euler-Bernoulli plate theory. The first wave propagation model in the presence of a thin elastic beam floating on the water was initiated by Greenhill (1887) over a century ago. Using a computational mode-matching technique, Fox and Squire (1994) discussed the first evaluated solutions of the Greenhill's (1887) mathematical model for the sake of geophysical interest. Later, many research attempts were made to study a thin sheet of ice having elastic properties (cf. Fox and Squire (1994), Balmforth and Craster (1999) and the literature cited therein). Sturova (2015) used Greenhill's function to deal with the radiation problem involving a submerged cylinder in water with ice cover. Also, some recent papers explain the effect of floating ice sheet/elastic plate on wave scattering problems (cf. Samanta and Chakraborty (2020) and Sarkar et al.(2021)).

In the present chapter, we study the effect of ice cover on waves scattering by obliquely incident wave by submerged wall with rectangular cross-section having a gap in a finite depth water. Due to the geometrical symmetry of the construction about its center line, the boundary value problem is split in two separate problems involving the symmetric part and antisymmetric part of the velocity potential function. Then the matching of eigen function expansion of velocity potential through the corner points of the barriers produces an integral equation. This integral equation is then solved by two methods, viz, multiterm Galerkin approximation method using ultraspherical Gegen-

baurer polynomial as basis functions and also boundary element method. Recently, utilizing same multi term Galerkin technique, Chakraborty and Mandal (2014,2015) solved scattering problem by rectangular trench. The boundary element method is also utilised by Mondal et.al. (2021) while studying a scattering problem circular arc shaped barrier. Utilising the solutions of the integral equations, we obtain the reflection and transmission coefficient which are then depicted in the graphs against the wave number. These graphs show that the presence of ice cover and height of the gap remarkably affects the reflection coefficients.

2. Formulation of the problem

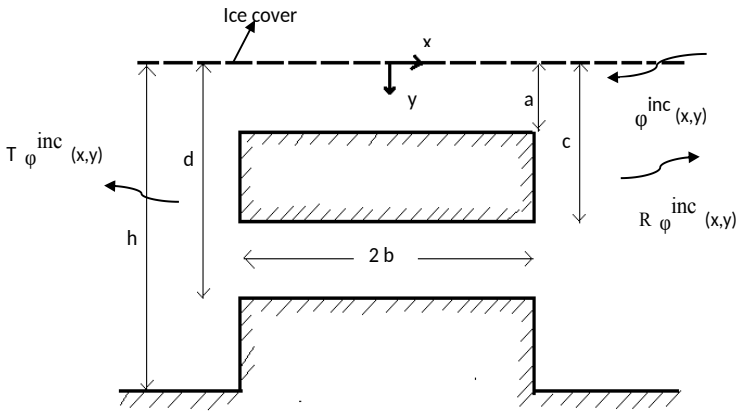

Figure 8.1: Geometrical configuration of the problem

We consider an irrotational motion in an inviscid, incompressible, and homogeneous fluid (water) with a constant density ρ_1. A Cartesian coordinate system is taken with y-axis directed vertically downward passing through the middle of the thick wall. The (x, z) plane denotes the rest position of a thin ice sheet floating on the water. This thin ice sheet is modeled as a thin elastic plate of infinite extent. The fluid occupies the region $0 < y < h$ below the ice-covered surface. The obstacle is of the form of a submerged thick wall with a gap whose position is given by $-b \leq x \leq b$, $y \in L \equiv \{(a, c) + (d, h)\}$.

The wall is at the depth a below the ice cover and the gap of the wall is at depth c below the ice cover surface with gap length $(d-c)$ and the width of the wall is $2b$. The geometrical configuration is depicted in figure 8.1.
Now we consider a train of waves coming from positive x- direction is incident obliquely on the the wall with angle of incidence α with x axis. Under the assumption of linearized theory of water wave the incident wave is represented by the velocity potential $Re\{\phi^{inc}(x,y)\ e^{i(\nu z-\sigma t)}\}$, where

$$\phi^{inc} = \frac{2\cosh\lambda_0(h-y)e^{-i\mu(x-b)}}{\cosh\lambda_0 h} \tag{8.1}$$

and λ_0 is the unique real positive root of the transcendental equation

$$u(1-\epsilon K+Du^4)\tanh uh = K. \tag{8.2}$$

Here $K = \sigma^2/g$, σ is the circular frequency of incoming wave train, g is gravitational acceleration and $D = \frac{Eh_0^3}{12(1-\upsilon^2)\rho_1 g}$, $\varepsilon = \frac{\rho_0 h_0}{\rho_1}$, where ρ_0 is the density of ice, ρ_1 is the density of water, h_0 is the small thickness of the ice-cover and E, υ are respectively the Young's modulus and Poisson's ratio of the ice and $\mu = \lambda_0\cos\alpha$, $\nu = \lambda_0\sin\alpha$. Assuming velocity potential to be of the form $Re\{\phi(x,y)\ e^{i(\nu z-\sigma t)}\}$, $\phi(x,y)$ satisfies the following boundary value problem.

$$(\nabla^2-\nu^2)\phi = 0; \qquad \text{in the fluid region,} \tag{8.3}$$

$$(D\frac{\delta^4}{\delta x^4}+1-\varepsilon K)\phi_y + K\phi = 0; \qquad \text{on y=0.} \tag{8.4}$$

$$\phi_x = 0, \qquad \text{on x=}\pm\text{ b,} \qquad y \in L \equiv \{(a,c)+(d,h)\}. \tag{8.5}$$

$$\phi_y = 0, \qquad \text{on } y = a,c,d; \qquad |x| < b. \tag{8.6}$$

$$\phi_y = 0, \qquad \text{on y=h;} \qquad |x| > b. \tag{8.7}$$

$$r^{1/3}\nabla\phi \qquad \text{is bounded as r} \to 0, \tag{8.8}$$

where r is the distance of submerged edge of the thick wall,

$$\phi(x,y) \sim \begin{cases} \phi^{inc}(x,y) + R\phi^{inc}(-x,y) \text{ as } x \to \infty, \\ T\phi^{inc}(x,y) \text{ as } x \to -\infty. \end{cases} \tag{8.9}$$

Here R and T are the reflection and transmission coefficients and are to be determined.

3. Method of solution

The geometrical symmetry of the thick wall about $x = 0$ allows us to split the velocity potential $\phi(x,y)$ into symmetric part $\phi_{sm}(x,y)$ and antisymmetric part $\phi_{ansm}(x,y)$ such that

$$\phi(x,y) = \phi_{sm}(x,y) + \phi_{ansm}(x,y) \tag{8.10}$$

where

$$\phi_{sm}(-x,y) = \phi_{sm}(x,y), \qquad \phi_{ansm}(-x,y) = -\phi_{ansm}(x,y). \tag{8.11}$$

Therefore, we consider only the region $x \geq 0$. Now $\phi_{sm,ansm}(x,y)$ satisfy equations (8.3) to (8.8) together with

$$\frac{\partial \phi_{sm}}{\partial x}(0,y) = 0, \qquad \phi_{ansm}(0,y) = 0 \qquad 0 < y < h. \tag{8.12}$$

Let the behavior of $\phi_{sm,ansm}(x,y)$ for large x be represented by

$$\phi_{sm,ansm}(x,y) \sim \frac{\cosh \lambda_0(h-y)}{\cosh \lambda_0 h}[e^{-i\mu(x-b)} + R_{sm,ansm}e^{i\mu(x-b)}] \qquad \text{as } x \to \infty \tag{8.13}$$

where R_{sm} and R_{ansm} are unknown constants. These constants are related to R and T by

$$R, T = \frac{1}{2}(R_{sm} \pm R_{ansm})\ e^{-2ib\mu}. \tag{8.14}$$

Now, the whole fluid region is divided into three regions
i) Region-I ($x > b$; $0 < y < h$);
ii) Region-II ($0 < x < b$; $0 < y < a$);
iii) Region-III ($0 < x < b$; $c < y < d$);
The eigen function expansions of $\phi_{sm,ansm}(x,y)$ satisfying equations (8.3), (8.4), (8.5), (8.6), (8.7), (8.12) for $x > 0$ in the different regions are given below.

Region I:

$$\phi_{sm,ansm}(x,y) = \psi(y;\lambda_0,h)[e^{-is_0(x-b)} + R_{sm,ansm}e^{is_0(x-b)}] + \sum_{n=1}^{\infty} A(n)_{sm,ansm}\ \bar{\psi}(y;\lambda_n,h)\ e^{-s_n(x-b)} + \sum_{n=I}^{II} A(n)_{sm,ansm}\ \psi(y;\lambda_n,h)\ e^{-i\epsilon_n s_n(x-b)} \tag{8.15}$$

where $R_{sm,ansm},\ A(n)_{sm,ansm}$ are unknown constants to be determined and

$$\psi(y;\lambda_n,h) = \frac{\cosh\lambda_n(h-y)}{\cosh\lambda_n h}\ ; \quad \bar{\psi}(y;\lambda_n,h) = \cos\lambda_n(h-y). \tag{8.16}$$

Here λ_n $(n = 0, I, II)$ satisfy the transcendental equation

$$K = u(1 - \epsilon K + Du^4)\tanh uh \tag{8.17}$$

and λ_n $(n = 1, 2, ...)$ satisfy the transcendental equation

$$u(1 - \epsilon K + Du^4)\tan uh + K = 0, \tag{8.18}$$

$$\epsilon_n = \begin{cases} 1, & for\ n = 0, I, \\ -1, & for\ n = II \end{cases}$$

and

$$s_n = \begin{cases} \sqrt{\lambda_n^2 + \nu^2}, & for\ n = 1, 2, 3, ... \\ \sqrt{\lambda_n^2 - \nu^2}, & for\ n = 0, I, II. \end{cases} \tag{8.19}$$

Region II:

$$\begin{aligned} \left\{ \begin{array}{l} \phi_{sm}(x,y) \\ \phi_{ansm}(x,y) \end{array} \right\} &= \left\{ \begin{array}{l} B(0)_{sm}\ \cos t_0 x \\ B(0)_{ansm}\ \sin t_0 x \end{array} \right\} \psi(y;\alpha_0,a) \\ &+ \sum_{n=I}^{II} \left\{ \begin{array}{l} B(n)_{sm}\ \cos t_n x \\ B(n)_{ansm}\ \sin t_n x \end{array} \right\} \psi(y;\alpha_n,a) \\ &+ \sum_{n=1}^{\infty} \left\{ \begin{array}{l} B(n)_{sm}\ \cosh\ t_n x \\ B(n)_{ansm}\ \sinh\ t_n x \end{array} \right\} \bar{\psi}(y;\alpha_n,a) \end{aligned} \tag{8.20}$$

where $B(n)_{sm,ansm}$ are unknown constants to be determined and $\pm\alpha_0$, α_I, α_{II}, $\pm i\alpha_n$ $(n = 1, 2, ...)$ are the roots of the equation

$$\alpha(1 - \epsilon K + D\alpha^4) \tanh\ \alpha a = K, \tag{8.21}$$

and

$$t_n = \begin{cases} \sqrt{\alpha_n^2 + \nu^2}, & for\ n = 1, 2, 3, ... \\ \sqrt{\alpha_n^2 - \nu^2}, & for\ n = 0, I, II. \end{cases} \tag{8.22}$$

Region III:

$$\left\{ \begin{array}{l} \phi_{sm}(x,y) \\ \phi_{ansm}(x,y) \end{array} \right\} = \left\{ \begin{array}{l} C(0)_{sm} \cosh \nu x \\ C(0)_{ansm} \sinh \nu x \end{array} \right\} + \sum_{n=1}^{\infty} \left\{ \begin{array}{l} C(n)_{sm} \cosh \xi_n x \\ C(n)_{ansm} \sinh \xi_n x \end{array} \right\} \cos \frac{n\pi(d-y)}{d-c} \tag{8.23}$$

where $C(n)_{sm,ansm}$ are unknown constants to be determined and

$$\xi_n = \sqrt{\left(\frac{n\pi}{d-c}\right)^2 + \nu^2}. \tag{8.24}$$

We now define

$$\frac{\partial}{\partial x}\phi_{sm,ansm}(b+0,y) = f_{sm,ansm}(y), \quad 0 < y < h. \tag{8.25}$$

Then

$$f_{sm,ansm}(y) = 0 \quad \text{for } y \,\epsilon\, L \tag{8.26}$$

and

$$\frac{\partial}{\partial x}\phi_{sm,ansm}(b \pm 0,y) = f_{sm,ansm}(y) \quad for\ y \,\epsilon\, \bar{L} \equiv (0,h) - L. \tag{8.27}$$

Also due to the edge condition (8.8) , we have the requirement

$$\begin{cases} f_{sm,ansm}(y) = O(|a-y|^{-1/3}) \quad as\ y \ \to\ a-0, \\ f_{sm,ansm}(y) = O(|y-c|^{-1/3}) \quad as\ y \ \to\ c+0, \\ f_{sm,ansm}(y) = O(|d-y|^{-1/3}) \quad as\ y \ \to\ d-0. \end{cases} \tag{8.28}$$

We shall now evaluate the various constants $A(n)_{sm,ansm},\ B(n)_{sm,ansm},\ C(n)_{sm,ansm}$ appearing in equation (8.15), (8.20) and (8.23) for different regions.

For Region-I

Using the expression of $\phi_{sm,ansm}(x,y)$ of equation (8.15) into (8.25) and then using Havelock's Inversion formula, we obtain

$$1 - R_{sm,ansm} = \frac{4i\lambda_0\ \cosh^2\ \lambda_0 h}{\mu\delta_0} \int_{\bar{L}} f_{sm,ansm}(y)\ \psi(y;\lambda_0,h)\ dy \tag{8.29}$$

with $\quad \delta_0 = 2\lambda_0 h + \sinh\ 2\lambda_0 h$; and

for n=I, II,

$$A(n)_{sm,ansm} = \frac{4i\lambda_n \cosh^2 \lambda_n h}{\epsilon_n s_n \delta_n} \int_{\bar{L}} f_{sm,ansm}(y)\ \psi(y;\lambda_n,h)\ dy \tag{8.30}$$

with $\delta_n = 2\lambda_n h + \sinh\ 2\lambda_n h\ \ (n = I, II)$,

for, n=1,2,3,.....,

$$A(n)_{sm,ansm} = -\frac{4\lambda_n}{s_n \delta_n} \int_{\bar{L}} f_{sm,ansm}(y)\ \bar{\psi}(y;\lambda_n,h)\ dy \tag{8.31}$$

with $\delta_n = 2\lambda_n h + \sin\ 2\lambda_n h\ \ (n = 1, 2, ...)$.

For Region-II

Again substituting equation (8.20) in (8.27) and applying Havelock's Inversion Formula, we have

for n=0, I, II

$$B(n)_{sm,ansm} = \frac{4\alpha_n \cosh^2 \alpha_n a}{t_n \gamma_n}\left(-\frac{1}{\sin t_n b},\ \frac{1}{\cos t_n b}\right) \int_0^a f_{sm,ansm}(y)\ \psi(y;\alpha_n,a)\ dy \tag{8.32}$$

with $\gamma_n = 2\alpha_n a + \sinh\ 2\alpha_n a$ and

for n=1,2,3,.....

$$B(n)_{sm,ansm} = \frac{4\alpha_n}{t_n \gamma_n}\left(\frac{1}{\sinh t_n b},\ \frac{1}{\cosh t_n b}\right) \int_0^a f_{sm,ansm}(y)\ \bar{\psi}(y;\alpha_n,a)\ dy \tag{8.33}$$

with $\gamma_n = 2\alpha_n a + sin\ 2\alpha_n a$.

For Region-III

Using equation (8.23) in (8.27) and applying Fourier Cosine Inversion, we get

$$C(0)_{sm,ansm} = \frac{1}{\nu(d-c)}\left(\frac{1}{\sinh\nu b}, \frac{1}{\cosh\nu b}\right)\int_c^d f_{sm,ansm}(y)\ dy, \tag{8.34}$$

$$C(n)_{sm,ansm} = \frac{2}{\xi_n(d-c)}\left(\frac{1}{\sinh\xi_n b}, \frac{1}{\cosh\xi_n b}\right)\int_c^d f_{sm,ansm}(y)\cos\frac{n\pi(d-y)}{d-c}\ dy. \tag{8.35}$$

3.1. Reduction to integral equation

Now due to the continuity of velocity potential across the gap, we match $\phi_{sm,ansm}(x,y)$ across the line $x = b$, $y \in \bar{L}$, which yields

$$\phi_{sm,ansm}(b+0,y) = \phi_{sm,ansm}(b-0,y), \quad y \in \bar{L} \tag{8.36}$$

which after using the expression of $\phi_{sm,ansm}(x,y)$ from equations (8.15), (8.20), (8.23) along with the equations (8.29) -(8.31), reduces to a integral equation

$$\int_{\bar{L}} \mathcal{K}_{sm,ansm}(u)\ M_{sm,ansm}(y,u)\ du = \psi(y;\lambda_0,h), \quad y \in \bar{L} \tag{8.37}$$

where

$$\mathcal{K}_{sm,ansm}(y) = \frac{4}{\beta\ (1+R_{sm,ansm})}\ f_{sm,ansm}(y), \quad y \in \bar{L}$$

with

$$\beta = \frac{\mu\delta_0}{\lambda_0\cosh^2\lambda_0 h} \tag{8.38}$$

and $M_{sm,ansm}(y,u)$ $(y,u \in \bar{L})$ are real and symmetric in y and u. and their expressions are given below.

Case-1: $\boldsymbol{y, u \in (0, a)}$

$$M_{sm}(y,u) = \beta \Bigg[\sum_{n=1}^{\infty} \Bigg(\frac{\lambda_n \ \bar{\psi}(y;\lambda_n,h) \ \bar{\psi}(u;\lambda_n,h)}{s_n \delta_n} + \frac{\alpha_n \coth t_n b \ \ \bar{\psi}(y;\alpha_n,a) \ \bar{\psi}(u;\alpha_n,a)}{t_n \gamma_n} \Bigg) - \frac{\alpha_0 \cot t_0 b \ \cosh^2 \alpha_0 a \ \ \psi(y;\alpha_0,a) \ \psi(u;\alpha_0,a)}{t_0 \gamma_0} - \sum_{n=I}^{II} \Bigg(\frac{\alpha_n \cot t_n b \ \cosh^2 \alpha_n a \ \ \psi(y;\alpha_n,a) \ \psi(u;\alpha_n,a)}{t_n \gamma_n} + \frac{i\lambda_n \ \cosh^2 \lambda_n h}{\epsilon_n s_n \delta_n} \ \psi(y;\lambda_n,h) \ \psi(u;\lambda_n,h) \Bigg) \Bigg], \tag{8.39}$$

$$M_{ansm}(y,u) = \beta \Bigg[\sum_{n=1}^{\infty} \Bigg(\frac{\lambda_n \ \bar{\psi}(y;\lambda_n,h) \ \bar{\psi}(u;\lambda_n,h)}{s_n \delta_n} + \frac{\alpha_n \tanh t_n b \ \ \bar{\psi}(y;\alpha_n,a) \ \bar{\psi}(u;\alpha_n,a)}{t_n \gamma_n} \Bigg) - \frac{\alpha_0 (-\tan t_0 b) \ \cosh^2 \alpha_0 a \ \ \psi(y;\alpha_0,a) \ \psi(u;\alpha_0,a)}{t_0 \gamma_0} - \sum_{n=I}^{II} \Bigg(\frac{\alpha_n (-\tan t_n b) \ \cosh^2 \alpha_n a \ \ \psi(y;\alpha_n,a) \ \psi(u;\alpha_n,a)}{t_n \gamma_n} + \frac{i\lambda_n \ \cosh^2 \lambda_n h}{\epsilon_n s_n \delta_n} \ \psi(y;\lambda_n,h) \ \psi(u;\lambda_n,h) \Bigg) \Bigg]. \tag{8.40}$$

Case-2: $\boldsymbol{y, u \in (c, d)}$

$$M_{sm}(y,u) = \beta \left[\sum_{n=1}^{\infty} \left(\frac{\lambda_n \ \bar{\psi}(y;\lambda_n,h) \ \bar{\psi}(u;\lambda_n,h)}{s_n \delta_n} \right.\right.$$
$$\left. + \frac{\coth \xi_n b}{2(d-c) \ \xi_n} \cos \frac{n\pi(d-y)}{d-c} \cos \frac{n\pi(d-u)}{d-c} \right)$$
$$\left. + \frac{\coth \nu b}{4(d-c) \ \nu} - \sum_{n=I}^{II} \left(\frac{i\lambda_n \ \cosh^2 \lambda_n h}{\epsilon_n s_n \delta_n} \ \psi(y;\lambda_n,h) \ \psi(u;\lambda_n,h) \right) \right], \tag{8.41}$$

$$M_{ansm}(y,u) = \beta \left[\sum_{n=1}^{\infty} \left(\frac{\lambda_n \ \bar{\psi}(y;\lambda_n,h) \ \bar{\psi}(u;\lambda_n,h)}{s_n \delta_n} \right.\right.$$
$$\left. + \frac{\tanh \xi_n b}{2(d-c) \ \xi_n} \cos \frac{n\pi(d-y)}{d-c} \cos \frac{n\pi(d-u)}{d-c} \right)$$
$$\left. + \frac{\tanh \nu b}{4(d-c) \ \nu} - \sum_{n=I}^{II} \left(\frac{i\lambda_n \ \cosh^2 \lambda_n h}{\epsilon_n s_n \delta_n} \psi(y;\lambda_n,h) \ \psi(u;\lambda_n,h) \right) \right]. \tag{8.42}$$

Case-3: For $y \in (0,a)$, $u \in (c,d)$ and $y \in (c,d)$, $u \in (0,a)$

$$M_{sm,ansm} = \beta \left[\sum_{n=1}^{\infty} \frac{\lambda_n \ \bar{\psi}(y;\lambda_n,h) \ \bar{\psi}(u;\lambda_n,h)}{s_n \delta_n} \right.$$
$$\left. - \sum_{n=I}^{II} \frac{i\lambda_n \ \cosh^2 \lambda_n h}{\epsilon_n s_n \delta_n} \ \psi(y;\lambda_n,h) \ \psi(u;\lambda_n,h) \right]. \tag{8.43}$$

Writing

$$J_{sm,ansm} = -i \ \frac{1 - R_{sm,ansm}}{1 + R_{sm,ansm}} \tag{8.44}$$

and then by using the relations (8.29) and (8.38), $R_{sm,ansm}$ is given by the relation

$$\int_{\bar{L}} \mathcal{K}_{sm,ansm}(y) \ \psi(y;\lambda_0,h) \ dy = J_{sm,ansm}. \tag{8.45}$$

Here the integral equation (8.37) can be solved to obtain the unknown function $\mathcal{K}_{sm,ansm}(u)$ which involves the unknown function $f_{sm,ansm}(u)$ as given in equation (8.38). Knowing $\mathcal{K}_{sm,ansm}(u)$, we can obtain $J_{sm,ansm}$ in terms of $R_{sm,ansm}$ from equation (8.45). Also by using (8.14) and (8.44) the reflection and transmission coefficients $|R|,\ and\ |T|$ in terms of $J_{sm,ansm}$ are given below as

$$|R| = \frac{|1+J_{sm}J_{ansm}|}{\Delta}\ ; \quad |T| = \frac{|J_{sm}-J_{ansm}|}{\Delta}$$

with

$$\Delta = [1 + (J_{sm})^2 + (J_{ansm})^2 + (J_{sm}J_{ansm})^2]^{1/2}. \tag{8.46}$$

3.2. Solution of the integral equation using two numerical methods

Here we proceed to solve the integral equation (8.37) in two disjoint intervals using the following methods.

3.2.1. Boundary element method

Noting the edge condition (8.8) and the relation (8.38) and (8.28), we find that the unknown function $\mathcal{K}_{sm,ansm}(u)$ satisfying the integral equation (8.37) have $\frac{1}{3}$ singularities at $y = a-;\ c+;\ d-$. Thus we write

$$\mathcal{K}_{sm,ansm}(y) = \sqrt[3]{(a-y)(y-c)(d-y)}\ G_{sm,ansm}(y) \tag{8.47}$$

where $G_{sm,ansm}(y)$ is a regular function in $y \in \bar{L} = [0,a] + [c,d]$.
Using the relation (8.47), the integral equation (8.37) can be rewritten as

$$\int_{\bar{L}} G_{sm,ansm}(u)\ \mathcal{M}_{sm,ansm}(y,u)\ du = \vartheta(y), \quad y\ \epsilon\ \bar{L} \tag{8.48}$$

where

$$\mathcal{M}_{sm,ansm}(y,u) = \sqrt[3]{(a-u)(u-c)(d-u)}\; M_{sm,ansm}(y,u),$$

$$\vartheta(y) = \psi(y;\lambda_0,h). \tag{8.49}$$

Since $\bar{L}$ consists of two intervals, so we divide the first interval $[0,a]$ into n_1 number of subintervals and the second interval $[c,d]$ into n_2 number of subintervals such that $[0,a] = \bigcup_{i=1}^{n_1}[a_{i-1},a_i]$ and $[c,d] = \bigcup_{j=1}^{n_2}[b_{j-1},b_j]$ with $a_0 = 0;\ a_i = a_0 + ir_1$; and $b_0 = c;\ b_j = b_0 + jr_2$; where $r_1 = \frac{a-0}{n_1}$ and $r_2 = \frac{d-c}{n_2}$.

Now we take $u = u1_i \in [a_{i-1},a_i],\quad i = 1,2,.....,n_1$ and $u = u2_j \in [b_{j-1},b_j],\quad j = 1,2,.....,n_2$, so

$$\begin{cases} u1_i = (1-\xi)a_{i-1} + \xi a_i \\ u2_j = (1-\xi)b_{j-1} + \xi b_j \end{cases} \qquad 0 \le \xi \le 1. \tag{8.50}$$

Also when y belongs to the line element $[a_{i-1},a_i],\ i = 1,2,....,n_1$, we write $y = y1_i = (1-\eta)a_{i-1} + \eta a_i$ and when y belongs to the line element $[b_{j-1},b_j],\ j = 1,2,.....,n_2$, we write $y = y2_j = (1-\eta)b_{j-1} + \eta b_j \quad 0 \le \eta \le 1$.

So equation (8.48) can be rewritten as

$$\begin{cases} \sum_{i=1}^{n_1}\int_0^1 G_{sm,ansm}(u1_i)\ \mathcal{M}_{sm,ansm}(y1_k,u1_i)\ r_1 d\xi \\ \qquad + \sum_{j=1}^{n_2}\int_0^1 G_{sm,ansm}(u2_j)\ \mathcal{M}_{sm,ansm}(y1_k,u2_j)\ r_2 d\xi = \vartheta(y1_k), \quad k = 1,2,.....,n_1, \\ \\ \sum_{i=1}^{n_1}\int_0^1 G_{sm,ansm}(u1_i)\ \mathcal{M}_{sm,ansm}(y2_l,u1_i)\ r_1 d\xi \\ \qquad + \sum_{j=1}^{n_2}\int_0^1 G_{sm,ansm}(u2_j)\ \mathcal{M}_{sm,ansm}(y2_l,u2_j)\ r_2 d\xi = \vartheta(y2_l), \quad l = 1,2,.....,n_2. \end{cases} \tag{8.51}$$

Now by boundary element method we consider that the unknown function of the integral equation takes constant value in each small subinterval(cf. Samanta et al. (2021)). So we assume $G_{sm,ansm}(u1_i) = G(i)_{sm,ansm}$ = constant where $u1_i \in [a_{i-1},a_i],\ i =$

$1, 2, ..., n_1$ and $G^{sm,ansm}(u2_j) = G(j)_{sm,ansm}$ = constant where $u2_j \in [b_{j-1}, b_j]$, $j = 1, 2, ..., n_2$. So under this approximation, integral equation (8.51) reduces to a system of linear equation written as

$$\sum_{i=1}^{n_1} G(i)_{sm,ansm} \begin{pmatrix} \mathcal{M}(k,i)_{sm,ansm} \\ \mathcal{M}(l,i)_{sm,ansm} \end{pmatrix} + \sum_{j=1}^{n_2} G(j)_{sm,ansm} \begin{pmatrix} \mathcal{M}(k,j)_{sm,ansm} \\ \mathcal{M}(l,j)_{sm,ansm} \end{pmatrix}$$

$$= \begin{pmatrix} \vartheta(k) \\ \vartheta(l) \end{pmatrix}, \qquad \begin{matrix} k = 1, 2, ..., n_1 \\ l = 1, 2, ..., n_2 \end{matrix} \tag{8.52}$$

where

$$\begin{cases} \mathcal{M}(k,i)_{sm,ansm} = \int_0^1 \mathcal{M}^{sm,ansm}(y1_k, u1_i)\ r_1 d\xi \\ \mathcal{M}(l,i)_{sm,ansm} = \int_0^1 \mathcal{M}^{sm,ansm}(y2_l, u1_i)\ r_1 d\xi \\ \mathcal{M}(k,j)_{sm,ansm} = \int_0^1 \mathcal{M}^{sm,ansm}(y1_k, u2_j)\ r_2 d\xi \\ \mathcal{M}(l,j)_{sm,ansm} = \int_0^1 \mathcal{M}^{sm,ansm}(y2_l, u2_j)\ r_2 d\xi \end{cases}$$

and

$$\vartheta(k) = \vartheta(y1_k)\ ; \qquad \vartheta(l) = \vartheta(y2_l).$$

Solving the system of equation (8.52) , we obtain the unknown constants $G(i)_{sm,ansm}$ for $i = 1, 2, ..., n_1$ and $G(j)_{sm,ansm}$ for $j = 1, 2, ..., n_2$. Hence $J_{sm,ansm}$ can be evaluated from equation (8.45) as

$$\begin{aligned} J_{sm,ansm} = &\sum_{i=1}^{n_1} G(i)_{sm,ansm} \int_0^1 \sqrt[3]{(a - y1_i)(y1_i - c)(d - y1_i)}\ \psi(y1_i; \lambda_0, h)\ r_1 d\eta \\ &+ \sum_{j=1}^{n_2} G(j)_{sm,ansm} \int_0^1 \sqrt[3]{(a - y2_j)(y2_j - c)(d - y2_j)}\ \psi(y2_j; \lambda_0, h)\ r_2 d\eta. \end{aligned} \tag{8.53}$$

3.2.2. Multiterm Galerkin method

To solve the integral equation (8.37), we approximate $\mathcal{K}_{sm,ansm}(y)$ as

$$\mathcal{K}_{sm,ansm}(y) \approx \mathcal{F}_{sm,ansm}(y), \quad y \, \epsilon \, \bar{L} \tag{8.54}$$

where $\mathcal{F}_{sm,ansm}(y)$ have multi-term Galerkin expansions in terms of suitable basis functions.

Since $\bar{L} = (0, a) + (c, d)$ consists of two disjoint intervals, so $\mathcal{F}_{sm,ansm}(y)$ can be expressed as

$$\mathcal{F}_{sm,ansm}(y) = \begin{cases} \sum_{n=0}^{N} a(n)_{sm,ansm} \; p(n)_{sm,ansm}(y), \; 0 < y < a, \\ \sum_{n=0}^{N} b(n)_{sm,ansm} \; q(n)_{sm,ansm}(y), \; c < y < d, \end{cases} \tag{8.55}$$

where $a(n)$ and $b(n)$ are unknown constants and $p(n)_{sm,ansm}(y)$, $q(n)_{sm,ansm}(y)$ are basis functions chosen as follows.

Choice of Basis Functions

For 0 < y < a

Here we have to consider the ice covered surface condition and the cube-root singularity of velocity near corner point (b, a). Thus $\mathcal{K}_{sm,ansm}(y) = \mathcal{K}(y)$ satisfies

$$(D\frac{\delta^4}{\delta x^4} + 1 - \varepsilon K)\mathcal{K}'(y) + K\mathcal{K}(y) = 0; \qquad \text{on y=0} \tag{8.56}$$

$$\mathcal{K}(y) \sim o(a - y)^{-\frac{1}{3}} \qquad \text{as } y \to a - 0. \tag{8.57}$$

If we define

$$\bar{\mathcal{K}}(y) = \mathcal{K}(y) - \frac{K}{1 - \epsilon K + Du^4} \int_0^a \mathcal{K}(u) \; du \quad 0 < y < a \tag{8.58}$$

then

$$\bar{\mathcal{K}}'(y) = 0, \quad on \quad y = 0 \tag{8.59}$$

$$\bar{\mathcal{K}}(y) \sim o(a-y)^{-\frac{1}{3}} \qquad \text{as } y \to a-0. \tag{8.60}$$

So, $(a^2-y^2)^{\frac{1}{3}}\,\bar{\mathcal{K}}(y)$ can be expanded in $(0,a)$ as a complete set of even ultraspherical Gegenbaurer Polynomials $C_{2m}^{\frac{1}{6}}(\frac{y}{a})$.
Thus we take

$$p(m)_{sm,ansm} = p(m)(y) = -\frac{d}{dy}\left[e^{-\frac{Ky}{1-\epsilon K+Du^4}} \int_0^a e^{\frac{K}{1-\epsilon K+Du^4}t}\bar{p}(m)(t)\,dt\right] \tag{8.61}$$

where $\bar{p}(m)(y)$ is chosen as

$$\bar{p}(m)(y) = \frac{2^{\frac{7}{6}}\,\Gamma(\frac{1}{6})(2m)!}{\pi\Gamma(2m+\frac{1}{3})a^{\frac{1}{3}}(a^2-y^2)^{\frac{1}{3}}}\,C_{2m}^{\frac{1}{6}}\left(\frac{y}{a}\right), \quad 0<y<a. \tag{8.62}$$

For c < y < d

Here we have to consider only the cube-root singular behavior of the velocity at the points (b,c) and (b,d). So a complete set $C_m^{\frac{1}{6}}(\frac{2y-c-d}{d-c})$ of ultraspherical Gegenbaurer Polynomials are used to for expansion of $\{(y-c)(d-y)\}^{\frac{1}{3}}\mathcal{K}_{sm,ansm}(y)$ in $c<y<d$. So we choose

$$q(m)_{sm,ansm}(y) = \frac{2^{\frac{1}{6}}\,\Gamma(\frac{1}{6})\,m!}{\pi\,\Gamma(m+\frac{1}{3})\left(\frac{d-c}{2}\right)^{\frac{1}{3}}\{(y-c)(d-y)\}^{\frac{1}{3}}}C_m^{\frac{1}{6}}\left(\frac{2y-c-d}{d-c}\right), \quad c<y<d. \tag{8.63}$$

Reduction of Integral equation to Linear system of equations

Substituting the approximations (8.55) in equation(8.37) and then multiply both

side first by $p(m)_{sm,ansm}(y)$ and then by $q(m)_{sm,ansm}(y)$ and then integrate over $(0,a)$ and (c,d) respectively , we obtain two linear systems of equations

$$\sum_{n=0}^{N} a(n)_{sm,ansm}\begin{pmatrix} \mathcal{G}(m,n)_{sm,ansm} \\ \mathcal{P}(m,n)_{sm,ansm} \end{pmatrix} + \sum_{n=0}^{N} b(n)_{sm,ansm}\begin{pmatrix} \mathcal{H}(m,n)_{sm,ansm} \\ \mathcal{Q}(m,n)_{sm,ansm} \end{pmatrix}$$

$$= \begin{pmatrix} d(m)^{(1)}_{sm,ansm} \\ d(m)^{(2)}_{sm,ansm} \end{pmatrix}, \qquad m = 0, 1, ...N \tag{8.64}$$

where

$$\begin{aligned}
\mathcal{G}(m,n)_{sm,ansm} &= \int_0^a \left\{ \int_0^a M_{sm,ansm}(y,u)\ p(n)_{sm,ansm}(u)\ du \right\}\ p(m)_{sm,ansm}(y)\ dy, \\
\mathcal{H}(m,n)_{sm,ansm} &= \int_0^a \left\{ \int_c^d M_{sm,ansm}(y,u)\ q(n)_{sm,ansm}(u)\ du \right\}\ p(m)_{sm,ansm}(y)\ dy, \\
\mathcal{P}(m,n)_{sm,ansm} &= \int_c^d \left\{ \int_0^a M_{sm,ansm}(y,u)\ p(n)_{sm,ansm}(u)\ du \right\}\ q(m)_{sm,ansm}(y)\ dy, \\
\mathcal{Q}(m,n)_{sm,ansm} &= \int_c^d \left\{ \int_c^d M_{sm,ansm}(y,u)\ q(n)_{sm,ansm}(u)\ du \right\}\ q(m)_{sm,ansm}(y)\ dy,
\end{aligned} \tag{8.65}$$

so that $\mathcal{P}(m,n)_{sm,ansm} = \mathcal{H}(m,n)_{sm,ansm}$, and

$$\begin{aligned}
d(m)^{(1)}_{sm,ansm} &= \int_0^a \psi(y;\lambda_0,h)\ p(m)_{sm,ansm}(y)\ dy \\
d(m)^{(2)}_{sm,ansm} &= \int_c^d \psi(y;\lambda_0,h)\ q(m)_{sm,ansm}(y)\ dy.
\end{aligned} \tag{8.66}$$

So, solving the equations (8.64) we find $a(n)_{sm,ansm}$ and $b(n)_{sm,ansm}$ and then by

using (8.45) we get a simplified form of $J_{sm,ansm}$ as

$$J_{sm,ansm} = \sum_{n=0}^{N} \left\{ a(n)_{sm,ansm}\ d(n)^{(1)}_{sm,ansm} \ +\ b(n)_{sm,ansm}\ d(n)^{(2)}_{sm,ansm} \right\}. \tag{8.67}$$

Coefficients of Linear system of Equation

The coefficient matrix of the linear system of equations (8.64) are calculated as follows

$$\begin{aligned}
\mathcal{G}(m,n)_{sm} = \beta \Bigg[& 4(-1)^{m+n} \sum_{r=1}^{\infty} \Bigg(\frac{\lambda_r \ \cos^2 \lambda_r h}{s_r \delta_r} \ \frac{J_{2n+\frac{1}{6}}(\lambda_r a) J_{2m+\frac{1}{6}}(\lambda_r a)}{(\lambda_r a)^{\frac{1}{3}}} \\
& + \frac{\alpha_r \coth t_r b \cos^2 \alpha_r a}{t_r \gamma_r} \ \frac{J_{2n+\frac{1}{6}}(\alpha_r a) J_{2m+\frac{1}{6}}(\alpha_r a)}{(\alpha_r a)^{\frac{1}{3}}} \Bigg) \\
& - \frac{\alpha_0 \ \cot t_0 b}{t_0 \gamma_0} \cosh^2 \alpha_0 a \ \frac{I_{2n+\frac{1}{6}}(\alpha_0 a) I_{2m+\frac{1}{6}}(\alpha_0 a)}{(\alpha_0 a)^{\frac{1}{3}}} \\
& - 4(-1)^{m+n} \sum_{r=I}^{II} \Bigg(\frac{\alpha_r \ \cot t_r b}{t_r \gamma_r} \cosh^2 \alpha_r a \ \frac{I_{2n+\frac{1}{6}}(\alpha_r a) I_{2m+\frac{1}{6}}(\alpha_r a)}{(\alpha_r a)^{\frac{1}{3}}} \\
& + \frac{i \ \lambda_r \ \cosh^2 \lambda_r h}{\epsilon_r s_r \delta_r} \ \frac{I_{2n+\frac{1}{6}}(\lambda_r a) I_{2m+\frac{1}{6}}(\lambda_r a)}{(\lambda_r a)^{\frac{1}{3}}} \Bigg) \Bigg],
\end{aligned} \tag{8.68}$$

$$\begin{aligned}
\mathcal{G}(m,n)_{ansm} = \beta \Bigg[& 4(-1)^{m+n} \sum_{r=1}^{\infty} \Bigg(\frac{\lambda_r \ \cos^2 \lambda_r h}{s_r \delta_r} \ \frac{J_{2n+\frac{1}{6}}(\lambda_r a) J_{2m+\frac{1}{6}}(\lambda_r a)}{(\lambda_r a)^{\frac{1}{3}}} \\
& + \frac{\alpha_r \tanh t_r b \cos^2 \alpha_r a}{t_r \gamma_r} \ \frac{J_{2n+\frac{1}{6}}(\alpha_r a) J_{2m+\frac{1}{6}}(\alpha_r a)}{(\alpha_r a)^{\frac{1}{3}}} \Bigg) \\
& - \frac{\alpha_0 \ (-\tan t_0 b)}{t_0 \gamma_0} \cosh^2 \alpha_0 a \ \frac{I_{2n+\frac{1}{6}}(\alpha_0 a) I_{2m+\frac{1}{6}}(\alpha_0 a)}{(\alpha_0 a)^{\frac{1}{3}}}
\end{aligned}$$

$$- 4(-1)^{m+n}\sum_{r=I}^{II}\left(\frac{\alpha_r\ (-\tan t_r b)}{t_r\gamma_r}\cosh^2\alpha_r a\ \frac{I_{2n+\frac{1}{6}}(\alpha_r a)I_{2m+\frac{1}{6}}(\alpha_r a)}{(\alpha_r a)^{\frac{1}{3}}}\right.$$
$$\left.+\ \frac{i\ \lambda_r\ \cosh^2\lambda_r h}{\epsilon_r s_r\delta_r}\ \frac{I_{2n+\frac{1}{6}}(\lambda_r a)I_{2m+\frac{1}{6}}(\lambda_r a)}{(\lambda_r a)^{\frac{1}{3}}}\right)\Bigg], \tag{8.69}$$

$\mathcal{H}(m,n)_{sm,ansm} =$

$$4\beta\left[\sum_{r=1}^{\infty}\frac{\lambda_r\ \cos\lambda_r h}{s_r\delta_r}\begin{pmatrix}(-1)^{\frac{n}{2}}\cos\lambda_r(h-\frac{c+d}{2})\text{ for even }n\\(-1)^{\frac{n-1}{2}}\sin\lambda_r(h-\frac{c+d}{2})\text{ for odd }n\end{pmatrix}\frac{J_{n+\frac{1}{6}}(\lambda_r\ \frac{d-c}{2})J_{2m+\frac{1}{6}}(\lambda_r a)}{(\lambda_r a)^{\frac{1}{6}}(\lambda_r\ \frac{d-c}{2})^{\frac{1}{6}}}\right.$$

$$\left.-\sum_{r=I}^{II}\frac{i\ \lambda_r\ \cosh\lambda_r h}{\epsilon_r s_r\delta_r}\begin{pmatrix}(-1)^{\frac{n}{2}}\cosh\lambda_r(h-\frac{c+d}{2})\text{ for even }n\\(-1)^{\frac{n-1}{2}}\sinh\lambda_r(h-\frac{c+d}{2})\text{ for odd }n\end{pmatrix}\frac{I_{n+\frac{1}{6}}(\lambda_r\ \frac{d-c}{2})I_{2m+\frac{1}{6}}(\lambda_r a)}{(\lambda_r a)^{\frac{1}{6}}(\lambda_r\ \frac{d-c}{2})^{\frac{1}{6}}}\right]. \tag{8.70}$$

$$\mathcal{Q}(m,n)_{sm} = \beta\left[2\sum_{r=1}^{\infty}\left\{\frac{2\lambda_r}{s_r\delta_r}\times\frac{J_{n+\frac{1}{6}}(\lambda_r\ \frac{d-c}{2})\ J_{m+\frac{1}{6}}(\lambda_r\ \frac{d-c}{2})}{(\lambda_r\ \frac{d-c}{2})^{\frac{1}{3}}}\times\right.\right.$$

$$\begin{pmatrix}(-1)^{\frac{n}{2}}\cos\lambda_r(h-\frac{c+d}{2})\text{ for even }n\\(-1)^{\frac{n-1}{2}}\sin\lambda_r(h-\frac{c+d}{2})\text{ for odd }n\end{pmatrix}\times\begin{pmatrix}(-1)^{\frac{m}{2}}\cos\lambda_r(h-\frac{c+d}{2})\text{ for even }m\\(-1)^{\frac{m-1}{2}}\sin\lambda_r(h-\frac{c+d}{2})\text{ for odd }m\end{pmatrix}$$

$$+\ \frac{\coth\xi_r b}{(d-c)\xi_r}\times\frac{J_{n+\frac{1}{6}}(\frac{r\pi}{2})J_{m+\frac{1}{6}}(\frac{r\pi}{2})}{(\frac{r\pi}{2})^{\frac{1}{3}}}\times$$

$$\left.\begin{pmatrix}(-1)^{\frac{n}{2}}\cos\frac{r\pi}{2}\text{ for even }n\\(-1)^{\frac{n-1}{2}}\sin\frac{r\pi}{2}\text{ for oddeven }n\end{pmatrix}\times\begin{pmatrix}(-1)^{\frac{m}{2}}\cos\frac{r\pi}{2}\text{ for even }m\\(-1)^{\frac{m-1}{2}}\sin\frac{r\pi}{2}\text{ for odd }m\end{pmatrix}\right\}$$

$$+\ \frac{12\ \pi\ 2^{\frac{1}{3}}\ \coth\nu b}{(d-c)\{\Gamma(\frac{1}{3})\}^4\ \nu}\ \delta_{0n}\delta_{0m}$$

$$-\sum_{r=I}^{II}\frac{4i\lambda_r}{\epsilon_r s_r\delta_r}\times\frac{I_{n+\frac{1}{6}}(\lambda_r\ \frac{d-c}{2})\ I_{m+\frac{1}{6}}(\lambda_r\ \frac{d-c}{2})}{(\lambda_r\ \frac{d-c}{2})^{\frac{1}{3}}}\times$$

$$\left(\begin{array}{l} (-1)^{\frac{n}{2}} \cosh\lambda_r(h-\frac{c+d}{2}) \text{ for even } n \\ (-1)^{\frac{n-1}{2}} \sinh\lambda_r(h-\frac{c+d}{2}) \text{ for odd } n \end{array} \right) \times \left(\begin{array}{l} (-1)^{\frac{m}{2}} \cosh\lambda_r(h-\frac{c+d}{2}) \text{ for even } m \\ (-1)^{\frac{m-1}{2}} \sinh\lambda_r(h-\frac{c+d}{2}) \text{ for odd } m \end{array} \right) \Bigg] \tag{8.71}$$

where $\delta_{0n} = 1$ for $n = 0$, and $\delta_{0n} = 0$ for $n \geq 1$.

$$\mathcal{Q}(m,n)_{ansm} = \beta \Bigg[2 \sum_{r=1}^{\infty} \Bigg\{ \frac{2\lambda_r}{s_r \delta_r} \times \frac{J_{n+\frac{1}{6}}(\lambda_r \ \frac{d-c}{2}) \ J_{m+\frac{1}{6}}(\lambda_r \ \frac{d-c}{2})}{(\lambda_r \ \frac{d-c}{2})^{\frac{1}{3}}} \times$$

$$\left(\begin{array}{l} (-1)^{\frac{n}{2}} \cos\lambda_r(h-\frac{c+d}{2}) \text{ for even } n \\ (-1)^{\frac{n-1}{2}} \sin\lambda_r(h-\frac{c+d}{2}) \text{ for odd } n \end{array} \right) \times \left(\begin{array}{l} (-1)^{\frac{m}{2}} \cos\lambda_r(h-\frac{c+d}{2}) \text{ for even } m \\ (-1)^{\frac{m-1}{2}} \sin\lambda_r(h-\frac{c+d}{2}) \text{ for odd } m \end{array} \right)$$

$$+ \frac{\tanh\xi_r b}{(d-c)\xi_r} \times \frac{J_{n+\frac{1}{6}}(\frac{r\pi}{2}) J_{m+\frac{1}{6}}(\frac{r\pi}{2})}{(\frac{r\pi}{2})^{\frac{1}{3}}} \times$$

$$\left(\begin{array}{l} (-1)^{\frac{n}{2}} \cos\frac{r\pi}{2} \text{ for even } n \\ (-1)^{\frac{n-1}{2}} \sin\frac{r\pi}{2} \text{ for oddeven } n \end{array} \right) \times \left(\begin{array}{l} (-1)^{\frac{m}{2}} \cos\frac{r\pi}{2} \text{ for even } m \\ (-1)^{\frac{m-1}{2}} \sin\frac{r\pi}{2} \text{ for odd } m \end{array} \right) \Bigg\}$$

$$+ \frac{12 \ \pi \ 2^{\frac{1}{3}} \ \tanh\nu b}{(d-c)\{\Gamma(\frac{1}{3})\}^4 \ \nu} \ \delta_{0n}\delta_{0m}$$

$$- \sum_{r=I}^{II} \frac{4i\lambda_r}{\epsilon_r s_r \delta_r} \times \frac{I_{n+\frac{1}{6}}(\lambda_r \ \frac{d-c}{2}) \ I_{m+\frac{1}{6}}(\lambda_r \ \frac{d-c}{2})}{(\lambda_r \ \frac{d-c}{2})^{\frac{1}{3}}} \times$$

$$\left(\begin{array}{l} (-1)^{\frac{n}{2}} \cosh\lambda_r(h-\frac{c+d}{2}) \text{ for even } n \\ (-1)^{\frac{n-1}{2}} \sinh\lambda_r(h-\frac{c+d}{2}) \text{ for odd } n \end{array} \right) \times \left(\begin{array}{l} (-1)^{\frac{m}{2}} \cosh\lambda_r(h-\frac{c+d}{2}) \text{ for even } m \\ (-1)^{\frac{m-1}{2}} \sinh\lambda_r(h-\frac{c+d}{2}) \text{ for odd } m \end{array} \right) \Bigg] \tag{8.72}$$

Also,

$$d(m)^{(1)}_{sm,ansm} = \frac{I_{2m+\frac{1}{6}}(\lambda_0 a)}{(\lambda_0 a)^{\frac{1}{6}}}, \tag{8.73}$$

$$d(m)^{(2)}_{sm,ansm} = \frac{(-1)^m \ e^{\lambda_0\left(h-\frac{c+d}{2}\right)} + \ e^{-\lambda_0\left(h-\frac{c+d}{2}\right)}}{2\cosh\lambda_0 h} \ \frac{I_{m+\frac{1}{6}}\left(\lambda_0\frac{d-c}{2}\right)}{\left(\lambda_0\frac{d-c}{2}\right)^{\frac{1}{6}}}. \tag{8.74}$$

4. Numerical Results

In this section, we will discuss about the reflection coefficient $|R|$ and transmission coefficient $|T|$ computed numerically by solving the integral equation using boundary element method (BEM) and multiterm Galerkin method for different values of non-dimensional parameters $a/h,\ b/h,\ c/h,\ d/h,\ \alpha,\ D/h^4,\ \epsilon/h$. The physical quantities $|R|,\ |T|$ evaluated by using the solution of integral equation (8.37) by BEM converges upto six decimal places by taking $n_1 = 25,\ n_2 = 25$. For the numerical solution of integral equation (8.37) using multiterm Galerkin method, it is first necessary to compute the infinite series given by (8.64) and (8.67) by truncating it as prescribed degree of accuracy. Choosing 250 terms in each series a six figure accuracy in the numerical results have been achieved. The accuracy can be further increased by taking more terms in the series as mentioned by Chakraborty and Mandal [2014,2015]. The energy identity $|R|^2 + |T|^2 = 1$ is verified here for different values of the parameters. The values of $|R|$ obtained by solving the integral equation by above mentioned two methods for different values of kh are presented in tables (8.1) to (8.3) for different values of parameters $a/h,\ b/h, c/h, d/h, \alpha$ with $\epsilon/h = 0.01;\ D/h^4 = 0.01$. The tables shows that the results by two methods agree with each other reasonably well. Also the numerical estimates of reflection coefficient for various values of the different parameters are explained graphically in Figure (8.2) to Figure (8.7) .

Table 8.1: Reflection coefficient for $\alpha = \frac{\pi}{4}$; $\frac{a}{h} = 0.2$; $\frac{c}{h} = 0.4$; $\frac{d}{h} = 0.6$; $\frac{b}{h} = 1.0$

Kh	BEM	Galerkin Method
0.5	0.669100	0.669105
1.0	0.566317	0.566319
1.5	0.187967	0.187968
2.0	0.096431	0.096434

In Fig.8.2, the values of $|R|$ are plotted against Kh to compare the present result with the result corresponding to scattering by a bottom standing thick barrier consid-

Table 8.2: Reflection coefficient for $\alpha = \frac{\pi}{3}$; $\frac{a}{h} = 0.2$; $\frac{c}{h} = 0.6$; $\frac{d}{h} = 0.8$; $\frac{b}{h} = 2.0$

Kh	BEM	Galerkin Method
0.5	0.418307	0.418310
1.0	0.099753	0.099755
1.5	0.344931	0.344931
2.0	0.418114	0.418117

Table 8.3: Reflection coefficient for $\alpha = \frac{\pi}{6}$; $\frac{a}{h} = 0.3$; $\frac{c}{h} = 0.5$; $\frac{d}{h} = 0.8$; $\frac{b}{h} = 1.0$

Kh	BEM	Galerkin Method
0.5	0.514193	0.514194
1.0	0.629259	0.629261
1.5	0.406748	0.406750
2.0	0.162717	0.162718

ered by Samanta and Chakraborty (2020) (Fig. 11(a) there). In our calculation we have taken $\frac{d-c}{h} = 0$ $a/h = 0.6$ $c/h = 0.8$ $b/h = 1.0$ $\alpha = 0$. A good agreement in the results is observed from Fig.8.2.

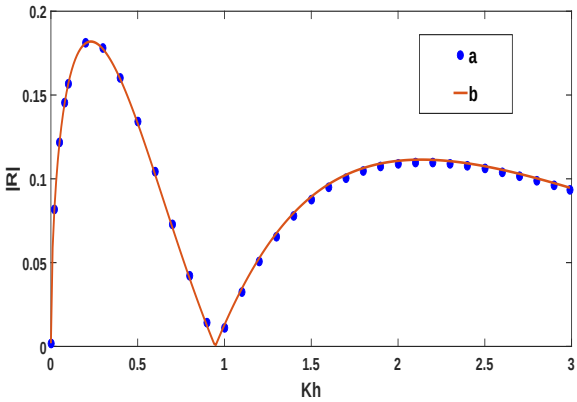

Figure 8.2: Reflection coefficient vs. wave number, **(a)** fully submerged barrier in cf. [Samanta and Chakraborty (2020)] with $a/h = 0.6$; $c/h = 0.8$; $b/h = 1.0$; **(b)** present paper with $a/h = 0.6$; $(d-c)/h = 0$; $b/h = 1.0$; $\alpha = 0^o$

In Fig. 8.3 , reflection coefficient ($|R|$) is depicted against wave number (Kh) for different values of elastic coefficient ($\frac{D}{h^4}$=0.01,0.1 and 1.0) and fixed values of $\epsilon/h = 0.01$, $a/h = 0.2$, $c/h = 0.6$, $d/h = 0.8$, $b/h = 1.0$, $\alpha = \frac{\pi}{4}$. It observed that $|R|$ exhibits oscillatory

behaviour and the frequency of oscillation is more for very small values of D/h^4.

Fig. 8.4 shows the behavior $|R|$ against Kh for variation in the width of the barrier,

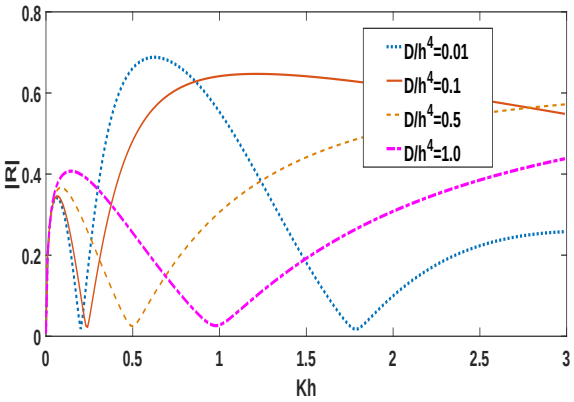

Figure 8.3: Reflection coefficient vs. wave number for different D/h^4, $\epsilon/h = 0.01$, $a/h = 0.2$, $c/h = 0.6$, $d/h = 0.8$, $b/h = 1.0$, $\alpha = \frac{\pi}{4}$

$\frac{b}{h} = 0.01, 0.1, 1.0, 2.0$ and $\epsilon/h = 0.01$, $D/h^4 = 0.01$, $a/h = 0.2$, $c/h = 0.6$, $d/h = 0.8$, $\alpha = \frac{\pi}{3}$. It is seen that $|R|$ exhibits oscillatory behaviour for barrier with large width which may be attributed due to multiple interaction of the waves with the barrier and the bottom of the water region. The amplitude of $|R|$ gradually increases with increasing width of the barrier. When the wall is comparatively thin ($b/h = 0.01$), the reflection coefficient first increases then decreases asymptotically to zero with increase of wave number and $|R|$ doesnot exhibit oscillatory behaviour. This shows that wide barrier induces multiple reflection of waves than thin barrier. This behavior of infinitely thin barrier observed in previous literature (cf. Porter and Evans (1995)).

The graphs in Fig. 8.5 depict the reflection coefficient $|R|$ against wave number with different values of incident wave angle $\alpha = 0, \frac{\pi}{6}, \frac{\pi}{4}$ and $\frac{\pi}{8}$ and fixed values of $\epsilon/h = 0.01$, $D/h^4 = 0.01$, $a/h = 0.2$, $c/h = 0.4$, $d/h = 0.6$, $b/h = 1.0$. From the figure it seen that $|R|$ exhibits oscillatory behaviour and increasing values of incident wave angle decreases the amplitude of $|R|$ and as the wave number increases. The graphs of $|R|$ against non dimensional wave number are depicted in Fig. 8.6 for different values of the gap ($\frac{d-c}{h}$=0.2,0.3,0.4) in the barrier with fixed values of $\epsilon/h = 0.01$, $D/h^4 = 0.01$, $a/h = 0.2$, $c/h = 0.4$, $d/h = 0.6$, $\alpha = \frac{\pi}{4}$. It is seen from the graph that $|R|$ exhibits oscillatory behaviour and an increasing in gap length induces more reflection and for large wave

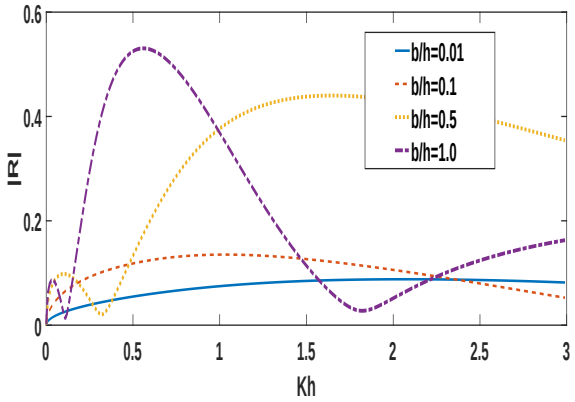

Figure 8.4: Reflection coefficient vs. wave number for different width b, ϵ/h = 0.01, D/h^4 = 0.01, a/h = 0.2, c/h = 0.6, d/h = 0.8, $\alpha = \frac{\pi}{3}$

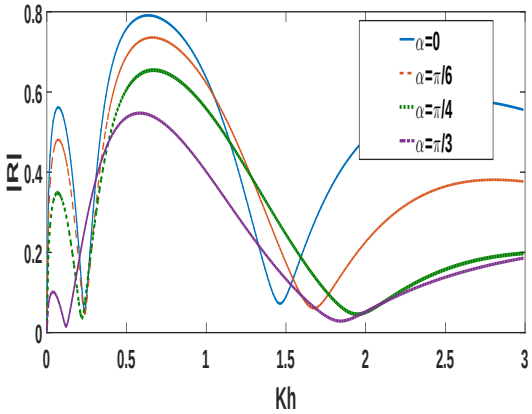

Figure 8.5: Reflection coefficient vs. wave number for different angle of inclination α, ϵ/h = 0.01, D/h^4 = 0.01, a/h = 0.2, c/h = 0.4, d/h = 0.6, b/h = 1.0

numbers, the $|R|$ corresponding to different gap length of the barrier almost coincide with each others.

In Fig.8.7 we have shown how the water depth affects the reflection coefficient. Here we have made all the parameters non-dimensional by parameter a. Here in Fig. 8.7, $|R|$ is plotted against Ka for different uniform height of the water body h/a $(= 1, 2, 3)$ for fixed values of ϵ/a = 0.01, D/a^4 = 0.01, c/a = 0.4, d/a = 0.6, $\alpha = \frac{\pi}{4}$. It is observed that $|R|$ shows the oscillatory behaviour. Also we have observed that with the increase in water depth the reflection coefficient decreases for a particular wave number. With increasing depth of water, the area occupied by the wall become comparatively less for

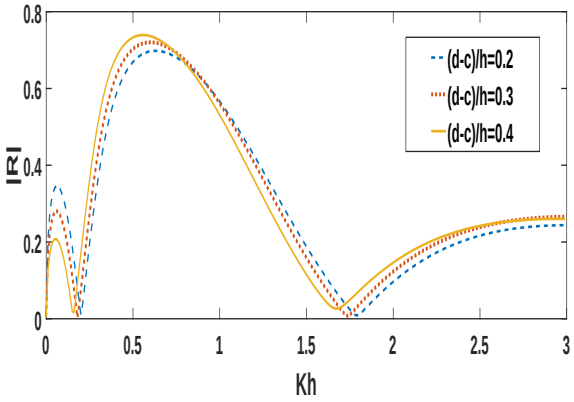

Figure 8.6: Reflection coefficient vs. wave number for different gap of wall $\frac{(d-c)}{h}$, ϵ/h = 0.01, D/h^4 = 0.01, a/h = 0.2, c/h = 0.4, d/h = 0.6, $\alpha = \frac{\pi}{4}$

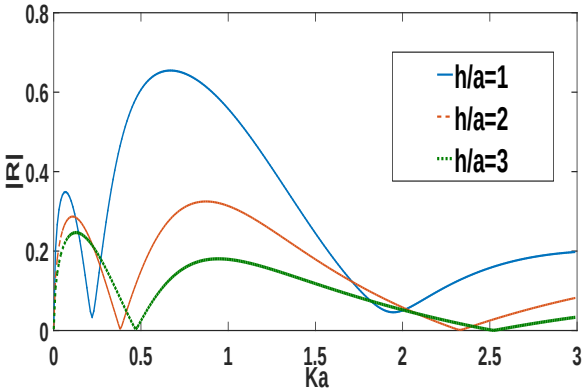

Figure 8.7: Reflection coefficient vs. wave number for different water depth h/a, ϵ/a = 0.01, D/a^4 = 0.01, c/a = 0.4, d/a = 0.6, $\alpha = \frac{\pi}{4}$

fixed values of c/a and d/a, so the reflection coefficient decreases accordingly.

5. Conclusion

The problem of obliquely incident wave scattering by a thick vertical rectangular wall with a gap in presence of ice cover is investigated. The corresponding boundary value problem is reduced to an integral equation in terms of unknown horizontal component of velocity across the gaps. This integral equation is solved by two methods, viz, boundary element method and multi-term Galerkin approximation method.

The solution of the integral equation obtained by two methods are matched to ensure the correctness of the methods. This BEM method is computationally simple compared to other methods. These results are depicted in a number of figures against non-dimensional wave numbers. The thickness of the barrier and flexural rigidity of the ice present in upper surface of water affects the reflection coefficient significantly. It is observed that large width of the thick barrier increases reflection of the wave and when thickness of ice cover increases the amplitude of reflection coefficient increases and more oscillation can be visible in the curves of $|R|$. The mathematical technique and analysis used here can be applied to wave structure interaction problems arising in several branches of marine engineering and mathematical physics problems.

Future scope of work

The present thesis is concerned with a study of numerical solution of integral equations with regular and singular kernel and their applications to water wave scattering problems by thin curved barrier and rectangular thick barrier present in water region.

The boundary element method (BEM) is a powerful computational technique, providing numerical solutions to the boundary value problems corresponding to a varied range of scientific and engineering problems. The method is easier to apply than the more traditional finite element method. The advantage of BEM over other numerical methods is that only the boundary of the domain needs to be discretized. Thus the solution of the boundary value problem at any arbitrary point of the domain can be found after determining the unknown boundary data.
In the present thesis, we have applied boundary element method to solve integral equations with regular and singular kernel, assuming the unknown function satisfying the integral equation, as constant in each line element and corresponding convergence analysis was done. This method can be applied to solve integral equations by assuming the unknown function satisfying the integral equation, as linear function or quadratic function of the argument. The necessary convergence analysis can be done for these cases. Also the boundary element method can be used to study water wave scattering problems involving obstacles of various geometrical shapes.
Water wave scattering problems involving barrier present in water with various bathymetry is important from the point of view of coastal engineering. The interaction of water waves with non uniform bottom topography is important in understanding the wave induced mass transport. This class of problems involving barriers present in water

region of nonuniform bathymetry can be studied.

The numerical scheme based on boundary element method is a simple numerical method which is applied to solve integral equations kernel of various forms. Particularly this method is quite useful in solving hypersingular integral equations of first and second kind with complicated kernel. We may mention here that hypersingular integral equation formulation provides an efficient method in solving boundary value problem associated with water wave propagation problems in two or three dimension involving obstacles in form of various geometrical shapes. There is much scope to study this class of problems involving barriers porous or rigid in form of thin plate, circular plate, cylindrical configurations using hypersingular integral equation formulation and applying boundary element method to solve the corresponding hypersingular integral equations. In addition to this boundary element method can be applied to solve a wide range of integral equations with regular as well as singular kernel arising in the continuum mechanics.

It is well known that the problem of scattering of water waves by porous coastal structures like rubble mound breakwaters are important in coastal engineering as the pores in the barrier attenuates wave action by dissipating the wave energy and thereby protects the coast line or harbour. Many researchers used sophisticated mathematical techniques to study scattering problems involving porous barrier with constant porosity. However when the porosity of the barrier is variable, then the literature concerning these scattering problems are rather limited. There is much scope to study water wave propagation problems in presence of barriers with variable porosity.

Bibliography

1. Abramowitz, M., and Stegun, I.A. (1965). Handbook of Mathematical functions. *Dover*, New York.

2. Balmforth, N.J. and Craster R.V. (1999). Ocean waves and ice sheets. *J. Fluid Mech.*, 395, 89-124.

3. Banerjea, S., Chakraborty, R., and Samanta, A. (2019). Boundary element approach of solving fredholm and volterra integral equations. *Int. J. Mathematical Modelling and Numerical Optimisation*, 9(1), 1-11.

4. Banerjea, S., Dutta, B. (2008). On a weakly singular integral equation and its application. *Appl. Math. Lett.*, 21, 729-734.

5. Banerjea, S., Kanoria M., Dolai D.P. and Mandal B.N. (1996). Oblique wave scattering by a submerged thin wall with gap in finite depth water. *Appl Ocean Res.*, 18 : 319-327.

6. Banerjea, S. and Mandal, B.N. (1993). Solution of a singular integral equation in a double interval arising in the theory of water waves. *Appl. Math. Lett.*, 6, 81-84.

7. Banerjea, S. and Mandal, B.N. (1995). On a singular integral equation with logarithmic and Cauchy kernel. *Int. J. Math. Edu. Sci. Tech.*, 26, 279-283.

8. Banerjea S. and Mandal B.N. (2009). Scattering of water waves by a submerged thin vertical wall with a gap. *ANZIAM J.*, 39, 318-331.

9. Becker, A.A. (1992). The boundary element method for engineering, A complete course. *McGraw Hill Book Company.*

10. Beer, G., Smith, I. and Duenser, C. (2008). The boundary Element Method with Programming. *Springer.*

11. Beer, G. and Watson, J.O. (1992). Introduction to Finite and Boundary Element Methods for Engineers. *Wiley*, New York.

12. Bhattacharya, S. and Mandal, B.N. (2008). Use of Bernstein Polynomials in Numerical Solutions of Volterra Integral Equations. *Appl. Math. Sci.*, 2(36), 1773-1787.

13. Brebbia, C.A., Dominguez, J. (1994). Boundary Elements: An Introductory Course. *WIT Press.*

14. Case, K.M. (1966). Singular solutions of certain integral equations. *J. Math. Phys.*, 7, 2125-2135.

15. Chakrabarti, A. (1980). Derivation of the solution of certain singular integral equation . *J. Indian Inst. Sci.*, 62, 147-157.

16. Chakrabarti, A. (1981). Solution of a singular integral equation. *J. Eng. Math.*, 15, 201-210.

17. Chakrabarti, A. (1984). Derivation of the solution of special integral equation. *J.Indian Inst. Sci.*, 65, 179-184.

18. Chakrabarti, A. (1986). A tractable pair of Cauchy singular integral equations. *J. Indian Inst. Sci.*, 66, 331-336.

19. Chakrabarti, A. (1989). Solution of two singular integral equations arising in water wave problems. *ZAMM*, 69, 457-459.

20. Chakrabarti, A. (2000). On the solution of the problem of scattering of surface water waves by the edge of an ice-cover. *Proc. R. Soc. Lond. A.*, 456, 1087-1099.

21. Chakrabarti, A. (2006). Solution of certain weakly singular integral equation. *IMA Journal of Appl. Math.*, 71, 534-543.

22. Chakrabarti, A. (2007). Solution of a simple hypersingular integral equation. *J. Integral Equation Applic.*, 19, 465-471.

23. Chakrabarti, A., Ahluwalia, D.S. and Manam, S.R. (2003). Surface water waves involving a vertical barrier in the presence of an ice-cover. *International J. of Eng. Sci.*, 41, 1145-1162.

24. Chakrabarti, A. and Chakrabarti, S. (1977). A note on certain singular integral equations with kernel $\frac{K(z,\zeta)}{z-\zeta}$. *Indian J. Pure and Appl. Math.*, 8, 327-334.

25. Chakrabarti, A. and George, A.E. (1994). A formula for the solution of the general Abel integral equation. *Appl. Math. Lett.*, 7, 87-90.

26. Chakrabarti, A. and Manam, S.R. (2003). Solution of the logarithmic singular integral equation. *Appl. Math. Lett.*, 16, 369-373.

27. Chakrabarti, A. and Mandal, B.N. (1998). Derivation of the solution of a simple hypersingular integral equation. *Int. J. Math. Educ. Sci. Tech.*, 29, 47-53.

28. Chakrabarti, A., Mandal, B.N., Banerjea, S. and Sahoo, T. (1995). Solution of a class of mixed boundary value problems for Laplace's equation arising in water wave scattering. *J. Indian Instt. Sci.*, 75, 577-585.

29. Chakrabarti, A., Mandal, B.N., Basu, U. and Banerjea, S. (1997). Solution of a class of hypersingular integral equation of second kind. *ZAMM*, 77, 319-320.

30. Chakraborty R. and Mandal B.N. (2014). Water wave scattering by rectangular trench. *J. Eng. Math.*, 89, 101-112.

31. Chakraborty R. and Mandal B.N. (2015). Oblique water wave scattering by a rectangular submarine trench. *ANZIAM J.*, 56, 286-298.

32. Chakrabarti, A. and Williams, W.E. (1980). A note on singular integral equations. *J. Inst. Math. Appl.*, 26, 321-323.

33. Chan, Y., Fannjiang, A.C. and Paulino, G.H. (2003). Integral equations with hyper singular kernels-theory and applications to fracture mechanics. *J. Eng. Sci.*, 41, 683-720.

34. Chowdhury, R. (2004). Water wave scattering by obstacles and surface discontinuities. *Thesis.*

35. Chung, H. and Fox, C. (2002). Calculation of wave-ice interaction using the WienerHopf technique. *New Zealand J. Math.*, 31(1), 1-18.

36. Crapper, G.D. (1984). Introduction to Water Waves. *Ellis Horwood.*

37. Das P., Dolai D.P. and Mandal B.N. (1997). Oblique wave diffraction by two parallel thin barriers with gaps. *J. Waterw. Port Coast Ocean Eng.*, 123, 163-171.

38. Dean W.R. (1945). On the reflection of surface waves by a submerged plane barrier. *Proc. of Cambridge Philosophical Soc.*, 41, 231-238.

39. Dean, R. G. and Ursell, F., (1959). Interaction of a fixed semi-immersed circular cylinder with a train of surface waves. *M.I.T. Hydrodynamics Laboratory*, Tech. Rep. no. 37.

40. Dragos, L. (1983). Method of fundamental solutions, A Novel theory of lifting surface in subsonic flow. *Arch. of Mechanics*, 35, 579-590.

41. Dragos, L. (1994). A collocation method for integration of Prandtl's equation. *ZAMM*, 74, 289-290.

42. Dragos, L. (1994). Integration of Prandtl's equation by the aid of quadratic formulae of Gauss type. *Quart. Appl. Math.*, 52, 23-29.

43. Dutta, B. and Banerjea, S. (2009). Solution of a hypersingular integral equation in two disjoint intervals. *Appl. Math. Lett.*, 22, 1281-1285.

44. Evans D.V. (1970). Diffraction of surface waves by a submerged vertical plate. *J. of Fluid Mech.*, 40, 433-451.

45. Evans, D.V. and Fernyhough, M. (1995). Edge waves along periodic coastlines. Part 2., *J. Fluid Mech.*, 297, 307-325.

46. Evans, D.V. and Morris, C.A.N. (1972a). The Effect of a Fixed Vertical Barrier on Obliquely Incident Surface Waves in Deep Water. *J. Inst. Maths Applics.*, 9, 198-204.

47. Evans, D.V. and Morris, C.A.N. (1972b). Complementary Approximations to the Solution of a Problem in Water Waves. *J. Inst. Maths Applics.*, 10, 1-9.

48. Evans, D. V. and Porter, M. A. (2011). Asymptotic reflection of linear water waves by submerged horizontal porous plates. *J. Eng. Math.*, 69, 135-154.

49. Estrada, R. and Kanwal, R.P. (1989). Integral equations with logarithmic kernels. *IMA Jour. of Appl. Math.*, 43, 133-155.

50. Estrada, R. and Kanwal, R.P. (2000). Singular Integral Equations. *Birkhauses*, Boston.

51. Fox C. and Squire V.A. (1994). On the oblique reflection and transmission of ocean waves at shore fast sea ice. *Phil. Trans. R. Soc. A.*, 347, 185-218.

52. Gakhov, F.D. (1966). Boundary value problems. *Pergamon*, Oxford.

53. Gayen, R., Mandal, B.N. and Chakrabarti, A. (2005). Water wave scattering by an ice-strip. *J. Eng. Math.*, 53, 21-37.

54. Gayen, R. and Mondal, A., (2014). A hypersingular integral equation approach to the porous plate problem. *Applied Ocean Research*, 46, 70-78.

55. Goldberg, Chen, (1994). Boundary Elements: An Introductory Course. *WIT Press.*

56. Gray, L.J., (1991). Evaluation of hypersingular integrals in the boundary element method. *Math. Comput. Modelling*, 15, No. 3-5, 165-174.

57. Greenhill A.G. (1887). Wave motion in hydrodynamics. *Am J Math.*, 9, 62-112.

58. Guiggiani, M., Krishnasamy G.,Rudolphi, T.J., Rizzo, F.J. (1992). A General Algorithm for the Numerical Solution of Hypersingular Boundary Integral Equations. *J. Appl. Mech.*, 59, 604-614.

59. Havelock, T. H., (1929). Forced waves on water. *Phil. Mag.*, 8, 569-576.

60. Ioakimidis, N.I. (1982). A natural interpolation formula for Cauchy-type singular integral equation with generalized kernels. *J. Comput. Phys.*, 48, 117-126.

61. Ioakimidis, N.I. (1982). Application of finite-part integrals to singular integral equations of crack problems in plane and 3D elasticity. *Acta Mech.*, 45, 31-47.

62. Kanoria M. (1999). Water wave scattering by a submerged thick wall with a gap. *Applied Ocean Research*, 21, 69-80.

63. Kanorai M., Dolai D.P. and Mandal B.N. (1999). Water wave scattering by thick vertical barriers. *J. Eng. Math.*, 35, 361-384.

64. Kanoria M. and Mandal B.N. (1996). Oblique wave diffraction by two parallel vertical barriers with submerged gaps in water of uniform finite depth. *J. Tech. Phys.*, 37, 187-204.

65. Kanoria M. and Mandal B.N. (2002). Water wave scattering by a submerged circular-arc-shaped plate. *Fluid dynamics research*, 31(5-6), 317.

66. Kaya, A.C., Erdogom, F. (1987). On the solution of integral equation with strongly singular kernels. *Quart. Appl. Math.*, 55(1), 105-122.

67. Kirkup, S. (2007). *The Boundary Element Method in Acoustics.*

68. Kirby J.T. and Dalrymple R.A. (1983). Propagation of obliquely incident water waves over a trench. *J. Fluid Mech.*, 133, 47-63.

69. Kohout, A. L. and Meylan, M. H., (2008). An elastic plate model for wave attenuation and ice floe breaking in the marginal ice zone. *J. Geophys. Res.*, 113.

70. Kreisel G. (1949) Surface waves. *Quart. Appl. Math.*, 7, 21-44.

71. Kuznetsov, N., McIver, P. and Linton, C. M. (2001). On uniqueness and trapped modes in the water-wave problem for vertical barriers. *Wave Motion*, 33, 283-307.

72. Lamb, H., (1932). Hydrodynamics. *Cambridge University Press*, England.

73. Lassiter J.B. (1972). The propagation of water waves over sediment pockets. *PhD thesis, Massachusetts Institute of Technology.*

74. Lee J.J. and Ayer R.M. (1981). Wave propagation over a rectangular trench. *J. Fluid Mech.*, 110, 335-347.

75. Lighthill, M. J., (1978). Waves in Fluids. *Cambridge University Press.*

76. Linton, C.M. and Chung, H. (2003). Reflection and transmission at the ocean/sea-ice boundary. *Wave Motion*, 38, 43-52.

77. Linton, C. M. and McIver, P. (2001). Handbook of mathematical techniques for wave/structure introductions. *Chapman and Hall/CRC, Boca Raton, FL.*

78. Liu Y. and Li H.J. (2012). Analysis of wave interaction with a submerged perforated semicircular breakwater through multipole method. *Appl. Ocean Res.*, 34, 164-172.

79. Liu H.W., Fu D.J. and Sun X.L. (2013). Analytic solution to the modified mild-slope equation for reflection by a rectangular breakwater with scour trenches. *ASCE J. Eng. Mech.*, 139, 39-58.

80. Luminita G. (2007). A Direct Boundary Element Approach with Linear Boundary Elements for the Compressible Fluid Flow Around Obstacles. *The XVI Conference on Applied and Industrial Mathematics CAIM.*

81. MacCammy, R.C. (1965). Pairs of column-type integral equations. *Proc. Amer. Math. Soc.*, 16, 871-875.

82. MacCammy, R.C. (1985). On singular integral equations with logarithmic or Cauchy kernels. *J. Math. Mech.*, 7, 355-376.

83. Mandal, B.N. (1986). Singular integral equation of first kind with Cauchy kernel revisited. *Indian J. Pure Appl. Math.*, 17, 1340-1344.

84. Mandal, B. N. (1987). A note on construction of potentials due to line multipoles in the theory of water waves. *Int. J. Math. Edu. Sci. Technol.*, 18, 561-565.

85. Mandal, B.N., Banerjea, S. and Dolai, D.P. (1995). Interface diffraction by a thin vertical barrier submerged in lower fluid. *Appl. Ocean Res.*, 17, 93-102.

86. Mandal, B.N., Bhattacharyya, S. (2007). Numerical solution of some classes of integral equations using Bernstein polynomials. *Appl. Math. Comput.*, 190, 1707-1716.

87. Mandal, B.N., Bhattacharyya, S. (2008). Numerical solution of a singular integro-differential equation. *Appl. Math. Comput.*, 195, 346-350.

88. Mandal, B.N., Chakrabarti, A. (2011). Applied singular integral equations, *CRC Press*.

89. Mandal, B.N., Chakrabarti, A. (2000). Water wave scattering by barriers. *WIT Press*, Southampton, Boston.

90. Mandal, B.N. and Gayen, R. (2002). Water waves scattering by two symmetric circular arc shaped thin plates. *J. Eng. Math.*, 44, 297-303.

91. Mandal, B.N. and Goswami, S.K. (1983). A note on singular integral equation. *Indian J. of Pure and Appl. Math.*, 14, 1352-1356.

92. Mandal B.N. and Kanoria M. (2000). Oblique wave-scattering by thick horizontal barrier. *J. Offshore Mech. Arctic Eng.*, 122(2), 100-108.

93. Martin, P.A. (1992). Exact solution of a simple hyper singular integral equation. *J. Integral Equation Appl.*, 4, 197-204.

94. Martin, P.A., Parsons, N.F. and Farina, L. (1997). Interaction of water waves with thin plates. Chap5, Mathematical techniques for water waves, ed. B.N. Mandal, *Comput. Mech. Publcs.*, Sothampton, Boston, 197-229.

95. McIver, P. (1999). Water-wave diffraction by thin porous breakwater. *J. Waterway Port Coastal and Ocean Eng.*, 125, 66-70.

96. McIver, M. and Urka U. (1995). Wave scattering by circular are shaped plates. *J. Eng. Math.*, 29(6), 575-589.

97. Mei, C.C. (1983). The Applied Dynamics of Ocean Surface Waves. *Wiley*, New York.

98. Mei, C. C. and Black, J. L. (1969). Scattering of surface waves by rectangular obstacles in water of finite depth. *J. Fluid Mech.*, 38, 499-511.

99. Mikhlin, S. G. (1957). Integral Equations. *Pergamon Press*, New York.

100. Miles, J.W. (1982). On surface wave diffraction by a trench. *J. Fluid Mech.*, 115, 315-325.

101. Mondal, A., Panda S. and Gayen R. (2017). Flexural-gravity wave scattering by a circular-arc-shaped porous plate. *Studies in Appl. Math.*, 138(1), 77-102.

102. Mondal, D. and Banerjea, S. (2016). Scattering of water waves by an inclined porous plate submerged in ocean with ice cover. *Quart. J. Mech. and Appl. Math.*, 69, 195-213.

103. Mondal, D. and Banerjea, S. (2016). Scattering of water waves by a porous circular arc- shaped barrier submerged in Ocean. *International J. Computational Methods and Experimental Measurements*, 4(4), 523-542.

104. Mondal D., Samanta A. and Banerjea S. (2021). Hypersingular Integral Equation Formulation of the Problem of Water Wave Scattering by A Circular Arc Shaped Impermeable Barrier Submerged in Water of Finite Depth. *The Quarterly J. Mech. and Appl. Math.*, 74(4), 491-505.

105. Muskhelishvili, N. I. (1953). Singular Integral Equations. *Noordhoff International Publishing.*

106. Newman, J.N. (1977). Marine Hydrodynamics. *MIT Press*, Cambridge.

107. Parsons, N.F. and Martin, P.A. (1992). Scattering of water waves by submerged plates using hypersingular integral equations. *Applied Ocean Research*, 14, 313-321.

108. Parsons, N.F. and Martin, P.A. (1994). Scattering of water waves by submerged curved plates and by surface-piercing flat plates. *Applied Ocean Research*, 16, 129-139.

109. Peters, A.S. (1963). A note on integral equations of the first kind with Cauchy kernel. *Comm. Pure and Appl. Math.*, 16, 57-61.

110. Porter, D., (1972). The transmission of surface waves through a gap in a vertical barrier. *Proc. Camb. Phil. Soc.*, 71, 411-421.

111. Porter, R. and Evans, D.V. (1995). Complementary approximations to wave scattering by vertical barriers. *J. Fluid Mech.*, 294, 155-180.

112. Pozrikidis, C., (2002). A practical guide to boundary element methods with the software library BEMLIB. *CRC Press*, London.

113. Samanta, A., Chakraborty, R. and Banerjea, S. (2022). Line element method of solving singular integral equations. *Indian J. pure appl. math.*, 53(2), 528-541.

114. Samanta, A. and Chakraborty, R. (2020). Scattering of water waves by thick rectangular barriers in presence of ice cover. *J. Ocean Eng. and Sci.*, 5, 278-293.

115. Sarkar, B., Paul, S. and De, S. (2021). Water wave propagation over multiple porous barriers with variable porosity in the presence of an ice cover. *Meccanica*, 56(7), 1771-1788.

116. Sasmal, A., Paul, S. and De, S. (2019). The influence of surface tension on oblique wave scattering by a rectangular trench. *J. Appl. Fluid Mech.*, 12, 233-241.

117. Sollitt, C.K. and Cross, R.H. (1972). Wave transmission through permeable breakwaters. *Proc. 13th Conf. on Coastal Engineering, ASCE* , 1827-1846.

118. Squire, V.A. (2007). Review of ocean and sea ice revisited. *Cold Regions Science and Technology*, 49, 110-133.

119. Stoker, J.J., (1957). Water Waves, The mathematical theory with applications. *Interscience Publishers*, New York.

120. Stokes, G. G., (1847). On the theory of oscillatory waves. Trans. *Cambridge Phil. Soc.*, 8 .

121. Sturova I.V. (2015). Radiation of waves by a cylinder submerged in water with ice floe or polynya. *J. Fluid Mech.*, 784, 373-395.

122. Sobhani S.M., Lee J.J. and Wellford(Jr.) L.C. (1988). Interaction of Periodic Waves with Inclined Portable Barrier. *Journal of Waterway, Port, Coastal, and Ocean Engineering*, 114, 745-761.

123. Sretensky, L.N. (1977). The Theory of Wave Motions of a Fluid. *Nauka*, Moscow.

124. Thorne, C. (1953). Multipole expansions in the theory of surface waves. *Proc. Camb. Phil. Soc.*, 49, 231-238.

125. Torri, T., Ohkubo, N., Hayashi, K., Matsuoka and Kanai, H., (2000). Development of a very large floating structure. *Nippon Steel Technical Report*, 82, 23-34.

126. Tsai, C. H. and Young, D. L. (2011). The method of fundamental solutions for water wave diffraction by thin porous breakwater. *Journal of Mechanics*, 27, 149-155.

127. Ursell F. (1947). The effect of a fixed vertical barrier on surface waves in deep water. *Proc. Cambridge Philosophical Soc.*, 43, 374-382.

128. Ursell, F., Dean, R.G. and Yu, Y.S., (1959). Forced small amplitude water waves: a comparison of theory and experiments. *J. Fluid Mech.*, 7, 33-52.

129. Wadhams, P. (1978). Wave decay in the mrginal ice zone measured from submarine. *Deep-sea Res.*, 25, 23-40.

130. Wang, C. M., Tay, Z.Y., Takagi, K. and Utsunomiya, T. (2010). Review of Methods for Mitigating Hydroelastic Response of VLFS Under Wave Action, *Appl. Mech. Reviews*, 63, 030802-18.

131. Wehausen, J. V. (1971). The motion of floating bodies. *Ann. Rev. Fluid Mech*, 3, 237-268.

132. Wehausen, J.V. and Laiton, E.V., (1960). Surface Waves. *Handbuch der Physik, Band IX, Springer Verlag*, Berlin.

133. Whitham, G.B. (1979). Lectures on Wave Propagation. *Springer-verlag*, New York.

134. Williams, W. E., (1978). A note on a singular integral equation. *J. Inst. Math. Appl.*, 22, 211-214.

135. Xie, J.J., Liu, H.W. and Lin, P. (2011). Analytical solution for long wave reflection by a rectangular obstacle with two scour trenches. *ASCE J. Eng. Mech.*, 137, 919-930.

136. Yu, X. (1995). Diffraction of Water Waves by Porous Breakwaters. *Journal of Waterway, Port, Coastal and Engineering*, 121(6), 275-282.

137. Yu, Y. S. and Ursell, F. (1961). Surface waves generated by an oscillating circular cylinder on water of finite depth: theory and experiments. *J. Fluid Mech.*, 11, 529-551.